# Gravity as an Emergent Force Via the Uncertainty Principle

Morgan W. Weinberg
(Dated: July 7, 2026)

The core concept of this paper is the relation between an accelerating field and time uncertainty. This relation distills from the derivation of Newton's Law of Gravitation via the uncertainty principle. It's shown, further, that this relation can be used to derive the Coulomb Force, suggesting that it may be a general principle in nature. Taking this concept further, this paper draws a connection between expanding space and acceleration—offering an explanation for the missing-mass problem in galaxies. The paper goes on to draw a connection between the expansion of space and time uncertainty, leading to a startling conclusion: The expansion of space is not a function of the energy contained therein, but conversely, the mass of the universe is created *in concert* with the expansion of space. Further, because this expansion is a function of time, the mass of the universe is a function of time and increases in lockstep therewith. It's deemed that the model of the universe presented herein obviates the need for dark matter and dark energy to explain our observations of the cosmos.

## I. DERIVATION OF NEWTON'S LAW OF GRAVITATION

Why Newton? Why not general relativity? Einstein's field equations reduce to the Newtonian limit for relatively low-energy gravitational systems—which constitute the bulk of the observable universe. Planetary motions in the Solar System are predicted by Newton's Laws to a high degree of precision. This includes the perihelion precession of Mercury, which Newtonian mechanics predicts with roughly 93% accuracy. With the relativistic effect of 43 (arcsec $cy^{-1}$) [1] factored in, the predicted value is brought to within .2% of the measured precession. To put this in perspective, Mercury's precession is measured in arc-seconds per *century*.

Considerably more interesting are the motions of bodies far away from massive objects, where accelerations are measured at 1E−9 m $s^{-2}$ and below. Importantly, this is the low-acceleration regime where galactic rotational-velocity curves start to diverge markedly from those predicted by Newtonian gravity (and general relativity). Observations repeatedly yield rotation curves that flatten out, which is in stark contrast to the expected profile—a Keplerian decline as seen in our Solar System. If Keplerian decline is expected in all gravitational systems, what's so special about galaxies?

The prevailing explanation for this discrepancy is that the mass needed to resolve flat rotation curves must exist but has yet to be directly detected because it doesn't interact with light—hence the term "dark matter"; but is this a problem of missing mass or missing physics?

The present thesis asserts that missing physics is at issue here, but before venturing down that road, a new take on gravity is presented that is based on the quantum principle of uncertainty. The aim is not to quantize gravity but to examine it in the context of the quantum realm and possibly gain new insights. Because we're ultimately interested in low-energy systems and low-acceleration regimes, the following analysis is non-relativistic.

$$E_f = \oint \vec{g_f} \cdot d\vec{A} = mc^2 \tag{1}$$

It is posited that a mass $m$ has a gravitational field $\vec{g_f}$ that, when integrated over a closed surface, is equivalent to the energy contained within the surface. In the rest frame of $m$, the net energy of this field $E_f$—as shown by Eq. (1)—is irrespective of distance. If $m$ is a point mass, and the closed surface is a sphere with radius $r$, Eq. (1) simplifies to:

$$g_f = \frac{mc^2}{4\pi r^2} \, . \tag{2}$$

It is further suggested that the field energy $E_f$ cannot be infinitesimally divided. There is a lower bound to the elements that comprise $E_f$, which is found at the Planck scale. Multiplying field $g_f$ times the Planck area $a_p$ gives the smallest measurable unit of energy $\Delta E$ in the field at a given offset $r$ from the point mass:

$$l_p = \sqrt{\frac{\hbar G}{c^3}} \, , \tag{3}$$

$$a_p = \pi {l_p}^2 \, , \tag{4}$$

$$a_p = \frac{hG}{2c^3} \, , \tag{5}$$

$$\Delta E = \frac{m \cancel{c^2}}{4\pi r^2} \frac{hG}{2 \cancel{c^3}} \, , \tag{6}$$

$$\Delta E = \frac{mhG}{8\pi r^2 c} \, . \tag{7}$$

Eq. (3) defines the Planck length $l_p$ [2], which, in turn, is used to define the Planck area $a_p$ as given by Eq. (4). The definition of Planck area $a_p$ here—with the inclusion of $\pi$ as a scalar—is slightly different from that typically found in publications. With the inclusion of $\pi$, the reduced Planck constant $\hbar$ in Eq. (3) distills to its non-reduced form $h$ in Eq. (5). If $a_p$ is defined as a point, then $\Delta E$ represents the energy of gravitational field $g_f$ at that point. It is imagined that particles in a gravitational field

interact with the field at these points.

With $\Delta E$ defined as the smallest measurable unit of energy in a field, the time needed to measure this energy—which is to say, the time $\Delta t_u$ needed for a particle to sense this energy at a point in the field—is given by the uncertainty principle:

$$\Delta E \Delta t_u \geq \frac{h}{4\pi} \, . \tag{8}$$

The time uncertainty $\Delta t_u$ is deemed to be an inherent property of a gravitational field—and possibly accelerating fields in general.

Plugging Eq. (7) into Eq. (8) gives the following relations:

$$\frac{m\cancel{h}G}{8\cancel{\pi} r^2 c} \Delta t_u \geq \frac{\cancel{h}}{4\cancel{\pi}} \, , \tag{9}$$

$$\frac{mG}{2r^2 c} \Delta t_u = 1 \, . \tag{10}$$

Notice that as Eq. (9) progresses to Eq. (10), the $\geq$ sign has been replaced with an equals sign. This will pin $\Delta t_u$ to its minimal value—with the understanding that $\Delta E$ has also been defined as a minimum.

It's well established that a gravitational field—and information, in general—travels at the speed of light for all observers. This is embodied by Eq. (11) where $t_f$ is the time it takes for the field to travel a distance of $\Delta r$:

$$\frac{\Delta r}{\Delta t_f} = c \, . \tag{11}$$

Multiplying Eq. (10) by Eq. (11) gives this:

$$\frac{mG}{2r^2 \cancel{c}} \Delta t_u \cancel{c} = \frac{\Delta r}{\Delta t_f} \, , \tag{12}$$

$$\frac{mG}{2r^2} = \frac{\Delta r}{\Delta t_f \Delta t_u} \, . \tag{13}$$

Non-relativistic acceleration is described by the familiar equation:

$$\Delta r = \frac{1}{2} a {\Delta t_p}^2 \, , \tag{14}$$

$${\Delta t_p}^2 = \frac{2\Delta r}{a} \, . \tag{15}$$

In Eq. (15), $\Delta t_p$ relates to a particle $p$ accelerating at rate $a$. Substituting ${\Delta t_p}^2$ in Eq. (15) for $\Delta t_f \Delta t_u$ in Eq. (13) gives Newton's equation:

$$\frac{mG}{\cancel{2}r^2} = \frac{\cancel{\Delta r} a}{\cancel{2}\cancel{\Delta r}} \, , \tag{16}$$

$$a = \frac{mG}{r^2} \, . \tag{17}$$

With this substitution, an equivalence between the terms ${\Delta t_p}^2$ and $\Delta t_f \Delta t_u$ is being asserted that clearly needs to be unpacked. Fig. 1 shows a particle accelerating leftward through a minute distance $\Delta r$ from one point in space to another. The points may be considered to be points in a field with the right point having a time uncertainty of $\Delta t_u$. The field, in the figure, is propagating left to right between the points—opposite the direction of acceleration—at $c$. These concepts, taken together, yield the following relations:

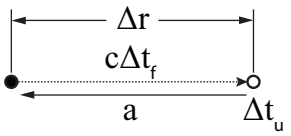


FIG. 1. Acceleration between discreet points in a field.

$$\Delta t_f = \frac{\Delta r}{c} \, ,$$

$${\Delta t_p}^2 = \frac{2\Delta r}{a} \, ,$$

$${\Delta t_p}^2 = \Delta t_f \Delta t_u \, , \tag{18}$$

$$\frac{2\cancel{\Delta r}}{a} = \frac{\cancel{\Delta r}}{c} \Delta t_u \, , \tag{19}$$

$$a = \frac{2c}{\Delta t_u} \, . \tag{20}$$

Plugging Eqs. (11) and (15) into Eq. (18) gives Eq. (19), which reduces to Eq. (20).

Applying direction to the magnitudes of acceleration and field speed—as shown in Fig. 1—gives the vector form of Eq. (20):

$$\vec{a} = -\frac{2\vec{c}}{\Delta t_u} \, . \tag{21}$$

In essence, Eqs. (18) through (21) relate the acceleration of a particle in a field to the field's speed of propagation and the time uncertainty of the field at the point coincident with the particle—where acceleration is opposite the direction of field propagation. The equivalence asserted in Eq. (18) is the finger in the dam that holds the above derivation of Newton's equation together. It's thus necessary and asserted to be correct. Eq. (15) relates ${\Delta t_p}^2$ to acceleration, which, along with Eq. (11) allow the $\Delta r$ terms to cancel, leaving Eqs. (20) and (21).

Notably, Eq. (21) has a large numerator. Plugging Earth's near-surface gravity acceleration of 9.81 m $s^{-2}$ into Eq. (21) gives a time uncertainty of 1.94 years.

Playing around with Eq. (10) also yields an interesting result. When the estimated mass of the universe—1.5E53 kg [3] and the estimated age of the universe—13.8 billion years [4] (4.36E17 s) are plugged into Eq. (10), the diameter—$2r$ calculates to 1.71E26 m, which is less than an order of magnitude from the estimated diameter of the universe of 8.8E26 m.

In Eq. (20), as acceleration goes to zero, time uncertainty goes to infinity. With $\Delta t_u$ set equal to the age

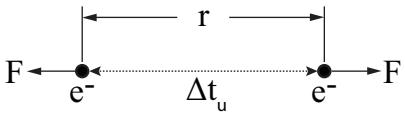


FIG. 2.

of the universe, acceleration $a$ calculates to 1.38E−9 m $s^{-2}$. Coincidentally, this value marks the beginning of the low-acceleration regime mentioned above, where galactic-rotation curves start to become anomalous.

## II. COULOMB FORCE

Fig. 2 shows two electrons separated by a distance $r$. To illustrate how Eq. (21) could be used in general, this equation is applied to the electron pair in the figure to determine the Coulomb force urging the electrons apart. Using the model that the electrostatic force is carried by virtual photons, a virtual photon emitted between the electrons would have an energy given by the uncertainty principle:

$$\begin{aligned} \Delta E \Delta t &\geq \frac{\hbar}{2} \ , \\ \Delta E &\geq \frac{\hbar}{2\Delta t} \ . \end{aligned} \tag{22}$$

The "effective mass" $m_e$ of this photon is as follows:

$$\begin{aligned} m_e &= \frac{\Delta E}{c^2} \ , \\ m_e &= \frac{\hbar}{2c^2 \Delta t} \ . \end{aligned} \tag{23}$$

Because $\Delta E$ is a minimum, the $\geq$ sign in Eq. (22) can be replaced with an equals sign. With the application of Eq. (21), the reactive force on an electron emitting the virtual photon is thus:

$$\begin{aligned} F_p &= ma \ , \\ F_p &= m_e \frac{2c}{\Delta t_u} \ , \\ F_p &= \frac{\hbar}{\cancel{2}c^{\cancel{2}}\Delta t} \frac{\cancel{2}c}{\Delta t_u} \ . \end{aligned} \tag{24}$$

The lifespan $\Delta t$ and the uncertainty $\Delta t_u$ of the virtual photon are equivalent and equate to $r/c$. Plugging this result into Eq. (24) gives the following:

$$\begin{aligned} F_p &= \frac{\hbar}{c \Delta t \Delta t_u} \ , \\ F_p &= \frac{\hbar c^{\cancel{2}}}{\cancel{c}r^2} \ , \\ F_p &= \frac{\hbar c}{r^2} \ . \end{aligned} \tag{25}$$

Eq. (25) gives the reactive force $F_p$ on an electron from the emission of a virtual photon. To translate this reactive force to the Coulomb force between the electrons, $F_p$ is multiplied by the Sommerfeld constant $\alpha$. This constant relates the potential energy $PE_c$ between two electrons at a distance $r$ and the energy $E_p$ of a photon of angular wavelength $r$ where:

$$\begin{aligned} \alpha E_p &= PE_c \ , \\ \alpha \frac{\partial E_p}{\partial r} &= \frac{\partial PE_c}{\partial r} \ , \\ \alpha &= \frac{F_c}{F_p} \ . \end{aligned}$$

Taking the partial derivative of these energies with respect to $r$ gives a relation between the Coulomb force and the force of a photon of energy $E_p$. With this relation, the Coulomb force is given by multiplying Eq. (25) by $\alpha$—the latter defined below:

$$\begin{aligned} \alpha &= \frac{e^2}{4\pi\epsilon_0 \hbar c} \ , \\ F_c &= \alpha \frac{\hbar c}{r^2} \ , \\ F_c &= \frac{e^2 \cancel{\hbar c}}{4\pi\epsilon_0 \cancel{\hbar c} r^2} \ , \\ F_c &= \frac{e^2}{4\pi\epsilon_0 r^2} \ . \end{aligned} \tag{26}$$

Eq. (26) is the familiar equation for the Coulomb force, where $e$ is the charge of an electron and $r$ is the distance between charges. While simplistic, the recovery of the Coulomb force is a quick sanity check of Eq. (21). Eq. (21) will be integral to the ideas presented in later sections.

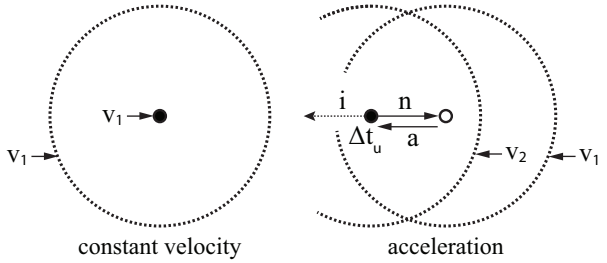


FIG. 3.

## III. INERTIA

If Eq. (21) can describe acceleration from an external field, can it also elucidate the mystery of inertia?

Imagine two capsules in space, separated by a certain distance, at rest with respect to each other. The second capsule fires its engine and starts accelerating. From the vantage point of an observer in the second capsule, the first capsule looks to be moving, and its relative velocity seems to be increasing. Conversely, an observer in the

first capsule sees the second capsule moving at an increasing velocity. From the perspective of either observer, the other is accelerating.

There is, however, additional information that these observers can use to determine who, in fact, is accelerating. The second observer, looking at the accelerometers in the cabin, could measure his rate of acceleration. The second observer—assuming that he was facing the direction of acceleration—would be pressed into his seat, which would be pushing against the inertia of his body. The first observer, looking at his instruments, would detect no such acceleration—remaining essentially weightless in his seat. Here, inertia is the source of truth. It informs which observer is *actually* accelerating.

At a certain point, the second observer looks out of his window and sees the first capsule moving at a velocity $v_1$. Assuming that the first capsule and its gravitational field are at rest with respect to each other, the second observer would see the first capsule *and its field* moving at $v_1$—as illustrated in Fig. 3. As the relative velocity increases, the first capsule and its field, which continue to remain at rest with respect to each other—from the perspective of the second observer, move in concert.

Does this hold in the opposite perspective—where the first observer is looking at the second capsule? If the engine of the second capsule were to be cut off, and it stopped accelerating, the capsule wouldn't have detached from its field. The second capsule and its field would be at rest with respect to each other. Therefore, even during acceleration, the second capsule's field must be accelerating along with the capsule.

It's posited that accelerating this field requires information flow—which, in effect, is how the second observer comes to realize that *he* is the one who is accelerating. Looking at Eq. (21), if this equation is run in reverse, acceleration coupled with time uncertainty—which is related to the measurable energy at a point in the field—can drive information flow in the field. Here, the acceleration of particles of and within the second capsule is informing the fields around those particles. Further, it's surmised that the inertia—the resistance to acceleration—experienced by the second observer as he is pressed into his seat is a result of that observer interacting with his *own* gravitational field. This interaction, during acceleration, is continuously re-informing his field.

Fig. 3 also shows a particle of the second capsule, on the right—accelerating its own field from $v_1$ to $v_2$. The field, at the particle's location, has a time uncertainty $\Delta t_u$. This, coupled with acceleration $\vec{a}$, drives information flow $\vec{i}$ into the field. With respect to Eq. (21), information flowing into the field flows in the direction of acceleration, and thus, the negative sign disappears in this case. However, inertia—represented as $\vec{n}$ in the figure—is also described by Eq. (21). In the frame of the inertial observer in the first capsule, the particle is accelerating at $\vec{a}$. In the frame of the particle, there is a force of $m\vec{a}$ (where $m$ is the particle mass) acting upon the particle, which is balanced by the equal but opposite inertial force of $m\vec{n}$.

If gravity can be described as information flow driving acceleration, inertia can be thought of as acceleration driving information flow. Here, inertia is the price of re-informing the field around an accelerating mass.

Notice that time uncertainty in Eq. (21) is inversely proportional to acceleration, which means that as acceleration approaches infinity, time uncertainty approaches zero. Perhaps time uncertainty, here, can be thought of as the urgency with which information must flow, where higher rates of acceleration require higher rates of information transfer. As acceleration goes to zero, time uncertainty goes to infinity, indicating that information flow is no longer necessary.

## IV. A GRAVITATIONAL FIELD IN EXPANDING SPACE

If photons are redshifted over time by expanding space as they propagate, can gravitational fields also be redshifted as they propagate? Are all propagating fields in expanding space subject to redshift? With respect to photons, cosmological redshift is literally the shifting of a photon's frequency to the red end of the spectrum as a consequence of its wavelength being stretched by expanding space. An observer of a redshifted photon will have noticed its energy having been decreased relative to its emitted frequency.

Gravitational fields, however, show no signs of dilution over time—with gravitational systems remaining stable over billions of years. Even at the outermost edges of galaxies, 1000s of light-years from their centers (that comprise the bulk of the galactic mass), there is no indication of a weakening field. In fact, the opposite is true; this field typically seems to have more strength than the mass of the galaxy can account for—as evidenced by flat rotation curves.

This is actually a clue. Unlike light, a gravitational field is intrinsically connected to its source. As the source translates or accelerates, the field must move in concert. If the source loses or gains energy, the field strength changes in proportion thereto. In short, the field requires a constant flow of information to maintain its connection with its source. With this in mind, it may be more correct to imagine a gravitational field in expanding space as being simultaneously stretched and re-informed, with the latter immediately undoing any sign of dilution. Furthermore, it's imagined that the tension between stretching and re-informing the field adds time uncertainty that, in turn, yields an additional acceleration component on top of the Newtonian term.

Eq. (7), restated below, gives the energy uncertainty at a point in a field. Taking the derivative with respect

to time gives the following:

$$\Delta E = \frac{mhG}{8\pi r^2 c} ,$$
$$\frac{d\Delta E}{dt} = \frac{-mhG}{4\pi r^3 c}\frac{dr}{dt} . \quad (27)$$

The expansion of space is given by:

$$\vec{v} = \vec{r}H_l , \quad (28)$$
$$\frac{dr}{dt} = rH_l . \quad (29)$$

Eq. (28) is recognizable as Hubble's law, which is usually written with the Hubble parameter $H_0$—a measure of intergalactic expansion. Notice that Eqs. (28) and (29) use the parameter $H_l$, which is proffered as a local measure of expansion (or "expansion parameter") at a specific point in a frame of reference. The case for the idea—that the expansion parameter measured by an observer is dependent on that observer's frame of reference—will be built slowly over the course of the following sections. This will, hopefully, lead to a reconciliation of $H_l$ and $H_0$.

Plugging Eq. (29) into Eq. (27) gives the following:

$$\frac{d\Delta E}{dt} = \frac{-mhG}{4\pi r^{\cancel{3}2}c}\cancel{r}H_l , \quad (30)$$
$$\frac{\Delta(\Delta E)}{\Delta t_u} = \frac{-mhGH_l}{4\pi r^2 c} , \quad (31)$$
$$\Delta E = \frac{mhGH_l}{4\pi r^2 c}\Delta t_u . \quad (32)$$

There's a lot going on between Eq. (30) and Eq. (32) that needs to be deconstructed. Eq. (30) shows the energy at a point in a gravitational field that is decreasing over time as a result of being stretched in expanding space. In Eq. (31), $d(\Delta E)$ and $dt$ are quantized to $\Delta(\Delta E)$ and $\Delta t_u$, with the presumption that any change in energy, at this scale, would be discrete over a discrete period of time. In Eq. (32), $\Delta(\Delta E)$ is simplified to $\Delta E$ with the observation that the latter *is* the change in energy in question.

Also, notice that the negative sign has been stripped from the definition of $\Delta E$. As discussed, the strength of this field, being a function of the source mass, does not dilute over time. If a mass is stable, its field must remain stable in concert. This means that a negative $\Delta E$ must be balanced with a positive $\Delta E$ as the field is reinformed. The $\Delta E$s cancel, which means there is no net energy transfer to or from the field as a consequence of expanding space. It may be more correct to imagine $\Delta E$ here as a potential change of energy that never actually takes place—where expansion creates a certain tension in the field, so to speak, that manifests as energy and time uncertainty, which are positive numbers.

Plugging Eq. (32) into the uncertainty equation (Eq. (8)) gives the following:

$$\Delta E \Delta t_u = \frac{h}{4\pi} ,$$
$$\frac{mh\cancel{G}GH_l}{\cancel{4\pi}r^2 c}{\Delta t_u}^2 = \frac{\cancel{h}}{\cancel{4\pi}} , \quad (33)$$
$$\Delta t_u = \frac{r\sqrt{c}}{\sqrt{mGH_l}} . \quad (34)$$

$\Delta E$, in Eq. (27), was already defined as a minimum, and with $\Delta t_u$ also defined as a minimum, the $\geq$ sign in the uncertainty equation has been replaced with an equals sign, similar to the case above. Note that the time uncertainty $\Delta t_u$ in Eq. (32) corresponds to $\Delta t_u$ in Eq. (8), as they are both measuring the same energy. This is reflected in the ${\Delta t_u}^2$ term of Eq. (33). Solving for $\Delta t_u$ gives Eq. (34)—a relation between time uncertainty $\Delta t_u$ and local-frame expansion $H_l$.

Eq. (20) may then be used to convert this time uncertainty to acceleration:

$$a = \frac{2c}{\Delta t_u} ,$$
$$a = \frac{2c\sqrt{mGH_l}}{r\sqrt{c}} , \quad (35)$$
$$a = \frac{2\sqrt{cH_l mG}}{r} . \quad (36)$$

The acceleration term defined by Eq. (36) is designated as the non-Newtonian or "expansion" component and is additive to the Newtonian term given by Eq. (17). Because the direction of field propagation is the same for both components, both accelerations point toward the field source. Combining these terms gives a complete equation for acceleration in the Newtonian limit:

$$a_n = \frac{mG}{r^2} + \frac{2\sqrt{cH_l mG}}{r} . \quad (37)$$

In Section VI, a more general form of Eq. (37) will be derived in the context of a system of particles. Before moving on, however, the similarity between Eq. (36) and the deep-MOND equation for acceleration should be discussed.

## V. THE RELATION TO MOND

MOND (Modified Newtonian Dynamics), proposed by Mordehai Milgrom in 1983 [5] [6] [7], offers an alternative to dark matter as an explanation for the flattening of galactic-rotation curves. MOND is an algorithm that separates regimes of acceleration according to an empirically-derived constant $a_0$. Gravitational accelerations far above $a_0$ remain Newtonian, whereas accelerations far below $a_0$, termed the "deep-MOND regime",

taper to the following relation:

$$a = \frac{\sqrt{a_0 m G}}{r} \ . \tag{38}$$

An interpolation function mathematically bridges the Newtonian and deep-MOND regimes. Milgrom's initial estimate of $a_0$ was slightly higher than the accepted value of 1.2E−10 m s$^{-2}$, originally estimated by Begeman et al. in 1991 [8]. Interestingly, $a_0$ has not materially wavered from this value in the ensuing decades since the early 1990s, even as the catalog of galaxies with measurable rotation curves has vastly expanded.

Note the congruence between Eqs. (38) and (36), with both having an acceleration $a \propto \sqrt{mG}/r$. Both of these equations satisfy the Baryonic Tully-Fisher Relation (BTFR), which holds that $v^4 \propto m$ [9] [10] [11]:

$$\begin{aligned} \frac{v^2}{\cancel{r}} &= a = \frac{\sqrt{a_0 m G}}{\cancel{r}} \ , \\ v^4 &= a_0 m G \ . \end{aligned} \tag{39}$$

In this relation, $v$ is the speed of a particle in circular orbit around a galaxy of mass $m$—at the outer edge where the Newtonian component is a small fraction of the net acceleration. The rotation curve, given by this relation, mathematically flattens out—as speed is independent of distance.

Three predictions stem from MOND: The rotation curves of isolated galaxies flatten out. The speed at the flat end of rotation curves raised to the power of four is proportional to the galaxy mass, and the constant $a_0$ demarks the transition to the non-Newtonian acceleration regime. These are specific predictions that leave MOND and the BTFR very exposed to falsification. Extensive galaxy surveys, however, repeatedly find MOND to be consistent with observations, and this holds for low-mass and high-mass galaxies with varying levels of surface brightness [12] [13] [14] [15] [16].

Another striking confirmation of the flatness prediction comes from a recent paper where the authors used weak-gravitational-lensing data from the KiDS survey to construct the extended rotation curves of isolated galaxies [17], which seem to remain flat even out to 1 Mpc with no sign of decline! This may prove to be disruptive to the mainstream understanding of the cosmos, which has traditionally been informed by rotation curves that typically extend out to tens of kpc.

Put succinctly, "If the universe is made of cold dark matter, why does MOND get any predictions right?" [18] It seems highly unlikely that the predictive successes of MOND are mere coincidences, but on the contrary, an admonition that our understanding of gravity in the low-acceleration regime is likely incomplete. In this respect, the BTFR and MOND serve as important guidestones along the path to a more complete comprehension of nature—on par with Kepler's discovery that the planets have elliptical orbits.

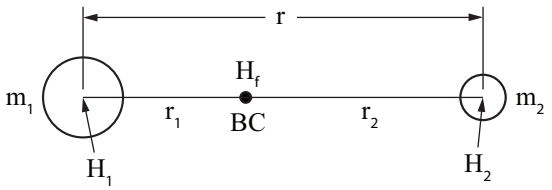


FIG. 4.

## VI. TWO-BODY SYSTEM

Fig. 4 shows a two-body system with masses $m_1$ and $m_2$, separated by distance $r$, with barycenter BC; and where $m_1$ is of larger mass than $m_2$. With Eq. (37), the attractive force between the two masses is thus:

$$F_1 = m_1 \left( \frac{m_2 G}{r^2} + \frac{2\sqrt{c H_2 m_2 G}}{r} \right) \ , \tag{40}$$

$$F_2 = m_2 \left( \frac{m_1 G}{r^2} + \frac{2\sqrt{c H_1 m_1 G}}{r} \right) \ , \tag{41}$$

$$F_1 = F_2 \ . \tag{42}$$

$F_1$ is the magnitude of the force on $m_1$ by $m_2$'s gravitational field, and vice versa for $F_2$. $F_1$ and $F_2$ must be equivalent, as vectorially, they are opposed and must cancel according to Newton's Third Law of Motion—which is to say, the momentum of the system must be conserved.

$H_2$, in Eq. (40), refers to the local expansion parameter at $m_2$; and conversely, $H_1$, in Eq. (41), refers to the local expansion parameter at $m_1$. For $F_1$ to be equivalent to $F_2$, $H_1$ and $H_2$ must differ, which will shortly be clear.

Here, it's posited that the frame of reference comprising the $m_1$–$m_2$ system has an expansion parameter $H_f$, where $H_1$ and $H_2$ are linear functions of $H_f$ as follows:

$$H_1 = k_1 H_f \ , \tag{43}$$

$$H_2 = k_2 H_f \ , \tag{44}$$

where $k_1$ and $k_2$ are constants.

With these relations, equating $F_1$ and $F_2$, gives the following:

$$\begin{aligned} m_1 \left( \frac{m_2 G}{r^2} + \frac{2\sqrt{c k_2 H_f m_2 G}}{r} \right) &= \\ m_2 \left( \frac{m_1 G}{r^2} + \frac{2\sqrt{c k_1 H_f m_1 G}}{r} \right) \ , & \\ \cancel{\frac{m_1 m_2 G}{r^2}} + \frac{2 m_1 \sqrt{c k_2 H_f m_2 G}}{r} &= \\ \cancel{\frac{m_2 m_1 G}{r^2}} + \frac{2 m_2 \sqrt{c k_1 H_f m_1 G}}{r} \ , & \end{aligned}$$

which, in turn, reduces to:

$$\begin{aligned}
\frac{2m_1\sqrt{k_2 H_f m_2 G}}{r} &= \frac{2m_2\sqrt{k_1 H_f m_1 G}}{r} \ , \\
m_1\sqrt{k_2 m_2} &= m_2\sqrt{k_1 m_1} \ , \\
\sqrt{m_1 k_2} &= \sqrt{m_2 k_1} \ , \\
\frac{k_1}{k_2} &= \frac{m_1}{m_2} \ . \qquad (45)
\end{aligned}$$

Taking the ratio of Eqs. (43) and (44) and plugging Eq. (45) into the result, yields this:

$$\frac{H_1}{H_2} = \frac{m_1 H_f}{m_2 H_f} \ , \qquad (46)$$

$$H_1 = k m_1 H_f \ , \qquad (47)$$

$$H_2 = k m_2 H_f \ . \qquad (48)$$

Eqs. (47) and (48) show that the expansion parameter at each mass is proportional to that mass. In separating these two equations from Eq. (46), a new constant $k$ is introduced—noting that the $k$s would cancel upon retaking the ratio of $H_1$ and $H_2$. Adding Eqs. (47) and (48) together gives this:

$$H_1 + H_2 = k(m_1 + m_2)H_f \ . \qquad (49)$$

If the sum of the local expansion parameters in the frame is set equal to the expansion parameter of the frame $H_f$, Eq. (49) can be solved for $k$:

$$H_1 + H_2 = H_f \ , \qquad (50)$$

$$1 = k(m_1 + m_2) \ , \qquad (51)$$

$$k = \frac{1}{m_1 + m_2} \ . \qquad (52)$$

The correctness of Eq. (50) will become more evident as the discussion continues. With this relation for $k$, Eqs. (47) and (48) can be rewritten as functions of the frame's expansion parameter $H_f$ and the masses in that frame:

$$H_1 = \frac{m_1}{m_1 + m_2} H_f \ , \qquad (53)$$

$$H_2 = \frac{m_2}{m_1 + m_2} H_f \ . \qquad (54)$$

What these relations are revealing is that the masses in a system govern the rates of expansion seen by the particles in that system. The expansion rate, however, given by Eq. (28)—which underpins the acceleration and force equations that follow—has no mass terms and is a function of distance! The next step is to reconcile Eqs. (53) and (54) with Eq. (28).

In Fig. 4, distances $r_1$ and $r_2$ are related to $m_1$ and $m_2$ as follows:

$$\frac{r_1}{r_2} = \frac{m_2}{m_1} \ . \qquad (55)$$

This ratio holds regardless of the motions of these masses. Whether they are in circular orbits, eccentric orbits, or accelerating toward each other in a straight line, the barycenter of $m_1$ and $m_2$ maintains the ratio given by Eq. (55). Versions of this equation with $r$ in the denominator of the distance ratio are deduced as follows:

$$\begin{aligned}
\frac{r_1}{r_2} + 1 &= \frac{m_2}{m_1} + 1 \ , \\
\frac{r_1}{r_2} + \frac{r_2}{r_2} &= \frac{m_2}{m_1} + \frac{m_1}{m_1} \ , \\
\frac{r_1 + r_2}{r_2} &= \frac{m_1 + m_2}{m_1} \ , \\
\frac{r_2}{r} &= \frac{m_1}{m_1 + m_2} \ , \qquad (56) \\
\frac{r_1}{r} &= \frac{m_2}{m_1 + m_2} \ . \qquad (57)
\end{aligned}$$

Applying Eq. (28) to the two-body system of Fig. 4, gives the expansion rates at $m_1$ and $m_2$:

$$v_1 = r H_2 \ , \qquad (58)$$

$$v_2 = r H_1 \ . \qquad (59)$$

With $m_2$ as an origin, space expanding from this point has an expansion rate of $v_1$ as measured at $m_1$. This is embodied by Eq. (58). Likewise, Eq. (59) gives the expansion rate $v_2$ relative to $m_1$—as seen by $m_2$.

Here, it's postulated that the expansion rate $v_1$ measured at $m_1$ should be consistent at a given point in time, regardless of the chosen origin along the line of expansion. This would likewise hold for $v_2$ as measured at $m_2$. In other words, **the expansion rate measured at a point in a reference frame—in a particular direction at a point in time—should be invariant with respect to an arbitrary origin of expansion along the line of measurement**.

Further, referring back to Eq. (27), the idea—that $dr/dt$ ($v_1$ and $v_2$ in the present example) relative to a reference mass should be consistent—is required by this equation, which relates a physical effect $d\Delta E/dt$ to an expansion rate $dr/dt$. It doesn't make sense that this physical effect should change as a result of choosing different coordinates.

Thus, with the barycenter set as the origin of expansion, the following relations can be written:

$$v_1 = r_1 H_f \ , \qquad (60)$$

$$v_2 = r_2 H_f \ . \qquad (61)$$

Notice that Eqs. (60) and (61) are functions of $H_f$, the expansion parameter at the barycenter, which is the same origin for both observers $m_1$ and $m_2$. Contrast this with the case above for Eqs. (58) and (59), where the observers see expansion rates from different perspectives and origins.

Equating Eqs. (58) and (59) with Eqs. (60) and (61)

distills as follows:

$$rH_2 = r_1 H_f \ , \tag{62}$$
$$rH_1 = r_2 H_f \ , \tag{63}$$
$$H_1 = \frac{r_2}{r} H_f \ , \tag{64}$$
$$H_2 = \frac{r_1}{r} H_f \ , \tag{65}$$
$$H_1 = \frac{r_2}{r_1} H_2 \ . \tag{66}$$

Plugging Eqs. (56) and (57) into Eqs. (64) and (65), recovers Eqs. (53) and (54):

$$H_1 = \frac{m_1}{m_1 + m_2} H_f \ , \tag{67}$$
$$H_2 = \frac{m_2}{m_1 + m_2} H_f \ . \tag{68}$$

Thus, given a two-body system of masses $m_1$ and $m_2$, with a frame of reference at the barycenter—with the frame having an expansion parameter of $H_f$, Eqs. (53) and (54) give the local expansion parameters at $m_1$ and $m_2$, respectively. As demonstrated, these local expansion parameters are functions of barycenter distances, which in turn are functions of mass. Importantly, these relations allow the force vectors—on $m_1$ by $m_2$ and conversely, on $m_2$ by $m_1$—to cancel, avoiding a possible inconsistency.

In somewhat of a leap, the above equations for a two-body system are generalized for an n-body system. Evidence to support this extrapolation will build in the following sections. The general form of Eqs. (53) and (54) is thus:

$$H_r = \frac{m_r}{m_t} H_f \ . \tag{69}$$

Eq. (69) relates the expansion parameter $H_r$ at the barycenter of a reference mass $m_r$ (or collection of masses) to that of another mass or collection of masses $m_t$, where $H_f$ is the expansion parameter at the barycenter of $m_t$. $m_t$ may include $m_r$, in which case, $H_f$ is the expansion parameter at the barycenter of the entire system.

With Eqs. (37) and (69), a general relation for the magnitude of acceleration relative to a reference mass $m_r$, in an n-body system of total mass $m_t$, is as follows:

$$\begin{aligned} a_n &= \frac{m_r G}{r^2} + \frac{2\sqrt{c H_r m_r G}}{r} \ , \\ a_n &= \frac{m_r G}{r^2} + \frac{2 m_r \sqrt{c H_f G}}{r\sqrt{m_t}} \ , \\ a_n &= \frac{m_r G}{r} \left( \frac{1}{r} + \frac{2\sqrt{c H_f}}{\sqrt{m_t G}} \right) \ . \end{aligned} \tag{70}$$

With the arguments surrounding Eqs. (60)–(66), Eq. (50) is assumed to have been correct. Extending this relation to the general case gives this:

$$H_f = \sum_{i=1}^{n} H_i \ . \tag{71}$$

Eq. (71) shows that in a system of $n$ bodies with an expansion parameter of $H_f$ at the barycenter, the sum of local expansion parameters for these bodies is equivalent to $H_f$.

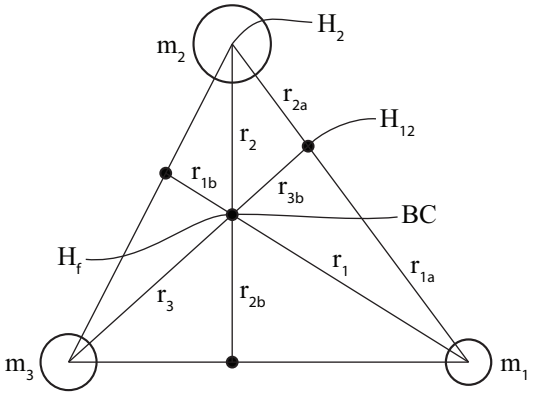


FIG. 5.

## VII. THREE-BODY SYSTEM

As a quick sanity check of the n-body-system equations, the concepts from the last section are applied to a three-body system and checked for consistency. Fig. 5 shows a three-body system of dissimilar masses. The center dot in the triangle marks the barycenter BC of the system, and the dots on the edges denote the centers of mass of the two bodies along each edge. The relations between distances and masses in this figure can be written as follows:

$$\frac{r_3}{r_{3b}} = \frac{m_1 + m_2}{m_3} \ , \tag{72}$$
$$r_{3c} = r_3 + r_{3b} \ , \tag{73}$$
$$r_{3c} = \left( \frac{m_1 + m_2}{m_3} \right) r_{3b} + r_{3b} \ , \tag{74}$$
$$r_{3c} = \left( \frac{m_1 + m_2}{m_3} + \frac{m_3}{m_3} \right) r_{3b} \ , \tag{75}$$
$$\frac{r_{3b}}{r_{3c}} = \frac{m_3}{m_1 + m_2 + m_3} \ , \tag{76}$$
$$\frac{r_3}{r_{3c}} = \frac{m_1 + m_2}{m_1 + m_2 + m_3} \ . \tag{77}$$

Equating rates of expansion at $m_3$ along the line ex-

tending from $H_{12}$ gives this:

$$v_3 = (r_3 + r_{3b})H_{12} \ , \tag{78}$$
$$v_3 = r_3 H_f \ , \tag{79}$$
$$H_{12} = \frac{r_3}{r_3 + r_{3b}} H_f \ . \tag{80}$$

Plugging Eq. (77) into Eq. (80) yields this:

$$H_{12} = \frac{m_1 + m_2}{m_1 + m_2 + m_3} H_f \ . \tag{81}$$

With $H_{12}$ marking the barycenter of $m_1$ and $m_2$, distance is related to mass as follows:

$$\frac{r_{1a}}{r_{2a}} = \frac{m_2}{m_1} \ , \tag{82}$$
$$\frac{r_{1a}}{r_{1a} + r_{2a}} = \frac{m_2}{m_1 + m_2} \ . \tag{83}$$

With a definition for $H_{12}$, the expansion parameter at $m_2$ can also be determined via the expansion rate at $m_1$:

$$v_1 = (r_{1a} + r_{2a})H_2 \ , \tag{84}$$
$$v_1 = r_{1a} H_{12} \ , \tag{85}$$
$$H_2 = \frac{r_{1a}}{r_{1a} + r_{2a}} H_{12} \ . \tag{86}$$

Plugging Eqs. (81) and (83) into Eq. (86) is thus:

$$H_2 = \frac{m_2}{\cancel{m_1 + m_2}} \frac{\cancel{m_1 + m_2}}{m_1 + m_2 + m_3} H_f \ ,$$
$$H_2 = \frac{m_2}{m_1 + m_2 + m_3} H_f \ . \tag{87}$$

Note the congruency between this equation and the general local-expansion relation given by Eq. (69), where $H_2$ is the expansion parameter at reference mass $m_2$. With Eq. (69) satisfied, agreement with Eq. (70) follows when $H_2$ is plugged into Eq. (37):

$$m_t = m_1 + m_2 + m_3 \ ,$$
$$H_r = \frac{m_2}{m_t} H_f \ ,$$
$$a_n = \frac{m_2 G}{r^2} + \frac{2\sqrt{c m_2 H_f m_2 G}}{r\sqrt{m_t}} \ ,$$
$$a_n = \frac{m_2 G}{r} \left( \frac{1}{r} + \frac{2\sqrt{c H_f}}{\sqrt{m_t G}} \right) \ .$$

Agreement with Eq. (71) is also observed upon taking the sum of the expansion parameters at the three masses. Note, the relations $H_1$ and $H_3$ below are readily derived with the same approach used for $H_2$:

$$H_1 = \frac{m_1}{m_t} H_f \ ,$$
$$H_2 = \frac{m_2}{m_t} H_f \ ,$$
$$H_3 = \frac{m_3}{m_t} H_f \ ,$$
$$H_1 + H_2 + H_3 = \frac{\cancel{m_t}}{\cancel{m_t}} H_f = H_f \ .$$

Here, the above n-body relations are recovered.

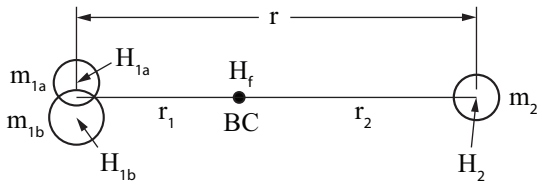


FIG. 6.

## VIII. SPLIT TWO-BODY SYSTEM

Fig. 6 has the same two-body system of Fig. 4 with mass $m_1$ having been split into two unequal parts, $m_{1a}$ and $m_{1b}$. In the figure, visually, the two parts are slightly offset. Mathematically, however, assume they are coincident. Using Eq. (70), the magnitude of the forces between $m_{1a}$, $m_{1b}$, and $m_2$ is thus:

$$m_t = m_{1a} + m_{1b} + m_2 \ ,$$
$$F_{1a2} = \frac{m_{1a} m_2 G}{r} \left( \frac{1}{r} + \frac{2\sqrt{c H_f}}{\sqrt{m_t G}} \right) \ ,$$
$$F_{1b2} = \frac{m_{1b} m_2 G}{r} \left( \frac{1}{r} + \frac{2\sqrt{c H_f}}{\sqrt{m_t G}} \right) \ ,$$
$$F_{12} = \frac{(m_{1a} + m_{1b}) m_2 G}{r} \left( \frac{1}{r} + \frac{2\sqrt{c H_f}}{\sqrt{m_t G}} \right) \ .$$

Looking at the above equations, the individual force on an element of $m_1$ is proportional to its mass, and the sum of those forces equates to the net force $F_{12}$ between $m_1$ and $m_2$, as consistency would demand.

## IX. RESTRICTED THREE-BODY SYSTEM

Fig. 7 shows a restricted three-body system with an isolated two-body system orbiting a relatively large mass. This is the relationship between the Earth, Moon, and the Sun. The force between the Earth and the Moon as calculated in the three-body reference frame, which has an expansion parameter of $H_{f1}$ at the Sun–Earth–Moon

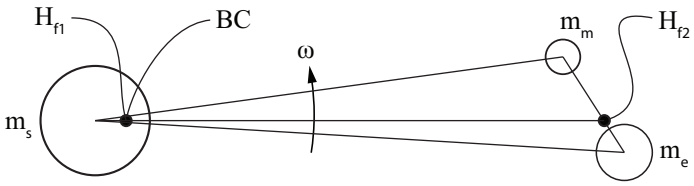


FIG. 7.

barycenter, is thus:

$$F_{em} = \frac{m_e m_m G}{r}\left(\frac{1}{r} + \frac{2\sqrt{cH_{f1}}}{\sqrt{(m_s + m_e + m_m)G}}\right) . \quad (88)$$

In the Earth–Moon reference frame, with an expansion parameter of $H_{f2}$, the force between the Earth and the Moon is this:

$$F_{em} = \frac{m_e m_m G}{r}\left(\frac{1}{r} + \frac{2\sqrt{cH_{f2}}}{\sqrt{(m_e + m_m)G}}\right) . \quad (89)$$

It should be necessary that $F_{em}$, as calculated in either reference frame, should be equivalent. Referring back to Fig. 5, which shows a three-body system with no clear subsystem, the force between masses $m_1$ and $m_2$—as calculated via Eq. (70)—is consistent in both the two-body and three-body frames:

$$\begin{aligned}
H_{12} &= \frac{m_1 + m_2}{m_1 + m_2 + m_3} H_f \ , \\
F_{12a} &= \frac{m_1 m_2 G}{r}\left(\frac{1}{r} + \frac{2\sqrt{cH_{12}}}{\sqrt{(m_1 + m_2)G}}\right) \ , \\
F_{12b} &= \frac{m_1 m_2 G}{r}\left(\frac{1}{r} + \frac{2\sqrt{cH_f}}{\sqrt{(m_1 + m_2 + m_3)G}}\right) \ , \\
F_{12a} &= F_{12b} \ .
\end{aligned}$$

Recall that this derives mathematically by enforcing consistency in the measurement of expansion rates with respect to arbitrary origins of expansion along a given vector. There doesn't seem to be any reason why this consistency should not be applicable in the case where two bodies of Fig. 5 happen to comprise a subsystem. Said another way, as shown by the above equations, the force between two bodies—as calculated in either the two- or three-body frames—is a function of all three masses and doesn't care how these bodies are moving relative to each other or whether they're part of a subsystem or not. Imagine a three-body system with chaotic motions where two bodies split off to form a subsystem. The forces between these bodies should be consistent immediately before and after the formation of this subsystem.

With this understanding, Eq. (88)—the relation for $F_{em}$ in the three-body reference frame—and Eq. (89)—the relation for $F_{em}$ in the two-body subsystem—can be considered equivalent. This, in turn, allows the following relation between the expansion parameter $H_{f1}$ of the three-body frame and the parameter $H_{f2}$ of the two-body frame to be written:

$$\begin{aligned}
\frac{H_{f2}}{m_e + m_m} &= \frac{H_{f1}}{m_s + m_e + m_m} \ , \\
H_{f2} &= \frac{m_e + m_m}{m_s + m_e + m_m} H_{f1} \ . \quad (90)
\end{aligned}$$

As expected, Eq. (90) parallels Eq. (81)—the equation above for $H_{12}$. Further, both Eqs. (81) and (90) are congruent with Eq. (69), restated below, when the reference mass $m_r$, in this equation, comprises two of the three bodies.

$$H_r = \frac{m_r}{m_t} H_f \ .$$

The observation that $m_r$ in Eq. (69) can refer to a subsystem may not seem that interesting, but this actually has an important ramification—external mass can affect the gravitational forces within subsystems! Looking at Eq. (88), the presence of the Sun's mass $m_s$ affects the force *between* the Earth and the Moon. It doesn't affect the Newtonian component of acceleration, which is purely a function of the Earth's and Moon's masses. It does, however, affect the expansion component, which is muted by the presence of the Sun. In actuality, it's muted by the total mass of the Solar System, which comprises the Sun, the planets, and the asteroid belt!

But the Solar System is a subsystem of the Milky Way, and therefore, the mass of the Milky Way must affect the forces within the Solar System—drastically reducing the expansion component relative to the Newtonian component. Traversing further up the hierarchy, the Milky Way is a member of the Local Group, which is, in turn, a member of the Virgo Supercluster, which is part of the Laniakea Supercluster complex.

**To what extent does external mass affect internal systems**? The universe has a lot of mass. Does all of this mass count? As the total system mass $m_t$ in Eq. (70) goes to infinity, the expansion component asymptotically goes to zero. If $m_t$ were set to the net mass of the universe, this effectively would be the case—any non-Newtonian acceleration components in galaxies and clusters of galaxies would be reduced to insignificance. However, we know that galaxies have flat rotation curves, and there are clusters where galaxies are moving too quickly to be bound by Newtonian gravity. If non-Newtonian motion is to be explained by modified gravity—specifically, as it's described by Eq. (70), it's not possible that the expansion parameters of galaxies and clusters are diluted by the entire mass of the universe.

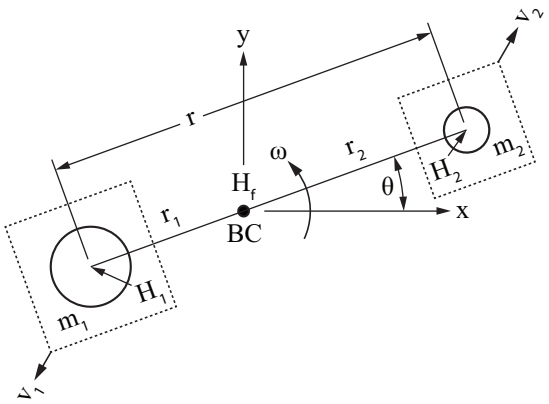


FIG. 8.

## X. EXPANSION PARAMETERS OF MOVING FRAMES

In the above relations, expansion parameters only ever equate to other expansion parameters—via distance or mass. There is no relation that describes expansion in a frame purely as a function of other metrics. So far, the mechanism by which expansion in a frame is manifested is unknown. Understanding this mechanism and how it relates to the expansion of the universe will be necessary to delve deeper into the mystery of flat galactic-rotation curves and the motions of galaxies with respect to each other.

Fig. 8 shows the same two-body system from Fig. 4 with each body having a coincident frame that moves relative to the parent frame—the latter fixed at the barycenter BC of the system. The x and y coordinates of frame two—which is coincident with the barycenter of $m_2$—relative to the BC frame are thus:

$$x = r_2 \cos\theta \ ,$$
$$y = r_2 \sin\theta \ .$$

Taking the derivative of $x$ and $y$ with respect to time gives the following:

$$\dot{x} = \dot{r_2} \cos\theta - r_2 \omega \sin\theta \ ,$$
$$\dot{y} = \dot{r_2} \sin\theta + r_2 \omega \cos\theta \ ,$$

where

$$\omega = \dot{\theta} \ .$$

Taking the sum of the squares of $\dot{x}$ and $\dot{y}$ gives the square of the speed of frame two relative to BC:

$$v_2{}^2 = \dot{x}^2 + \dot{y}^2 \ , \tag{91}$$
$$v_2{}^2 = \dot{r_2}{}^2 + (r_2\omega)^2 \ . \tag{92}$$

Notice here, in Eq. (92), that speed $v_2$ squared is simply the sum of the squares of the radial and transverse components of vector $\vec{v}_2$.

Recall Eq. (55), which gives a relation between distance and mass for this two-body system. Taking the derivative of this equation with respect to time is thus:

$$r_2 = \frac{m_1}{m_2} r_1 \ ,$$
$$\dot{r_2} = \frac{m_1}{m_2} \dot{r_1} \ .$$

Plugging these equations into Eq. (92) gives this:

$$v_2 = \frac{m_1}{m_2} \sqrt{\dot{r_1}{}^2 + (r_1\omega)^2} \ .$$

With $r_1$ substituted for $r_2$, the speed of frame one—which is coincident with the barycenter of $m_1$—relative to the BC frame is similar to $v_2$:

$$v_1 = \sqrt{\dot{r_1}{}^2 + (r_1\omega)^2} \ .$$

Taking the ratio of the above two speed equations gives a result that intuitively parallels Eq. (55):

$$\frac{v_2}{v_1} = \frac{m_1}{m_2} \frac{\cancel{\sqrt{\dot{r_1}{}^2 + (r_1\omega)^2}}}{\cancel{\sqrt{\dot{r_1}{}^2 + (r_1\omega)^2}}} \ , \tag{93}$$
$$\frac{v_1}{v_2} = \frac{m_2}{m_1} \ . \tag{94}$$

Akin to Eq. (55), Eq. (93)—wherein the radial and transverse components of $\vec{v}_1$ and $\vec{v}_2$ cancel—shows that the ratio of $v_2$ to $v_1$ is irrespective of the paths of motion. Eq. (93) distills to Eq. (94), which shows that the relative speed between bodies one and two (and thus frames one and two) is purely a function of their masses.

Again, Eq. (94) is a natural extension of Eq. (55). If the distances relative to the barycenter of a system are a function of mass, then it follows that the derivatives of those distances—specifically, the derivatives of the distance vectors—with respect to time should obey the same relation. With this in mind, in general, if expansion parameters can be related via distance, they should also be relatable via speed.

Eq. (69) can be used to derive the ratio between the expansion parameters at $m_1$ and $m_2$:

$$H_1 = \frac{m_1}{m_t} H_f \ , \tag{95}$$
$$H_2 = \frac{m_2}{m_t} H_f \ , \tag{96}$$
$$\frac{H_1}{H_2} = \frac{m_1}{m_2} \ , \tag{97}$$
$$H_1 = \frac{m_1}{m_2} H_2 \ . \tag{98}$$

Similar to Eq. (69), Eqs. (97) and (98) can be regarded as general relations that relate the expansion parameter $H_1$ at the barycenter of $m_1$—representing a mass or collection of masses—to the expansion parameter $H_2$ at the

barycenter of $m_2$—representing a second mass or collection of masses.

Plugging Eq. (94) into Eq. (98), relates expansion parameters to relative speeds:

$$\frac{H_1}{H_2} = \frac{v_2}{v_1} \,, \tag{99}$$

$$H_1 = \frac{v_2}{v_1} H_2 \,. \tag{100}$$

The interpretation of Eq. (100) is thus: An observer in reference frame two, moving with respect to a common frame at BC, would measure a different expansion parameter relative to $m_1$ than would an observer in reference frame one relative to $m_2$—when their speeds differ—with the ratio of measured expansion parameters being equivalent to the ratio of their relative speeds.

Recognizing that speeds $v_1$ and $v_2$ are relative to BC—which is to say, relative to this common frame, Eq. (99) can be extended as follows:

$$\frac{H_1}{H_2}\frac{r_f}{r_f} = \frac{v_2}{v_1} \,, \tag{101}$$

$$H_1 = \frac{v_2}{r_f} \,, \tag{102}$$

$$H_2 = \frac{v_1}{r_f} \,. \tag{103}$$

Here, an abstract parameter $r_f$, termed the "frame size", with the units of distance, is introduced. As will become evident, this factor is dynamic and is a function of speed and mass. However, for a given collection of bodies, $r_f$ is a function of speed with respect to the barycenter of that collection. When the speeds in Eqs. (102) and (103) are taken with respect to a common frame, the frame size $r_f$ is equivalent for both observers. This isn't to say $r_f$ necessarily remains constant over time. It can vary, but it varies by the same amount for both observers such that they always agree on its value.

If, for the sake of argument, the speed of frame one were taken directly relative to frame two and vice versa, an observer in each frame would measure the same relative speeds. These observers, however, would not be moving relative to a common frame, and thus, $r_f$ in Eqs. (102) and (103) would not be equivalent.

Because $H_1$ and $H_2$ are also functions of mass and are constant with respect to the expansion parameter of the common frame—$H_f$, $r_f$, in Eqs. (102) and (103) must vary with speed. This is illustrated by equating Eqs. (95) and (96) with Eqs. (102) and (103), respectively:

$$\frac{m_1}{m_t} H_f = \frac{v_2}{r_f} \,, \tag{104}$$

$$\frac{m_2}{m_t} H_f = \frac{v_1}{r_f} \,, \tag{105}$$

$$r_f = \frac{m_t}{H_f}\frac{v_2}{m_1} = \frac{m_t}{H_f}\frac{v_1}{m_2} \,. \tag{106}$$

As demonstrated by Eq. (106), for the left side of Eqs. (104) and (105) to remain constant, the frame size $r_f$ must increase and decrease in concert with speed. The greater the speed, the larger the frame size. This concept will be revisited below when the redshift of light is considered from the perspective of a moving reference frame.

Eq. (106) also describes $r_f$ in terms of the parent frame's expansion parameter $H_f$ and mass. Notice that as $H_f$ goes to zero, the frame size $r_f$ goes to infinity, which results in local expansion parameters $H_1$ and $H_2$ going to zero in concert with $H_f$.

With the above concepts in mind, a general set of relations for moving frames is as follows:

$$H_f = \frac{v_f}{r_f} \,, \tag{107}$$

$$r_f = \frac{v_f}{k_f m_r} \,, \tag{108}$$

$$k_f = \frac{H_i}{m_i} = \frac{H_f}{m_t} \,. \tag{109}$$

Eq. (107) can be interpreted as thus: For an observer moving relative to a parent frame at a speed of $v_f$, there exists a frame size $r_f$ such that the ratio of $v_f$ to $r_f$ gives the expansion parameter $H_f$ of the moving frame. Another observer, moving relative to the same parent frame with a speed of $v_{f2}$, for example, would see a different expansion parameter equal to the ratio of $v_{f2}$ to $r_f$.

Recognize that Eq. (107) is essentially Hubble's law (Eq. (28)) with the parameters having been rearranged, but these two equations and their parameters have different interpretations. In Eq. (28), $\vec{v}$ is the velocity at which space—with an expansion parameter of $H_l$—expands at a distance of $\vec{r}$. In contrast, under Eq. (107), expansion parameters are functions of speed and frame size. Also, in contrast to Eq. (28)—where $\vec{v}$ and $\vec{r}$ are vectors, all of the parameters in Eq. (107) are scalars. Speed $v_f$ and frame size $r_f$, in this equation, have no direction.

All of the parameters in Eq. (28) are measured in the same reference frame, and the same situation applies to Eq. (107), where all parameters are measured in the parent frame. Speed $v_f$ of the moving frame can be thought of as a scalar property of the moving frame relative to the parent frame. Likewise, $H_f$ is also a scalar property of the moving frame that relates to the parent frame through frame size $r_f$. Inasmuch as every point in the moving frame will have the same speed $v_f$ relative to the parent frame, any given point in the moving frame will have the same expansion parameter $H_f$. Interestingly, however, with a point established in the moving frame as having an expansion parameter of $H_f$, a second point at a certain distance will *not* have the same expansion parameter. This phenomenon will be discussed in detail in Section XVIII.

Generally, in the case where there is a frame moving relative to a rest frame, the relativistic effects of time dilation and length contraction need to be considered—especially as speeds approach $c$. However, because all of the parameters in Eq. (107) are measured in the rest frame (or parent frame), relativistic effects are not of

concern here.

Eq. (108) defines $r_f$ as a function of the frame speed $v_f$, a reference mass $m_r$, and a constant $k_f$, termed the "frame constant". For a given frame constant and reference mass, **the frame size $r_f$ with respect to an observer is dynamic and linearly proportional to the observer's speed $v_f$ relative to the frame**. In the two-body system of Fig. 8, for example, from the perspective of either moving frame, $r_f$ changes in proportion to any change in speed relative to BC. As shown by Eq. (106), both frames always agree on the value of $r_f$.

Eq. (109) defines frame constant $k_f$—which has the units of ($kg^{-1}s^{-1}$)—as expansion parameter per unit mass. As evidenced by Eqs. (69) and (98), **no matter how the mass in a system is divided, this ratio holds**. It's postulated that this applies to all systems—from a simple two-body system to a massive spiral galaxy. For example, a two-body child system within a galaxy would share the same frame constant as that of the parent galaxy. In essence, $k_f$ can be thought of as a state that applies equally to the system as a whole or any subsystem or element thereof.

This state is a function of mass and expansion parameter, and one metric can vary independently of the other. It's concluded, therefore, that **the expansion parameter of a frame is a property of the frame irrespective of the mass contained therein**.

Further, looking at the relation for $k_f$, the internal dynamics of the system within the frame are immaterial. It's concluded, therefore, that **the positions of particles in a system within a parent frame and the motions of those particles relative to that frame have no bearing on the frame's expansion parameter**.

Interestingly, $1/k_f$ has the units of mass-time (kg-s), which seems to be somewhat unique. The Planck constant, which has the units of action, is similar—with units of (J-s). The uncertainty principle, which employs this constant, can be rearranged to give units of mass-time as follows:

$$\Delta E \Delta t \geq \frac{\hbar}{2} \, ,$$
$$\Delta m \Delta t \geq \frac{\hbar}{2c^2 \Delta t} \, .$$

One possible deduction is that the frame constant $k_f$, based on its units, is related to action.

Eqs. (107)–(109) align with the observation made at the beginning of the section that expansion parameters only ever relate to other expansion parameters—as $k_f$ is a function of expansion parameter. While earlier discussions focused on relating expansion parameters via mass and distance, they may also be related through speed—an important concept that will prove to be integral in the following sections.

## XI. THE EXPANSION PARAMETER—AS SEEN BY LIGHT

Continuing the line of reasoning from the previous section, the following question is posed: Can the expansion parameter seen by light be examined in the context of a photon traveling in a frame moving relative to a parent frame?

The standard interpretation of redshift is as follows: As a photon travels through space, over time, the expansion of space stretches the photon—increasing its wavelength. Increasing distance (and time) correlates with increasing redshift as described here:

$$v = \dot{r} = rH_0 \, , \tag{110}$$
$$\dot{\lambda} = \lambda H_0 \, . \tag{111}$$

Eq. (110) is Hubble's law, and Eq. (111) is Hubble's law applied to light, where $\lambda$ is the emitted wavelength.

Given the arguments of the previous section, an alternative interpretation is that $H_0$ is the expansion parameter of a photon in a moving frame as a *result* of moving at $c$ relative to a parent frame. In either point of view, the photon is stretched over time *and distance* according to $H_0$, which is a literal description of observed redshift that is agnostic of an underlying mechanism. Under this alternative interpretation, Eq. (110) is rearranged akin to Eq. (107) such that $H_0$ is a function of speed $c$ and frame size $r_0$:

$$H_0 = \frac{c}{r_0} \, . \tag{112}$$

The interpretation of Eq. (112) is thus: A photon in a moving frame—traveling at $c$ relative to a parent frame with a frame size of $r_0$—has an expansion parameter of $H_0$. In the previous section, with regard to Eq. (107), the frame size was defined as an abstract parameter. Is this still the case for Eq. (112)? What does $r_0$ actually represent?

This will be covered in detail in Section XV, but in the case where $v_f$, in Eq. (107), goes to the extent of speed in the universe—$c$, $H_f$ goes to the extent of expansion parameter—$H_0$, and $r_f$ goes to the extent of distance—$r_0$. At the other extreme—where $v_f$ goes to zero, both $H_f$, and $r_0$ go to zero. While $r_f$ is abstract, at these two extents, it corresponds to a physical distance.

Thus, if $H_0$ demarks the expansion parameter of the universe, it's surmised that $r_0$ represents the size of the universe. When terms of Eq. (112) are arranged according to Eq. (110), its interpretation changes: $c$ is the rate at which space expands at a distance of $r_0$—where the universe has an expansion parameter of $H_0$. Both interpretations are deemed to be correct. Therefore, it's concluded that the universe is expanding at $c$.

Eqs. (107) and (112) further suggest that a frame moving at a subluminal speed relative to the same parent frame in which light travels (which is the frame of the universe) would also have an expansion parameter—and

one that would be less than $H_0$. Because—as discussed in the previous section—both $r_f$ *and* $H_f$ vary with speed, the expansion parameter $H_f$ as seen by a frame moving at a subluminal speed $v_f$ in the universe is unclear. And what is meant by a speed "relative to the universe"? Does the universe have a frame? This topic and the reconciliation of $H_f$ with $H_0$ will be addressed in the following sections.

#### 1. *Hubble time*

Taking the inverse of $H_0$ gives the age of the universe. The estimated age of the universe is 13.787 billion years [4], which, working backwards, translates to a Hubble parameter equal to:

$$t = 13.787 \times 10^9 \,\mathrm{yr} \Rightarrow 435.075 \times 10^{15} \,\mathrm{s} \;,$$
$$H_0 = 2.298 \times 10^{-18} \,\mathrm{m\,s^{-1} m^{-1}} \;,$$
$$H_0 = 70.92 \,\mathrm{km\,s^{-1} Mpc^{-1}} \;.$$

This relationship is well known, and the inverse of the Hubble parameter is termed the "Hubble time". Recent measurements of the Hubble parameter vary based on the chosen method, but they tend to fall within this range: 67-74 km s$^{-1}$ Mpc$^{-1}$ [19] [20], which averages to 70.5 km s$^{-1}$ Mpc$^{-1}$. Early-universe techniques place $H_0$ at the low end of the range, whereas late-universe analyses pin $H_0$ towards the upper end. The discrepancy between these results is termed the "Hubble tension". Combining a variety of late-universe methods, places $H_0$ towards the upper-middle of the range—72 Â± 8 km s$^{-1}$ Mpc$^{-1}$ [21].

The definition of $H_0$—and the derivative thereof with respect to time—as a function of Hubble time $t_0$ is as follows:

$$H_0 = \frac{1}{t_0} \;, \tag{113}$$

$$\frac{dH_0}{dt} = \frac{-1}{{t_0}^2} \frac{\cancel{dt_0}^{\,1}}{\cancel{dt}} \;, \tag{114}$$

$$\dot{H_0} = -{H_0}^2 \;. \tag{115}$$

Here, $t_0$ is the proper time in an inertial rest frame. Both $dt_0$ and $dt$ are measured in the same frame and are thus equivalent. Notice that the subscript 0 in $t_0$, $H_0$, and $r_0$ refers to the current values of each parameter in the inertial reference frame.

It seems highly unlikely that the agreement between the Hubble time and the estimated age of the universe is *simply* an interesting coincidence. The most straightforward explanation is that time and the expansion of the universe are directly related—as described by Eq. (113). Otherwise, it must be presumed that the trajectory of time happens to have intersected the trajectory of the universe's expansion parameter—where one is the inverse of the other—at precisely the point where humanity has the capability of measuring both quantities.

Returning to the discussion of $r_0$ in Eq. (112), taking the derivative of Eq. (112) vs. time gives the following:

$$\frac{d}{dt}(H_0) = \frac{d}{dt}\left(\frac{c}{r_0}\right) \;, \tag{116}$$

$$-{H_0}^2 = -\frac{c}{{r_0}^2}\dot{r_0} \;, \tag{117}$$

$$(r_0 H_0)^2 = c\dot{r_0} \;, \tag{118}$$

$$c^2 = c\dot{r_0} \;, \tag{119}$$

$$\dot{r_0} = c \;. \tag{120}$$

The first derivative of $H_0$ with respect to time—which was defined by Eq. (115)—is plugged into Eq. (116), which thus distills to Eq. (120). This latter equation shows that $r_0$ expands at $c$; and further, because the rate is constant, $r_0$ has *always* been expanding at $c$. As mentioned, it's posited that $r_0$ defines the size of the universe. It's further imagined that all observers, in their rest frames, see $r_0$ as expanding at $c$; and from the perspective of these observers, a universe expanding at $c$ would appear to be of infinite size.

## XII. TIME-DRIVEN COSMOLOGY

The idea that the universe is describable by constant, linear expansion at $c$ is referred to as "coasting cosmology". This is not a new idea [22][23]. Constant, linear expansion at $c$ is a stark contrast to the evolution of the universe prescribed by ΛCDM—the current standard model of cosmology, which holds that there was a brief period of exponential expansion—termed "inflation"—immediately after the Big Bang. Inflation ostensibly solves the "flatness problem".

The flatness problem is as follows: In order for the present universe to be spatially flat—which has been confirmed by numerous experiments [4][24][25]—the ratio of the total energy density to the critical density at the birth of the universe must have been equal to one—out to 59 decimal places [26]. Any deviation from this initial condition would've been magnified many times over as the universe expanded—either resulting in the universe quickly collapsing in on itself or expanding exponentially—and the flat universe we know wouldn't exist. Moreover, without the critical density of the early universe having been fine-tuned, *we* wouldn't exist to be able to contemplate it.

Flatness is typically gauged by the spatial-curvature density, or $\Omega_K$, where $\Omega_K = 1 - \Omega$ and $\Omega$ is the total-energy density parameter—the ratio of total density to the critical density. The Planck results, for example, measure $\Omega_K$ at 0.001Â±0.002 [4]. During inflation, which lasted from 10E-36 to 10E-32 seconds, the universe—expanding many times the speed of light—grew from the size of a proton to the size of a grapefruit, which, in effect, drives $\Omega_K$ to zero [27][28].

Within that first nanosecond after the birth of the universe, inflation ends as abruptly as it starts, and

for 10 billion years—according to ΛCDM—the universe expanded roughly linearly but started to accelerate in growth thereafter as the total density transitioned from being dominated by matter—comprising dark and baryonic matter—to dark energy. Current estimates hold that the energy of the universe is comprised of: mostly dark energy—at 70%, dark matter at 25%, and ordinary "baryonic" matter at only 5% [29].

Here, an alternative cosmological model called "Time-Driven Cosmology" is proposed with a flat spacetime—where, in every reference frame, the universe expands linearly at the speed of light. The universe expands forever at $c$ while the expansion parameter of the universe, $H_0$, asymptotically tapers to zero—as shown by Eq. (115) above. This happens *not* because the universe contains the exact amount of mass needed to slow the expansion parameter to zero after an infinite amount of time, but because the inverse of time *mathematically* tapers to zero.

Similarly, space doesn't expand as a consequence of energy density. The opposite is true: Energy is created as a consequence of the expansion of space, which, in turn, is purely a function of time. As space expands, energy is borrowed from the vacuum in concert, which ultimately manifests as the mass that comprises the material structure of the universe. The good news is: Because the universe will never stop expanding, the loan never has to be repaid!

Special relativity sets a speed limit of $c$ to all motion in the universe that conveys information. The implication is that in a universe that obeys this speed limit, information can never be lost or destroyed. A given particle, regardless of distance, can never travel faster than the information flow from a second particle. Space—as the medium for fields and light, which is to say information—should also be subject to this limit. Photons traveling from one point in space to another—if the space between those points were expanding faster than $c$—would be redshifted to an infinitely long wavelength, which would effectively destroy the information carried by those photons.

It's posited that our universe is describable by special relativity—where all events that have led to the present structure of the universe fall within the light cone that extends from the initial event that gave birth to the universe—ostensibly, the Big Bang. All events are time-like related and can be traced back to this initial event.

## XIII. THE HUBBLE FRAME

Under the principle that there should be no preferred frame, all observers in their respective rest frames should see the most distant coordinate—which demarks the size of the universe $r_0$—receding at $c$. More generally, in all frames, an observer should see a given coordinate receding at a speed between 0 and $c$ that varies linearly with distance. In addition, the recessional speed $v$ between any two coordinates should be seen as a constant over time as shown here:

$$v = rH_0 \ , \tag{121}$$

$$\frac{dv}{dt} = \frac{dr}{dt}H_0 + r\frac{dH_0}{dt} \ , \tag{122}$$

$$\dot{v} = r{H_0}^2 - r{H_0}^2 \ , \tag{123}$$

$$\dot{v} = 0 \ . \tag{124}$$

At a given distance $r$ between any two points in space, that distance expands according to Eq. (110), which is Hubble's law. Taking the derivative of Eq. (110) with respect to time gives Eq. (121). Plugging in Eq. (115) gives Eq. (122), which shows that the rate of speed increase at a given $H_0$ is canceled by the rate of $H_0$ decrease at a given distance—leaving the recessional speed constant over time. It stands to reason that if the most distant coordinate recedes at the constant rate of $c$, intermediate coordinates should recede at constant rates as well.

Bodies that move in sync with these receding coordinates—also referred to as "comoving" coordinates—are said to be moving in the "Hubble flow". This system of receding coordinates can be imagined as the cosmic rest frame or the "Hubble frame" for short. A body at rest in the Hubble frame would be seen as receding from an observer—also at rest in the frame—such that there was no relative speed or "peculiar speed" between the body and the coordinate coincident with that body—which is receding. Typically, however, bodies such as galaxies are found having peculiar speeds relative to the Hubble frame. Why, in nature, there would be an expectation to find bodies moving in the Hubble flow will be explored in Section XXI.

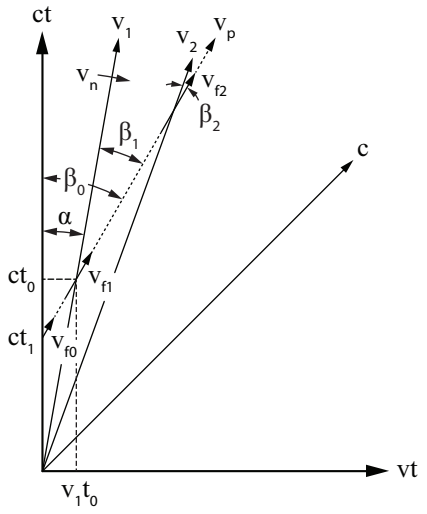


FIG. 9.

This system of moving coordinates can be visualized in Fig. 9, which is a spacetime diagram with time axis $ct$ and space axis $vt$—where the rest frame is a coordinate in the Hubble frame. The rest frame, by definition, is only moving in time—along $ct$—while $v_1$, $v_2$, and $c$ describe

coordinates moving at varying speeds relative to the rest frame according to Eq. (110). These are termed "Hubble coordinates". It can also be imagined that $v_1$, $v_2$, and $c$ represent the world lines of moving frames coincident with these coordinates. The inverse slope of a world line in the diagram ($vt/ct = v/c$) gives its speed relative to the rest frame. Thus, a line where $v = c$ is drawn at 45°.

Note, Fig. 9 only shows the right side of the complete spacetime diagram, which is mirrored about the $ct$ axis. Imagine coordinates $v_1$, $v_2$, and $c$ as all having mirrored counterparts—with the left and right $c$ world lines establishing a light cone.

As demonstrated by Eq. (123), the velocity of any given Hubble coordinate remains constant over time; and thus, in the diagram, the world lines for these coordinates are drawn with straight lines. Notice that, when the clocks of these world lines are all run in reverse, the world lines all converge at a point in spacetime that demarks the universe's initial event. Accordingly, an observer in the rest frame of any Hubble coordinate, moving backwards in time along the $ct$ axis, would see bodies in the Hubble flow converging on his location, making it appear to the observer that he is at the center of the universe.

The world line of an inertial frame moving at speed $v_p$ relative to the rest frame of a Hubble coordinate is also drawn in the diagram. Notice that the $v_p$ world line does not intersect the point of convergence of Hubble coordinates. However, an observer in the $v_p$ rest frame would see the universe as existing in its own light cone—expanding at $c$ in all directions—with a point of convergence at the intersection of these world lines at a Hubble time of zero in the frame. Thus, an observer in this rest frame, and, by extension, any inertial observer, can imagine himself as being located at the center of the universe.

Nonetheless, it's reasoned that the Universe had only one initial event—demarked by a single point in spacetime—this event establishing the Hubble frame. The implication is that the Hubble frame constitutes a *preferred* frame—where motion with respect to this frame is discernible. While it may seem outlandish that there would be a preferred frame in the universe, there is evidence for this case. For example, an observer moving along the $v_p$ world line would see blueshift in light observed from the right side of the $ct$ axis and redshift from the opposite direction. We see this effect—based on our motion in the Milky Way and the Milky Way's peculiar speed—as a dipole in the cosmic microwave background (CMB) where one side of a spherical survey is slightly blueshifted relative to the other.

Notice that the $v_p$ world line crosses coordinates in the Hubble frame at angles that decrease over time starting with $\beta_0$—relative to the rest frame, followed by $\beta_1$ relative to $v_1$, and finally $\beta_2$ with respect to $v_2$. Decreasing angles translate to decreasing relative speeds, and thus, the frame moving along the $v_p$ world line is decelerating with respect to coordinates in the Hubble frame—which is to say decelerating in the Hubble frame.

As the frame moving at $v_p$ intersects a Hubble coordinate, its speed relative to that coordinate is defined as $v_f$. Specifically, $v_f$ is defined as the peculiar speed relative to the coincident Hubble coordinate. More broadly, $v_f$ can be understood as the peculiar speed relative to the overall Hubble flow (or Hubble frame). This is in contrast to $v_p$, which is defined as the speed with respect to a fixed Hubble coordinate.

This can be visualized in the diagram. Notice that the $v_p$ world line is broken into a series of segments: $v_{f0}$, $v_{f1}$, and $v_{f2}$—where each segment represents the peculiar speed $v_f$ at the coincident Hubble coordinate. At time $t_1$—where the frame moving at $v_p$ crosses the $ct$ axis of the rest frame, $v_{f0}$ is equivalent to $v_p$—as evidenced by both segments having the same angle $\beta_0$ with respect to the Hubble coordinate. At the point where the moving frame intersects coordinate $v_1$, relative to $v_1$, $v_f$ has decelerated to $v_{f1}$; and at $v_2$, relative to $v_2$, $v_f$ has further slowed to $v_{f2}$.

As the moving frame continues along the $v_p$ world line, it will asymptotically approach the slope of the Hubble-frame coordinate of the same slope—which is to say the same speed. After an infinite amount of time, the moving frame will come to rest in the Hubble frame. Light, with a $v_p = c$, will asymptotically approach the edge of the light cone—defined by the $c$ coordinate in the diagram. Keeping in mind that the diagram is mirrored, there is no direction where a frame with a non-zero peculiar speed will not decelerate relative to the Hubble frame.

As the $v_p$ world line crosses the $v_1$ coordinate, $v_1$ becomes the rest frame, which would look identical to the frame of Fig. 9—with the most distant coordinate receding at $c$. Relative to this frame, the peculiar speed would not be $v_{f0}$ but $v_{f1}$—and the blueshift in the dipole would be slightly less than before.

From the diagram, the following equation can be written:

$$v_n t_0 = v_p(t_0 - t_1) \ . \tag{124}$$

As time progresses, coordinate $v_n$ rotates clockwise about the origin—tracking the $v_p$ world line as it intersects Hubble coordinates. At time $t_0$, $v_n$ has rotated an angle $\alpha$ relative to time axis $ct$ and is coincident with $v_1$—which is to say, at $t_0$, $v_n$ is equivalent to $v_1$. Looking at the diagram, in the timespan $t_0 - t_1$, a particle moving at speed $v_p$ will have traveled the same distance as a particle moving at the current value of $v_n$—which is $v_1$. With $t_0$ defined as the Hubble time, $v_n$ and $t_0$ in Eq. (124) are dynamic with respect to time, while $v_p$ and $t_1$ are constant.

Taking the derivative of Eq. (124) with respect to time

gives the following:

$$\frac{dv_n}{dt}t_0 + v_n\frac{dt_0}{dt} = \cancelto{0}{\frac{dv_p}{dt}}(t_0 - t_1) + v_p(\frac{dt_0}{dt} - \cancelto{0}{\frac{dt_1}{dt}}) , \quad (125)$$

$$\dot{v}_n t_0 + v_n = v_p . \quad (126)$$

As before, both $dt_0$ and $dt$ refer to changes in time in the rest frame and thus cancel. Speed $v_p$ is constant in the rest frame over time, and thus, $dv_p/dt$ is zero. With these considerations, Eq. (125) reduces to Eq. (126).

Plugging Eq. (113)—the relation between Hubble time $t_0$ and the Hubble parameter $H_0$—into Eq. (126), gives this:

$$\dot{v}_n\frac{1}{H_0} + v_n = v_p , \quad (127)$$

$$\dot{v}_n = (v_p - v_n)H_0 . \quad (128)$$

In the diagram, at time $t_1$, the coincident coordinate $v_n$ is in line with the $ct$ axis of the rest frame and thus has a speed of zero in the frame. With this in mind, the following equations are written:

$$v_f = v_p - \cancelto{0}{v_n} , \quad (129)$$

$$\dot{v}_n = (v_f - \cancelto{0}{v_n})H_0 = v_f H_0 , \quad (130)$$

$$v_f \cancel{H_0} = (v_p - v_n)\cancel{H_0} , \quad (131)$$

$$v_f = v_p - v_n , \quad (132)$$

$$\dot{v}_f = \cancelto{0}{\dot{v}_p} - \dot{v}_n , \quad (133)$$

$$a_f = \dot{v}_f = -v_f H_0 . \quad (134)$$

In Eq. (129), at a $v_n$ of zero, $v_f$ is equivalent to $v_p$. This is shown in the diagram where $v_{f0}$ and $v_p$ have the same slope relative to the $ct$ axis—and thus the same speed. With Eq. (129), Eq. (128) can be rewritten as Eq. (130), which gives the acceleration of the floating coordinate $v_n$ as it traces the moving frame in the reference frame of the coincident Hubble coordinate—which is to say the Hubble frame.

Plugging Eq. (130) into Eq. (128) gives Eq. (131), which reduces to Eq. (132). Notice the inclusion of the $v_n$ term in Eq. (132), which correctly indicates that after an infinitesimal amount of time, $v_f$ will be slightly smaller than $v_p$. Importantly, because $v_f$ is always relative to the reference frame of the coincident coordinate, which changes over time, this equation is only valid within this infinitesimal time period. Taking the derivative of Eq. (132) with respect to time gives Eq. (133), where, as before, $\dot{v}_p$ is zero. Like Eq. (132), Eq. (133) is only correct for an infinitesimal span of time.

Eq. (134), which follows from Eqs. (130) and (133), gives the deceleration $a_f$ of a frame moving relative to the coincident Hubble coordinate—which is to say deceleration in the Hubble frame—as a function of its peculiar speed $v_f$ in the frame. Because both $v_f$ and $a_f$ are always measured in the frame of the coincident coordinate, Eq. (134) is deemed to be valid at all times. Notice that $v_f$ is a scalar—with no direction, and thus, so is deceleration $a_f$. In the specific case where the peculiar speed of a given frame is zero, that frame is considered to be at rest in the Hubble frame.

Notice further that in static—non-expanding—space, which is described by an $H_0$ of zero in Eq. (134), there is no deceleration. A static universe, with an $H_0$ of zero, would be of infinite age and size—and *frameless*. In contrast, the present model holds that the universe is finite and perpetually expanding at $c$. It's surmised that this constitutes a frame against which peculiar speed $v_f$ and acceleration $a_f$ can be defined.

However, even our finite universe does look to be limitless. It's only finite on paper! All inertial observers see themselves as being at the center of the universe. Further, a given inertial observer can also have a peculiar speed relative to the universe—while curiously, always seeing himself at its center. This observer can certainly travel to other regions of the universe and see other galaxies, but in his rest frame, the universe will always be expanding at $c$ in every direction.

## XIV. MASS OF THE UNIVERSE

Eq. (134), when applied to light, holds that a photon is decelerated in the Hubble frame as follows:

$$a_f = -cH_0 . \quad (135)$$

This deceleration, which can be described as a photon losing energy over time as it travels through expanding space, manifests as redshift.

The following equations explore the idea that the redshift of a photon can be equivalently imagined in two different contexts: traveling through expanding space and traveling against a decelerating field:

$$\dot{\lambda} = \lambda H_0 ,$$

$$p = \frac{h}{\lambda} , \quad (136)$$

$$\dot{p} = \frac{-h}{\lambda^2}\dot{\lambda} , \quad (137)$$

$$\dot{p} = \frac{-h}{\lambda^{\cancel{2}}}\cancel{\lambda}H_0 , \quad (138)$$

$$m_e a_f = \dot{p} = \frac{-h}{\lambda}H_0 , \quad (139)$$

$$m_e = \frac{E}{c^2} = \frac{p}{c} = \frac{h}{c\lambda} , \quad (140)$$

$$\frac{\cancel{h}}{\cancel{\lambda}}\frac{1}{c}a_f = -\frac{\cancel{h}}{\cancel{\lambda}}H_0 , \quad (141)$$

$$a_f = -cH_0 .$$

Eq. (111), which gives Hubble's law applied to the wavelength of light, is restated above. The momentum of a photon as a function of wavelength is given by Eq. (136)

and the change in momentum over time $\dot{p}$ by Eq. (137). Plugging Eq. (111) into Eq. (137) gives Eq. (138), which reduces to Eq. (139)—the latter relating the effective mass of a photon $m_e$ and deceleration $a_f$ to the change in momentum. With the definition of $m_e$ in Eq. (140), Eq. (139) distills to Eq. (135).

Referring back to Eq. (20), acceleration implies time uncertainty. Equating this relation with the deceleration of a photon in the Hubble frame—as given by Eq. (135)—yields the following:

$$\cancel{c}H_0 = \frac{2\cancel{c}}{\Delta t_u} \,, \tag{142}$$

$$H_0 = \frac{1}{t_0} = \frac{2}{\Delta t_u} \,, \tag{143}$$

$$\Delta t_u = 2t_0 \,. \tag{144}$$

Plugging Eq. (114) into Eq. (142) gives Eq. (144). Eq. (144) asserts that the time uncertainty of the universe $t_u$ is double the Hubble time $t_0$, which, as argued, is the age of the universe. Notably, this time uncertainty will *always* be double the age of the universe. Is the time and energy of the universe perpetually on loan—one that never expires? Is the universe a vacuum fluctuation? In 1973, this question was originally posed by Edward Tryon in a paper of the same title [30].

With the relation between $H_0$ and time uncertainty $t_u$ given by Eq. (143), the energy uncertainty of the universe $E_u$ is derived via the uncertainty principle:

$$\Delta E_u \Delta t_u \geq \frac{\hbar}{2} \,,$$

$$\Delta t_u = \frac{2}{H_0} \,,$$

$$\Delta E_u \frac{2}{H_0} \geq \frac{\hbar}{2} \,, \tag{145}$$

$$\Delta E_u = \frac{\hbar H_0}{4} \,. \tag{146}$$

As before, replacing the $\geq$ sign with an equals sign in Eq. (146) pins $\Delta E_u$ at its minimum.

To recap, each observer in his respective rest frame will see the most distant coordinate of the universe receding at $c$. The distance to this coordinate $r_0$—as given by Eq. (112)—is equivalent in all directions. This establishes a sphere where points on that sphere have time and energy uncertainties as described by Eqs. (144) and (146), respectively. As such, Eq. (7) may be used to calculate the mass within that sphere—which is to say the mass of the universe:

$$\Delta E_u = \frac{m_0 hG}{8\pi {r_0}^2 c} \,, \tag{147}$$

$$\Delta E_u = \frac{m_0 \hbar G}{4{r_0}^2 c} \,, \tag{148}$$

$$\frac{m_0 \cancel{\hbar} G}{\cancel{4}{r_0}^2 c} = \frac{\cancel{\hbar} H_0}{\cancel{4}} \,, \tag{149}$$

$$m_0 = \frac{cH_0 {r_0}^2}{G} \,, \tag{150}$$

$$r_0 = ct_0 = \frac{c}{H_0} \,, \tag{151}$$

$$m_0 = \frac{c\cancel{H_0} c^2}{G\cancel{H_0^2}} \,, \tag{152}$$

$$m_0 = \frac{c^3}{GH_0} = \frac{c^3 t_0}{G} \,. \tag{153}$$

Eq. (7) is restated as Eq. (147) with $m_0$ and $r_0$ corresponding to the mass and radius of the universe in a given frame. In Eq. (149), Eq. (148) is equated with Eq. (146), which, via Eq. (112), reduces to Eq. (153). Eq. (153) shows that the mass of the universe $m_0$ is directly proportional to the Hubble time $t_0$ and thus inversely proportional to the Hubble parameter $H_0$.

Specifically, $m_0$—as described by Eq. (153)—is the rest mass of the universe in the rest frame of an inertial observer at a Hubble time of $t_0$, which is the proper time in the frame. It's surmised that all inertial observers agree on the value of $t_0$ in their own frames, and thus all inertial observers should agree on the mass of the universe $m_0$.

But other questions remain: Do observers in other frames on different world lines agree on the *mass density* of the universe? Does the cosmological principle still hold? By what reasoning does $m_0$ only reflect rest mass? What accounts for the kinetic and potential energies of bodies in the Hubble flow? These questions will be addressed in Sections XX and XXI.

With an $H_0$ of 70 km s$^{-1}$ Mpc$^{-1}$, $m_0$ calculates to:

$$H_0 = 70\,\mathrm{km\,s^{-1}Mpc^{-1}} \,,$$
$$H_0 = 2.27 \times 10^{-18}\,\mathrm{m\,s^{-1}m^{-1}} \,,$$
$$m_0 = 1.78 \times 10^{53}\,\mathrm{kg} \,.$$

Note that Eq. (153) has previously been arrived at via other lines of reasoning [31][32]. For example, the relation between mass density $\rho_0$ and $H_0$—which emerges from the Friedmann model of an expanding universe [33]—

reduces as follows:

$$
\begin{aligned}
&G\rho_0 \simeq {H_0}^2 \ , \\
&m_0 \sim \rho_0 {r_0}^3 \ , \\
&r_0 = \frac{c}{H_0} \ , \\
&m_0 \sim \frac{\cancel{{H_0}^2}}{G} \frac{c^3}{\cancel{H_0^3}} \ , \\
&m_0 \sim \frac{c^3}{GH_0} \ .
\end{aligned}
$$

With Eq. (153) and mass–energy equivalence, the energy of the universe $E_0$ is thus:

$$
\begin{aligned}
&E_0 = m_0 c^2 \ , \\
&E_0 = \frac{c^5 t_0}{G} = \frac{c^5}{GH_0} \ . \qquad (154)
\end{aligned}
$$

Taking the derivative of $E_0$ with respect to time gives this:

$$
\begin{aligned}
&\frac{dE_0}{dt} = \frac{c^5}{G} \frac{dt_0}{\cancel{dt}}^{\,1} \ , \qquad (155) \\
&P_0 = \frac{c^5}{G} \ . \qquad (156)
\end{aligned}
$$

Eq. (156), which gives the rate at which energy is added to the universe, is recognizable as the Planck power—theoretically, the upper power limit in the universe. Interestingly, there are no parameters in this equation—only constants.

In brief, Time-Driven Cosmology is the consequence of the universe running at two limits: the speed of light, which governs the rate of expansion, and Planck power, which caps the rate at which the universe gains energy. Further, it's posited that these two rates are directly coupled—one doesn't occur independently of the other. As space expands, energy is borrowed from the vacuum, and borrowing energy from the vacuum causes space to expand.

It's imagined that matter manifests via vacuum fluctuations. It's gathered that these were more energetic and dense in the early universe as Planck power was distributed across a relatively small volume.

## XV. EXPANSION PARAMETERS IN THE HUBBLE FRAME

From Sections X and XI: A frame moving in a parent frame sees an expansion parameter $H_f$ that varies linearly with that frame's speed in the parent frame. For a given $H_f$, frame size $r_f$ also varies linearly with speed. With this in mind, the following equations are written:

$$
\begin{aligned}
&H_f = \frac{v_x}{r_0} \ , \qquad (157) \\
&v_x = r_f H_0 \ , \qquad (158) \\
&r_0 H_f = r_f H_0 \ . \qquad (159)
\end{aligned}
$$

Referring back to Fig. 8 and Eqs. (102) and (103), frame two—moving at speed $v_2$ relative to a parent frame of size $r_f$—sees an expansion parameter of $H_1$. Recall from Section X that frame size $r_f$ is an abstract parameter. Frame one moving at the lower speed $v_1$ relative to the same frame sees a smaller expansion parameter of $H_2$. As described by these equations, for a given frame size $r_f$, the expansion parameter varies linearly in proportion to the frame speed.

It's thus imagined that there is a speed $v_x$ relative to a parent frame of size $r_0$ where the moving frame sees an expansion parameter $H_f$ proportional to that speed. This is embodied by Eq. (157). At $v_x = c$, Eq. (157) is equivalent to Eq. (112)—where a frame moving at $c$ sees an expansion parameter of $H_0$. As $v_x$ goes to zero, $H_f$ goes to zero. Here, $r_0$ is both the frame size *and* the size of the universe—as described in Section XI.

For a given $H_f$ in Eq. (157), there is a speed $v_f$ and frame size $r_f$ that satisfy Eq. (107). It's postulated that $v_f$ is also *some* function of $v_x$ with the following stipulations: As $v_x$ goes to zero, $v_f$ goes to zero, and as $v_x$ goes to $c$, $v_f$ goes to $c$. Here, unless $v_f$ is equivalent to $v_x$—which is assumed not to be the case—it's impossible for these two speeds to be linearly related, as that would violate one of the above stipulations.

Because $H_f$ varies according to $v_x$—as described by Eq. (157), for Eq. (107) to hold—*where $v_f$ is a non-linear function of $v_x$*, $r_f$ must also vary as a function of $v_x$. With this in mind, Eq. (158) is written according to the following reasoning: In congruence with Eq. (108), $r_f$ is a linear function of $v_x$. As $v_x$ goes to zero, $r_f$ goes to zero; and as $v_x$ goes to $c$, $r_f$ goes to $r_0$—the two limits in terms of distance. Yet, for $r_f$ to go to $r_0$, the expansion parameter in Eq. (158) *must* be $H_0$.

Combining Eqs. (157) and (158) gives Eq. (159), which is a relation between expansion parameters and frame sizes. Referring back to Section VI, notice the symmetry between Eqs. (62)–(63) and Eq. (159). In Eq. (62), for example, recall that $r$ is the distance between two masses; $H_f$ is the expansion parameter of the two-mass frame; $H_2$ is the expansion parameter at mass two; and $r_1$ is the distance between the barycenter of the two-mass system to mass one. In comparison, $r$ and $H_f$ in Eq. (62) correspond to $r_0$ and $H_0$, respectively, in Eq. (159)—where these parameters define the parent frame; and $r_1$ and $H_2$ correspond to $r_f$ and $H_f$—which, in their respective equations, define a child frame.

Eqs. (157) and (158) have interesting implications. As a consequence of traveling at $c$—where $v_x$ goes to $c$, light sees the two extents of the universe: its expansion parameter $H_0$ and its size $r_0$. At the other extreme, where

$v_x$ goes to zero, both the expansion parameter $H_f$ and frame size $r_f$ go to zero in concert.

A relation similar to Eq. (159) is derived by equating Eq. (112) to Eq. (158):

$$\begin{aligned} H_0 &= \frac{c}{r_0} \ , \\ H_0 &= \frac{v_x}{r_f} \ , \\ cr_f &= v_x r_0 \ . \end{aligned} \tag{160}$$

Notice that Eq. (160) is reproduced by multiplying Eq. (159) by Eq. (157):

$$\begin{aligned} \frac{r_f}{H_f} &= \frac{r_0}{H_0} \ , \\ \frac{r_f}{\cancel{H_f}} \frac{\cancel{H_f}}{v_x} &= \frac{r_0}{H_0} \frac{1}{r_0} \ , \\ \frac{r_f}{v_x} &= \frac{r_0}{c} \ . \end{aligned} \tag{161}$$

Eq. (161) reduces as follows:

$$\begin{aligned} \frac{r_f}{v_x} &= \frac{\cancel{r_0}}{H_0} \frac{1}{\cancel{r_0}} \ , \\ \frac{r_f}{v_x} &= \frac{1}{H_0} = t_0 \ . \end{aligned}$$

As noted, $r_f$ is an abstract parameter that doesn't reflect a measurable quantity. The same is true for $v_x$, which is also an abstract parameter that isn't directly observable. These are the only two abstract parameters used in the equations of this section. Interestingly, their quotient yields a non-abstract parameter: the inverse of $H_0$, which is the Hubble time $t_0$.

Plugging the relations for $r_0$ and $r_f$—Eqs. (112) and (107), respectively—into Eq. (159), yields the following:

$$\begin{aligned} r_0 H_f &= r_f H_0 \ , \\ r_0 &= \frac{c}{H_0} \ , \\ r_f &= \frac{v_f}{H_f} \ , \\ \frac{c}{H_0} H_f &= \frac{v_f}{H_f} H_0 \ , \\ c{H_f}^2 &= v_f {H_0}^2 \ , \end{aligned} \tag{162}$$

$$H_f = \sqrt{\frac{v_f}{c}} H_0 \ . \tag{163}$$

Eq. (163) relates the expansion parameter $H_f$—seen by a moving frame with a speed of $v_f$—to $H_0$. Notice that as $v_f$ goes to $c$, $H_f$ goes to $H_0$; but this leaves the question: Relative to what is $v_f$ measured in this case?

The answer to this question can be divined from Eq. (162):

$$\begin{aligned} c &= r_0 H_0 \ , \\ c{H_f}^2 &= v_f {H_0}^2 \ , \\ r_0 \cancel{H_0} {H_f}^{\cancel{2}} &= v_f {H_0}^{\cancel{2}} \ , \end{aligned} \tag{164}$$

$$\begin{aligned} r_0 H_f &= v_x \ , \\ v_x H_f &= v_f H_0 \ . \end{aligned} \tag{165}$$

Eq. (112) is plugged into Eq. (162), which gives Eq. (164). Plugging Eq. (157) into Eq. (164), reduces to Eq. (165).

Recalling Eq. (134) from Section XIII, both sides of Eq. (165) appear to be decelerations. $v_x H_f$ is a deceleration relative to the moving frame, and $v_f H_0$ is a deceleration relative to the Hubble frame—where $v_f$ is a peculiar speed in the Hubble frame.

Plugging Eqs. (112) and (157) into Eq. (165) yields a direct relation between $v_f$ and $v_x$:

$$\begin{aligned} v_x \frac{v_x}{r_0} &= v_f H_0 \ , \\ \frac{{v_x}^2}{r_0 H_0} &= v_f \ , \\ v_f &= \frac{{v_x}^2}{c} \ . \end{aligned} \tag{166}$$

Notice that Eq. (166) conforms to the above requirements: As $v_f$ goes to zero, $v_x$ goes to zero, and as $v_f$ goes to $c$, $v_x$ goes to $c$. As anticipated, $v_f$ is *not* a linear function of $v_x$. Similarly, looking at Eq. (165), as $v_f$ goes to zero, $v_x H_f$ goes to zero; and as $v_f$ goes to $c$, $v_x H_f$ goes to $cH_0$—the deceleration as seen by light.

There's an interesting parallel between Eqs. (166) and (18):

$$\begin{aligned} {v_x}^2 &= c v_f \ , \\ \Delta {t_p}^2 &= \Delta t_f \Delta t_u \ . \end{aligned}$$

Recall, in Eq. (18), that $\Delta t_f$ is distance over $c$.

All parameters in Eq. (163) are non-abstract, measurable quantities. An observer moving at peculiar speed $v_f$ would measure a dipole in the CMB. The Hubble parameter $H_0$ (and its inverse, the Hubble time $t_0$) are measurable. The expansion parameter $H_f$ of a frame moving at $v_f$ is also measurable. As $v_f$ goes to $c$, $H_f$ goes to $H_0$—which is the expansion parameter as seen by light. This was surmised in Section XI where it was reasoned that, at subluminal speeds, moving frames would see expansion parameters less than $H_0$.

In Section XIII, it was reasoned that a frame with a peculiar speed relative to the Hubble frame is decelerating in that frame. Building on this concept, in Section XIV, it was shown that the redshift of light could be imagined in two contexts—both having the same result: one where the wavelength of a photon is expanded over time according to $H_0$ and the other where a photon is decelerated according to $cH_0$.

The following section will investigate the case where the peculiar speed $v_f$ of the frame is less than $c$, which—

akin to light—incurs measurable physical effects. As described by Eq. (163), a frame moving with a peculiar speed of $v_f$ will have an expansion parameter of $H_f$. This, in turn, will result in an increase in the acceleration between particles in the system contained by the frame—as given by Eq. (70). Interestingly, the physical effect that manifests from a frame that is decelerating in the Hubble frame is an increase in acceleration within that decelerating frame.

## XVI. GALACTIC-ROTATION CURVES

In this section, Eqs. (163) and (70), restated below, are applied to a selection of nearby galaxies from the SPARC (Spitzer Photometry & Accurate Rotation Curves) database to derive their rotation curves, which are then checked against observations:

$$H_f = \sqrt{\frac{v_f}{c}} H_0 \ ,$$
$$a_n = \frac{m_r G}{r}\left(\frac{1}{r} + \frac{2\sqrt{cH_f}}{\sqrt{m_t G}}\right) \ .$$

The SPARC database comprises a large catalog of galaxies that vary in mass, gas fraction, effective radii, and surface brightness [34]. As a cohesive dataset spanning a broad range of morphologies, the SPARC data provide an ideal test of modified-gravity as well as dark-matter halo models, the latter being the primary focus of the cited paper. The complete SPARC catalog contains too many galaxies to analyze here—where the intent is a quick sanity check of the above equations. A subset of the catalog was selected to be examined based on proximity to the Milky Way—with the cutoff set to 5 Mpc. These galaxies are listed in Tables II and III of Appendix XXIV. This appendix also includes the corresponding rotation curve for each galaxy as generated via Eq. (70). Distance estimates, listed in Table II, were sourced from the *NASA/IPAC Extragalactic Database* [35].

Appendix XXIII is a synopsis of the procedure used to generate the rotation curves of Appendix XXIV. In short, discs are modeled as zero-thickness plates of varying density with respect to radius. Bulges (one galaxy in the selection has a bulge—NGC 6946) are modeled as spheres where density varies according to radius as well. Discs and bulges are broken into finite elements, and Eq. (70) is solved for each element, where $r$ is the distance from the center of mass of that element to an offset from the center of rotation. The net acceleration $a_n$—toward the center of rotation—at a given offset is the vector sum of the accelerations with respect to each disc and bulge element. Net acceleration $a_n$ is solved across a range of offsets for a given galaxy from the inner to the outermost data points—thereby establishing a rotation curve. The outermost data point, for each galaxy, is listed under the "$r_{max}$" column in Table II.

Looking at Eq. (70), when applied to galaxies, there are two free parameters: $m_t$, which is the total galactic mass, and $H_f$, the expansion parameter of the moving frame containing the galaxy. The total mass $m_t$ is constrained by estimates of the matter comprising the stellar populations, dust, and gas. In practice, $H_f$ is adjusted to fit a given galaxy's rotation curve, but the resulting value should comport with Eq. (163). This equation has two free parameters: $v_f$ and $H_0$, which are only free to a certain extent. Even considering the Hubble tension, estimates of $H_0$ fall within a relatively narrow range. The same holds for the peculiar speed $v_f$ of a body, which can be gauged via the CMB dipole and relative motions.

Each galaxy in the SPARC database includes curve fits for 12 different dark-matter halo models. To fit a given model, SPARC researchers adjusted the following free parameters: bulge mass-to-light ratio ($\Upsilon_b$), stellar-disk mass-to-light ratio ($\Upsilon_d$), galaxy distance, and disk inclination. This highlights another advantage of the SPARC catalog—as fitting the sundry dark-matter models required adjustments to these parameters, yielding a variety of stellar-mass models per galaxy from which to source data.

Looking at the two rotation curves for NGC 2976 in Appendix XXIV, for example, the curve with an $\Upsilon_d = 0.48$ was generated via the Burkert-Flat model (referred to simply as the "Burkert model" going forward), whereas the curve with an $\Upsilon_d = 0.60$ was generated via the DC14-LCDM model. The stellar-disk Newtonian curves in these figures—drawn as dashed blue lines—come directly from the SPARC catalog. The curves show the Keplerian decline that would be expected with only the stellar-disk mass as the source of centripetal acceleration—where that acceleration is purely Newtonian gravity. Notice that the stellar-disk curve from the Burkert model, with a smaller $\Upsilon_d$, looks like a scaled-down version—vertically—of the DC14-LCDM model's curve.

In addition to the stellar disk, Newtonian curves for the gas disk and the bulge (where appropriate) are published in the SPARC catalog for each dark-matter model of each galaxy. Table II of Appendix XXIV relates a given galaxy to the dark-matter model used as the source of Newtonian curves for the components of that galaxy. These curves were translated to density profiles and fed into the finite-element analysis of Appendix XXIII—generating the net rotation curve for the galaxy in question. All source Newtonian curves from the SPARC catalog were reproduced in the figures of Appendix XXIV. The Newtonian contribution from the gas disk is drawn as a dashed magenta line (with the larger dashes), and the bulge contribution is shown as a dotted green line. The net rotation curve is shown as a solid cyan line.

Variance in the free parameters of distance and inclination can result in the error bars of one model looking offset or scaled (or both) relative to those of another model with respect to the axes of distance and speed. This can be seen when comparing the Burkert and DC14-LCDM models of NGC 2976—where the error bars of the Burk-

ert model peak at roughly 88 km s$^{-1}$ at 2.1 kpc vs. a maximum speed of 81 km s$^{-1}$ at 2.2 kpc for the error bars of the DC14-LCDM model.

The gas curves of these two models both peak at roughly 30 km s$^{-1}$ but at different distances—with the Burkert curve peaking at 1.75 kpc vs. 1.8 kpc for the DC14-LCDM curve. The gas curves for a given galaxy are more consistent between models than the stellar curves, which are subject to being modified via the additional free parameter of mass-to-light ratio.

The rotation curves of the galaxies in Appendix XXIV were generated via the dark-matter model offering the best fit—as referenced in Table II. With density profiles for the stellar and gas disks (and bulge when relevant)—derived from the given Newtonian curves for these components, the expansion parameter $H_f$ for a given galaxy is calibrated to fit the net rotation curve to the error bars associated with the source model. Referring, again, to NGC 2976, notice that the Burkert model (with a lower $\Upsilon_d = 0.48$) prefers the higher $H_f$ of 1.9 than the DC14-LCDM model (with an $\Upsilon_d = 0.60$)—where fitting the curve favors an $H_f$ of .20. It's concluded that, for NGC 2976, the expansion parameter $H_f$ lies somewhere between .20 and 1.9 km s$^{-1}$ Mpc$^{-1}$.

Table III shows the expansion parameter $H_f$ for each galaxy in Table II used to generate that galaxy's rotation curve. Table III also includes the galactic mass $m_t$ as well as the frame constant $k_f$—defined by Eq. (109)—for each galaxy, which is computed via $H_f$ and $m_t$. The galactic mass $m_t$ is calculated via the density curves of the associated dark-matter model. Because $m_t$ is derived from data gleaned from the SPARC catalog, $m_t$ is only a free parameter to the extent that there are 12 models per galaxy from which to source density curves. Out of the 29 galaxies listed in Table II, 12 used density profiles derived from the Burkert model, 5 used density profiles derived from the coreNFW LCDM model, and the rest used a combination of the remaining models.

Solving Eq. (163) for $v_f$ for the cases where $H_f = .20$ and 1.9 gives the following:

$$v_f = c\left(\frac{H_f}{H_0}\right)^2 ,$$

$$v_f(.2) = 299\,792\,\mathrm{km\,s^{-1}}\left(\frac{.2}{70}\right)^2 = 0.3\,\mathrm{km\,s^{-1}} ,$$

$$v_f(1.9) = 299\,792\,\mathrm{km\,s^{-1}}\left(\frac{1.9}{70}\right)^2 = 221\,\mathrm{km\,s^{-1}} .$$

This predicts a peculiar speed $v_f$ for NGC 2976 between .3 and 221 km s$^{-1}$.

As touched upon earlier, an observer with a peculiar speed will see a dipole in the CMB. In the case of the Milky Way, the amplitude of this dipole suggests that our galaxy has a speed of 565 km s$^{-1}$ relative to the CMB [4].

Similarly, if the motion of a galaxy relative to the Milky Way is known, the peculiar speed of that galaxy relative to the CMB can be deduced. However, while the recessional component of a galaxy's relative velocity can be resolved by measuring its redshift—while accounting for cosmic redshift, determining the transverse component of the galaxy's velocity is more challenging [36].

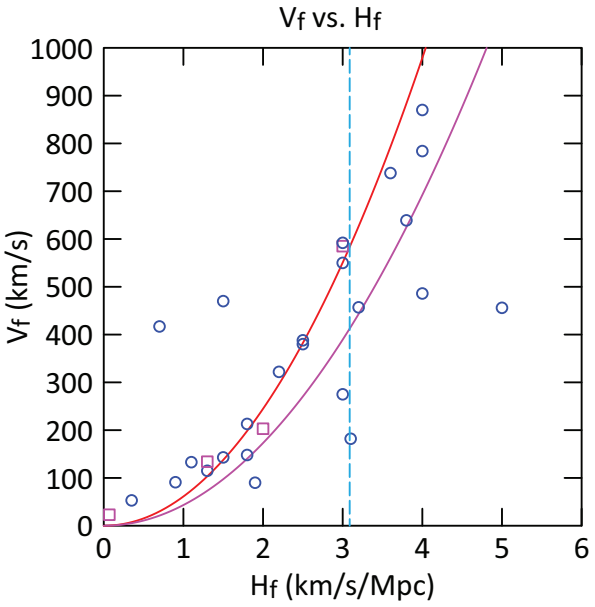


FIG. 10.

If, for example, a galaxy were found along the axis of the Milky Way's dipole moving away from the blue-shifted side of the dipole with a peculiar speed of 565 km s$^{-1}$, it could be deduced that the galaxy was at rest relative to the CMB frame—but only in the radial direction. If the galaxy had a transverse velocity, it would have a dipole perpendicular to that of the Milky Way.

Conversely, if a galaxy were found perpendicular to the axis of the Milky Way's dipole with zero recessional peculiar speed, it could be concluded to be moving in parallel with the Milky Way—with a peculiar speed of 565 km s$^{-1}$—but only if its transverse velocity were verified to be zero.

It's surmised, however, that the speeds of galaxies with respect to the CMB that are derived purely from redshift data—without resolution of those galaxies' transverse velocities relative to us—are still useful data. Given a large enough data set, if Eq. (163) is valid, it seems reasonable that data points should concentrate along a trend line that comports with this relation.

Peculiar speeds relative to the CMB—based on redshift data—of the galaxies in Appendix XXIV are listed in Table II under the column, "CMB redshift". These speeds were sourced from the *NASA/IPAC Extragalactic Database*. Notice that the CMB redshift for NGC 2976 is 90 km s$^{-1}$, which is nearly in the middle of the above estimated range: 0.3–221 km s$^{-1}$.

Fig. 10 is a plot of peculiar speed $v_f$ vs. expansion parameter $H_f$ for the galaxies in Appendix XXIV. The

data points come from Tables II and III—with the value for $v_f$ approximated by the CMB-redshift estimate published for a given galaxy and where the value for $H_f$ is that which gives the best fit for that galaxy's rotation curve. Circles in the figure indicate fair to excellent curve fits, while squares denote poor curve fits. Four galaxies have poor fits, which are highlighted in Table III. This table also notes the outlying galaxies relative to the data trend in the plot.

The left curve in the figure, drawn in red, traces Eq. (163). Galaxies plotted in Fig. 10 proximate to the left curve—assuming accurate values for $H_f$—have CMB redshifts that are nearly equal to their true peculiar velocities. A second curve to the right, drawn in magenta, accounts for uncertainty in the data—including that which stems from transverse velocities being unresolved. It's reckoned that the latter would tend to leave peculiar velocities underestimated. The right curve relates the true peculiar speed $v_f$ to $H_f$ as follows—where $v_2$ is the published CMB redshift:

$$
\begin{aligned}
{v_f}^2 &= {v_2}^2 + {v_2}^2 \ , \\
v_f &= \frac{1}{\sqrt{2}} \ .
\end{aligned}
$$

A galaxy plotted near the right curve thus has a true peculiar speed $v_f$ that is approximately $\sqrt{2}$ times greater than the published CMB redshift. This scalar is the ratio of the magnitude of a vector—comprised of two orthogonal components of equal length—to the length of either component. This scalar seems to be congruent with variation in the present dataset—as about 83% of the galaxies plotted in Fig. 10 are near or contained within the left and right curves. In general, the data trend seems to comport with Eq. (163).

Looking at the rotation curves in Appendix XXIV, a similar percentage (about 86%) of the galaxies listed in Table III have good fits. The quality of fit for these galaxies was determined visually—no statistical analysis was performed. Again, the intent here was to present a thesis with basic sanity checks made along the way.

NGC 2915 is an example of a galaxy having both a poor fit and, further, one that is significantly off trend in Fig. 10. With an $H_f$ of 12, the ($H_f$, $v_f$) coordinate for NGC 2915 is outside the bounds of the figure. It's not clear if this galaxy has a high peculiar speed, which would translate to a high $H_f$, or has more mass than estimated in the SPARC data, or both.

Poor curve fits don't necessarily indicate a discrepancy in galactic mass, as the distribution thereof could also be at issue. Referring again to NGC 2976, the stellar disks in the Burkert and DC14-LCDM models ($\Upsilon_d = .48$ and $\Upsilon_d = .60$, respectively) have different masses, but both yield rotation curves with good fits. This example also highlights the sensitivity that $H_f$ has with respect to mass—where just a 25% increase in $\Upsilon_d$ translates to a nearly 90% reduction in $H_f$.

The rotation curves of two galaxies were fit using disk mass-to-light ratios that were not specifically cited in one of the 12 dark-matter models. For NGC 0247, an $\Upsilon_d$ of 1.0 was used, which is about midway between the DC14 flat and coreNFW LCDM models: 0.50 and 1.52, respectively. The error bars for NGC 0247 came from the coreNFW LCDM model.

For NGC 6789, an $\Upsilon_d$ of 1.0 was used as well, which is about the midpoint of that of the Lucky13 LCDM and DC14 LCDM models: 0.69 and 1.20, respectively. The error bars for NGC 6789 were sourced from the DC14 LCDM model.

As $r$ goes to infinity in Eq. (70), the reference mass $m_r$ approaches the total mass $m_t$—as the galaxy looks increasingly like a point mass to an orbiting particle. Thus, at large distances, Eq. (70) reduces to Eq. (37) as follows:

$$
\begin{aligned}
a_n &= \frac{m_r G}{r} \left( \frac{1}{r} + \frac{2\sqrt{cH_f}}{\sqrt{m_t G}} \right) \ , \\
m_r &\to m_t \ , \\
a_n &= \frac{\cancelto{0}{m_t G}}{\cancel{r^2}} + \frac{2\sqrt{cH_f m_t G}}{r} \ , \\
a_n &= \frac{2\sqrt{cH_f m_t G}}{r} \ , \\
\frac{{v_{flat}}^2}{\cancel{r}} &= \frac{2\sqrt{cH_f m_t G}}{\cancel{r}} \ , \\
v_{flat} &= \sqrt{2}(cH_f m_t G)^{\frac{1}{4}} \ .
\end{aligned}
\tag{167}
$$

Note that as $m_t$ approaches a point mass, the local expansion parameter $H_l$—as seen by a particle of negligible mass in the field—approaches the frame's expansion parameter $H_f$. Further, in this regime, the Newtonian component of Eq. (37) loses significance in relation to the expansion component and thus, at a certain distance, this can be ignored. Here, Eq. (37) reduces to Eq. (36).

Assuming circular motion, Eq. (167) gives the asymptotic speed $v_{flat}$ that is approached by particles as the expansion component of centripetal acceleration becomes dominant. Table III includes $v_{flat}$ calculations for each galaxy via this equation. As mentioned above, a sample of isolated galaxies from the KiDS survey has been found with rotation curves that remain flat for hundreds of kpc [17]. In Section XVIII, the question of how far a flat rotation curve can extend will be explored.

### 1. *The Milky Way*

Fitting the Milky Way's rotation curve is left as a future exercise, but with an estimate of its peculiar speed $v_f$ and (baryonic) mass $m_t$ [37], the following parameters

are easily calculated: $H_f$, $k_f$, and $v_{flat}$.

$$
\begin{aligned}
&m_t = 8.43 \times 10^{10}\,\mathrm{M}_\odot = 1.68 \times 10^{41}\,\mathrm{kg}\ , \\
&v_f = 565\,\mathrm{km\,s^{-1}}\ , \\
&H_f = 3.04\,\mathrm{km\,s^{-1}Mpc^{-1}}\ , \\
&k_f = 5.88 \times 10^{-61}\,\mathrm{kg^{-1}s^{-1}}\ , \\
&v_{flat} = 191\,\mathrm{km\,s^{-1}}\ .
\end{aligned}
$$

The parameter $v_{flat}$ predicts that the Milky Way's rotation curve flattens to 191 km s$^{-1}$, which comports with recent observations that extend out to 25 kpc [38][39]. Yoshiaki Sofue has compiled a "grand" rotation curve for the Milky Way that extends out to 400 kpc [40]. From 40 to 100 kpc, $v_{flat}$ aligns well with this curve. Beyond 100 kpc, uncertainty in the data increases, and the error bars encompass a wide range of rotational velocities—from roughly 100 to 200 km s$^{-1}$.

The frame constant $k_f$, defined as the expansion parameter per unit mass, applies to all bodies in the system, which, in the case of the Milky Way, would include the Solar System. With the definition of $k_f$ given by Eq. (109), Eq. (70) can be simplified as follows:

$$
\begin{aligned}
k_f &= \frac{H_i}{m_i} = \frac{H_f}{m_t}\ , \\
a_n &= \frac{m_r G}{r}\left(\frac{1}{r} + 2\sqrt{\frac{c}{G}k_f}\right)\ , && (168) \\
a_n &= \frac{m_r G}{r^2} + \frac{2}{r}\sqrt{\frac{c}{G}k_f}\ , && (169) \\
k_e &= \frac{2}{\cancel{r}}\sqrt{\frac{c}{G}k_f}\left(\frac{r^{\cancel{2}}}{m_r G}\right)\ , && (170) \\
k_e &= \frac{2r}{m_r G}\sqrt{\frac{c}{G}k_f}\ . && (171)
\end{aligned}
$$

Plugging Eq. (109) into Eq. (70) gives Eq. (169), which defines $a_n$ as the sum of the two components of acceleration—the Newtonian and the expansion components. $k_e$, in Eq. (171), is the ratio of these components, which is an indication of their relative strength. Notice that $k_e$, which is a function of $r$, shows that the transition from the Newtonian to the non-Newtonian regime is linear with respect to distance.

Note that Section XVIII, as suggested, will explore the expansion component of acceleration at large distances—far beyond the extent of the typical rotation curve. Here, it will be shown that curves do not stay flat indefinitely. However, from the front end of the curve to the portion where it flattens out—which is typically on the order of Mpc, Eqs. (70) and (169) are sufficiently accurate.

When applied to the Solar System, Eq. (171) shows that the acceleration regime is entirely Newtonian:

$$
\begin{aligned}
&m_r = 1\,\mathrm{M}_\odot = 1.988\,47 \times 10^{30}\,\mathrm{kg}\ , \\
&r = 1\,\mathrm{AU} = 149\,597\,870.7\,\mathrm{km}\ , \\
&k_e = 3.66 \times 10^{-30}\ .
\end{aligned}
$$

At the average radius of Earth's orbit, the Newtonian component is 30 orders of magnitude larger than the non-Newtonian component.

At 4.25 ly—the distance to Proxima Centauri, the expansion component is still negligible at 25 orders of magnitude less than the Newtonian component:

$$
\begin{aligned}
&r = 4.2465\,\mathrm{ly} = 4.017 \times 10^{13}\,\mathrm{km}\ , \\
&k_e = 9.84 \times 10^{-25}\ .
\end{aligned}
$$

Clearly, the effects of modified gravity are not detectable in or near the Solar System, where motions—within the precision of our measurements—remain Newtonian.

### *2. MOND*

Well before Proxima Centauri—at around .111 ly (7300 AU), the strength of the Sun's gravitational field drops below the MOND constant $a_0$ of 1.2E−10 m s$^{-2}$. According to MOND, as discussed, this constant marks the transition to the non-Newtonian acceleration regime, but, as just demonstrated, the Sun's gravity remains Newtonian well past Proxima Centauri! In principle, MOND *does* account for such scenarios with a concept called the "external-field effect" (EFE)—where modified gravity is muted in systems that are in the presence of relatively strong external fields.

In contrast, under the present thesis, non-Newtonian effects in a galaxy are quantified by the frame constant $k_f$—which applies to all bodies and systems of bodies that are gravitationally bound to and part of the host galaxy. Looking at the Milky Way, at small scales—the scale of our Solar System and even out to nearby stars, $k_f$ is too small for non-Newtonian effects to be observed. Non-Newtonian motion is only observed at galactic scales—where distances are such that the non-Newtonian acceleration component is dominant.

The vertical dashed cyan line in Fig. 10 is drawn at an $H_f$ of 3.09 km s$^{-1}$ Mpc$^{-1}$, which is the value of $H_f$ that corresponds to the MOND constant $a_0$ of 1.2E−10 m s$^{-2}$. Equating the deep-MOND-regime relation, Eq. (38), with Eq. (36), distills as follows:

$$
\begin{aligned}
&\frac{\sqrt{a_0 \cancel{m_t} G}}{\cancel{r}} = \frac{2\sqrt{cH_M \cancel{m_t} G}}{\cancel{r}}\ , \\
&a_0 = 4cH_M\ , \\
&H_M = \frac{1}{4c}a_0\ , \\
&H_M = 3.09\,\mathrm{km\,s^{-1}Mpc^{-1}}\ .
\end{aligned}
$$

The expansion parameter corresponding to the MOND constant $a_0$ is designated as $H_M$. With Eq. (163), $H_M$ equates to a frame speed $v_M$ of 583 km s$^{-1}$, which is where the dashed blue line intersects the left red curve in Fig. 10. The blue line intersects the right magenta curve at 412 km s$^{-1}$. Interestingly, the Milky Way's peculiar speed of 565 km s$^{-1}$ is near $v_M$, and correspondingly, its

expansion parameter of 3.04 km s$^{-1}$ Mpc$^{-1}$ is close to $H_M$. The MOND constant $a_0$ was arrived at empirically and is the number that yields the best curve fits—on average—for the many galaxies tested against MOND. Ultimately, is $a_0$ simply a gauge of the average peculiar speed of galaxies in the cosmos?

## XVII. THE LOCAL GROUP

The salient question in Section IX was: "To what extent does external mass affect internal systems"? And from this, the immediate follow-on question is: What defines a system?

Here, a system is defined as a hierarchy of bodies and materials in stable orbits. These bodies move in unison such that the barycenter travels inertially. As such, all of the particles in a system are interconnected. Furthermore, it is reasoned that **all of the elements of a system share the same frame constant** $k_f$.

Is the top node in the hierarchy of systems typically a galaxy? a cluster of galaxies? To dig into this question, the main galaxies in the Local Group—Andromeda, Triangulum, and the Milky Way—are investigated to see where the evidence points. Eq. (69) shows that as mass is added to a system, the expansion parameter of a reference mass in that system decreases in concert. In general, this relation can be used as a starting point to explore the effects of combining galaxies into a system.

For example, if the Milky Way and Andromeda comprised a system, the Milky Way's expansion parameter $H_f$, estimated above at 3.04 km s$^{-1}$ Mpc$^{-1}$, would be diluted by the system mass $m_t$, which would now include Andromeda's mass:

$$H_r = \frac{m_r}{m_t} H_f \ ,$$
$$v_{flat} = \sqrt{2 m_r} \left( \frac{c H_r G}{m_t} \right)^{\frac{1}{4}} \ . \qquad (172)$$

Also, note that Eq. (167), the relation for $v_{flat}$, takes a different form when the reference mass is only a portion of the system mass:

Assuming that the Milky Way and Andromeda are of roughly equal mass [41], which is fair for a quick illustrative calculation, $m_r$, which corresponds to the Milky Way here, and $m_t$ are as follows:

$$m_r = 1.68 \times 10^{41} \, \text{kg} \ ,$$
$$m_t = 3.36 \times 10^{41} \, \text{kg} \ .$$

For a rough calculation, the peculiar speed $v_f$ of the two-galaxy frame is assumed to be that of the Milky Way, which, in turn, leaves the frame constant $H_f$ for the system at 3.04 km s$^{-1}$ Mpc$^{-1}$.

$$v_f = 565 \, \text{km} \, \text{s}^{-1} \ ,$$
$$H_f = 3.04 \, \text{km} \, \text{s}^{-1} \text{Mpc}^{-1} \ .$$

With these new parameters, $H_r$, $k_f$, and $v_{flat}$ for the Milky Way recalculate as follows:

$$H_r = 1.52 \, \text{km} \, \text{s}^{-1} \text{Mpc}^{-1} \ ,$$
$$k_f = 2.94 \times 10^{-61} \, \text{kg}^{-1} \text{s}^{-1} \ ,$$
$$v_{flat} = 135 \, \text{km} \, \text{s}^{-1} \ .$$

The expansion parameter of the Milky Way $H_r$ is now half its previous value. The frame constant $k_f$, which now applies to the system as a whole—with double the mass—also gets reduced by one half. In concert, Eq. (172) gives a significantly lower value for $v_{flat}$—135 km s$^{-1}$ than the above value of 191 km s$^{-1}$. Interestingly, looking at $v_{flat}$, this two-galaxy system has a significantly lower energy state—both in terms of kinetic and potential energies—than the case where the galaxies are independent. This is with all else being equal—including mass and peculiar speed. The potential large disparity in energy states is an additional distinction in terms of what defines a system.

Based on Yoshiaki Sofue's work, it's possible that the Milky Way's rotation curve does flatten to 135 km s$^{-1}$. Recall that past 100 kpc, the error bars of Sofue's grand rotation curve allow for rotational velocities from 100 to 200 km s$^{-1}$ [40]. With neither value of $v_{flat}$—135 or 191 km s$^{-1}$—ruled out, the question as to whether the Milky Way and Andromeda comprise a system remains unresolved. Clearly, an analysis of Andromeda's and the Milky Way's rotation curves would offer further evidence in a particular direction, but a look at Triangulum (M33) has the potential to be more informative.

The mass of M33 is an order of magnitude less than Andromeda (M31) and the Milky Way [42][43]. The implication is that if M33 is part of a system comprising one or both of its larger neighbors, its expansion parameter would be reduced by an order of magnitude in comparison to its non-system value. Further, the distance between M33 and M31 is estimated at 200-240 kpc [44], which opens the possibility that M33 could be a satellite of M31. An analysis of M33's rotation curve should provide a clear indication if this is indeed the case.

Fig. 11 shows M33's rotation curve, which was generated using the same methodology—outlined in Appendix XXIII—that was employed for the rotation curves of Appendix XXIV. Density profiles for the stellar disk and gas components were derived from Newtonian curves rendered by Corbelli et al. 2014 [43].

The net rotation curve was fit with the following values for $m_t$ and $H_f$:

$$m_t = 7.51 \times 10^9 \, \text{M}_\odot = 1.49 \times 10^{40} \, \text{kg} \ ,$$
$$H_f = 3.3 \, \text{km} \, \text{s}^{-1} \text{Mpc}^{-1} \ ,$$
$$v_f = 666 \, \text{km} \, \text{s}^{-1} \ ,$$
$$k_f = 7.17 \times 10^{-60} \, \text{kg}^{-1} \text{s}^{-1} \ ,$$
$$v_{flat} = 106 \, \text{km} \, \text{s}^{-1} \ .$$

With these values for $m_t$ and $H_f$, $v_{flat}$ calculates to 106 km s$^{-1}$, which aligns with the rotation curve in the figure.

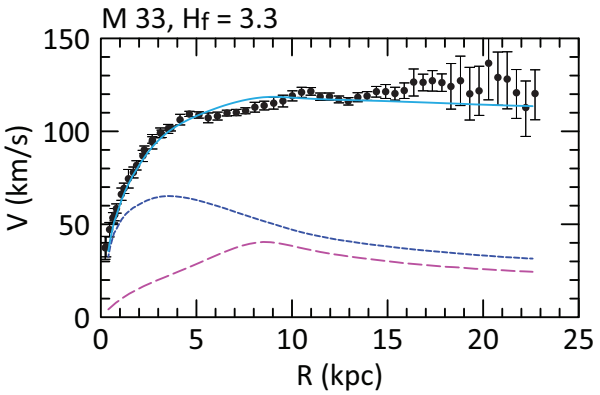


FIG. 11. The net rotation curve is drawn as a solid cyan line, and the Newtonian curves for the stellar and gas disks are drawn with dashed blue and magenta lines, respectively, with the magenta line having the larger dashes. Data are from Corbelli et al. 2014 [43].

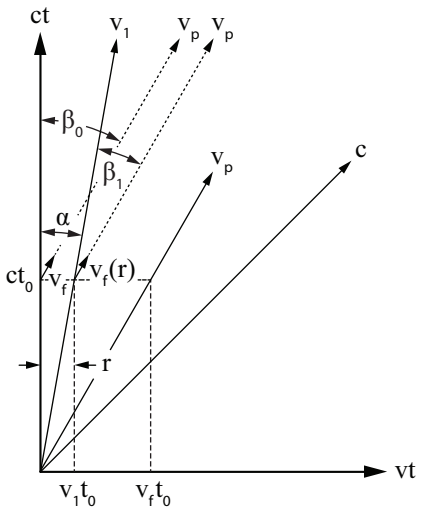


FIG. 12.

The total mass $m_t$, gleaned via these density profiles, is in line with estimates from Corbelli's 2014 paper and a previous paper—Corbelli et al. 2003, which placed M33's mass at $5.4 - 8.4\text{E}9\ M_\odot$ [42].

The expansion parameter $H_f$ of 3.3 km s$^{-1}$ Mpc$^{-1}$ translates to a peculiar frame speed $v_f$ of 666 km s$^{-1}$. This is not too far from the estimated peculiar speed of the Milky Way—at 565 km s$^{-1}$—and that of the Local Group—620 km s$^{-1}$. Two SPARC galaxies from Appendix XXIV that are also considered part of the Local Group—NGC 3109 and UGCA 444—have similar values for $H_f$: 3.6 and 3.2 km s$^{-1}$ Mpc$^{-1}$, respectively.

The frame constant $k_f$ for M33 is an order of magnitude larger than that of the Milky Way. Given that M31 has a similar mass and peculiar speed to that of the Milky Way, M31's frame constant should also be an order of magnitude smaller than that of M33. As such, while M33 is certainly gravitationally influenced by M31, the two galaxies do not constitute a system—based on the stipulation that all particles in a system share the same frame constant.

It's thus unlikely that M31 and the Milky Way comprise a system. Further, based on their expansion parameters—which range between 3.04 and 3.6 km s$^{-1}$ Mpc$^{-1}$, each of the aforementioned galaxies in the Local Group (The Milky Way, M31, M33, NGC 3109, and UGCA 444) is seemingly independent of the others and does not likely constitute an element of a larger system.

Further investigation into the Local Group with the above questions in mind will be instructive. This should include an analysis of the rotation curves of M31 and the Milky Way, and the smaller pressure-supported galaxies, including the Globular Clusters on the outskirts of M31 and the Milky Way.

## XVIII. RELATIVE EXPANSION PARAMETER

If rotation curves can remain flat for hundreds of kpc, can they remain flat for hundreds of Mpc? Can they remain flat indefinitely? To address this question, building on the framework of Section XIII, the concept of a "relative expansion parameter" $H_f(r)$—as an extension of the "frame expansion parameter" $H_f$—will be investigated with distance taken into account.

Fig. 12, similar to Fig. 9, is a spacetime diagram with a frame moving at speed $v_p$ in the rest frame of a Hubble coordinate. Recall from Section XIII that deceleration—as given by Eq. (163)—is calculated in the reference frame of the coincident coordinate—which is to say in the Hubble frame. In contrast to Fig. 9, the rest frame of Fig. 12 is that of the coincident coordinate—which is always the coordinate crossed by the moving frame at $t_0$ (the Hubble time). Notice that the moving frame is crossing the coordinate of the rest frame at $t_0$. At this moment, $v_f$ is equivalent to $v_p$.

Recall that while $v_f$ is measured relative to the coincident Hubble coordinate, $v_p$ is measured relative to a fixed coordinate, or alternatively said, relative to an observer that is static in the Hubble frame. Thus, while $v_p$ remains constant over time relative to this observer, $v_f$ is always decreasing. Looking at the diagram, $v_f$ decreases with distance as well. Notice, at distance $r$ in the rest frame, peculiar speed $v_f(r)$, which is measured relative to coincident coordinate $v_1$, is less than $v_f$—as shown by angle $\beta_1$—which is less than $\beta_0$. Here, peculiar speed $v_f(r)$ is defined as the peculiar speed at offset $r$ in the rest frame.

As distance $r$ in the rest frame increases, peculiar speed $v_f(r)$ decreases. At distance $v_f t_0$ from the $ct$ axis, the slope of the coincident Hubble coordinate is equivalent to that of $v_p$. Across this distance—where the angle between $v_p$ and the coincident coordinate is zero—a first

observer in the frame at the $ct$ axis would gauge that a second observer has a peculiar speed $v_f(r)$ of zero. Further, with the frame expansion parameter $H_f$ being a function of $v_f$—as described by Eq. (163), this first observer would also gauge that the second observer sees the frame as having an expansion parameter $H_f$ of zero.

This raises a question: In previous sections, the expansion parameter of the parent frame $H_f$ was deemed to be invariant with respect to motion and position—a value that was agreed upon by all particles in the system. Is this still the case? The answer is yes. From the perspective of the first observer, the frame has an expansion parameter of $H_f$. Importantly, the second observer also agrees with this value and sees the frame as having the same expansion parameter of $H_f$. However, the first observer sees the second observer as existing in a frame with a smaller, relative expansion parameter of $H_f(r)$; and in congruence, the second observer sees the first as existing in the same relative frame—where each observer agrees on the value of other's relative expansion parameter $H_f(r)$.

Recognize that in the spacetime diagram of Fig. 12, there is no preferred observer in the moving frame. From the perspective of a first observer, a second observer at distance $v_f t_0$ has a peculiar speed $v_f(r)$ of zero. And likewise, from the perspective of the second observer, the first observer has a peculiar speed $v_f(r)$ of zero. Neither observer is preferred, and both agree that the other has a peculiar speed of zero. With Eq. (163), which relates peculiar speed to expansion parameter, each observer would see the other as existing in a frame with an expansion parameter of zero.

Further, because there is no preferred direction in the frame, two observers orthogonal to the first two—also at a distance of $v_f t_0$—would agree that the frame has an expansion parameter of zero as well, but only with respect to each other! If these four observers formed a square, a pair of neighboring observers would be closer than $v_f t_0$, in which case, each observer in this pair would see the other as having a non-zero expansion parameter.

As a practical matter, at the scale of the typical rotation curve, $H_f(r)$ does not deviate with any significance from $H_f$. However, at large scales—typically on the order of Mpc, $H_f(r)$ can be substantially lower than $H_f$.

To explore the relation between expansion parameter and distance, refer again to Fig. 12. Angles $\beta_0$ and $\beta_1$ in the diagram are related to speed as follows:

$$tan(\beta_0) = \frac{v_f}{c} \,, \tag{173}$$

$$tan(\beta_1) = \frac{v_f(r)}{c} \,. \tag{174}$$

Note that $v_f$ in Eq. (173) is relative to the coincident Hubble coordinate of the rest frame; and $v_f(r)$, which is the peculiar speed at offset $r$, is relative to coincident coordinate $v_1$.

Similarly, a relation between distance $r$ in the rest frame and angle $\alpha$ is as follows:

$$tan(\alpha) = \frac{r}{ct_0} \,. \tag{175}$$

Expanding upon the equations above gives this:

$$\beta_1 = \beta_0 - \alpha \,, \tag{176}$$

$$tan(\beta_1) = tan(\beta_0 - \alpha) \,, \tag{177}$$

$$\frac{v_f(r)}{c} = tan\left(arctan\left(\frac{v_f}{c}\right) - arctan\left(\frac{r}{ct_0}\right)\right) \,, \tag{178}$$

$$\frac{v_f(r)}{c} = \left(\frac{v_f}{c} - \frac{r}{ct_0}\right)\left(1 + \left(\frac{v_f}{c}\right)\left(\frac{r}{ct_0}\right)\right)^{-1} \,, \tag{179}$$

$$v_f(r) = (v_f - rH_0)\left(1 + \frac{v_f r H_0}{c^2}\right)^{-1} \,. \tag{180}$$

Eq. (176) is derived with simple geometry. Imagine $v_1$ rotating counter-clockwise $\alpha$ degrees about the origin in the diagram. This would bring $v_1$ in line with the $ct$ axis—where $\beta_1$ would be equivalent to $\beta_0$.

Plugging Eqs. (173), (174), and (175) into Eq. (178), reduces to Eq. (179) via trigonometry and simplification. Plugging Eq. (113) into Eq. (179) gives Eq. (180).

Notice that, as $r$ goes to zero in Eq. (180), $v_f(r)$ goes to $v_f$. This is as expected, as both speeds in this case would be relative to the same coincident coordinate. Thus, $v_f(0) = v_f$. As $r$ goes to $v_f t_0$ (or alternatively, $v_f/H_0$), $v_f$ goes to zero, which begs the question: What happens when $r$ goes beyond $v_f t_0$? Can $v_f$ go negative?

While velocity, which has direction, can be negative, it doesn't make physical sense for speed—which is the magnitude of velocity (which has no direction)—to be negative. This comports with Eq. (134)—where a non-negative peculiar speed $v_f$ translates to deceleration in the Hubble frame. Looking at the spacetime diagram, all peculiar motion decelerates in the Hubble frame—including light, which asymptotically approaches the edge of the light cone.

Conversely, a negative $v_f$ would result in positive acceleration in the Hubble frame, which, according to the diagram, could only happen with time running in reverse! Further, would a body perpetually accelerating in the Hubble frame—which is to say the universe—be guaranteed to stay within the universe? Is deceleration the universe's way of ensuring that nothing can escape?

Additionally, looking at the relation for $H_f$ given by Eq. (163), a negative $v_f$ would result in $H_f$ being imaginary and thus ill-defined. For this and the above reasons, it's posited that $v_f$ only has physical meaning as a non-negative value.

A relation for the expansion parameter $H_f(r)$—as seen by observers separated by distance $r$—is given by Eq. (163), where the peculiar speed in this equation is

the value agreed upon by the observers—$v_f(r)$:

$$H_f(r) = \sqrt{\frac{v_f(r)}{c}} H_0 \ , \tag{181}$$

$$H_f(r)^2 = \frac{v_f(r)}{c} {H_0}^2 \ . \tag{182}$$

Plugging Eqs. (182) and (163) into Eq. (179) gives the following:

$$\frac{H_f(r)^2}{{H_0}^2} = \left( \frac{{H_f}^2}{{H_0}^2} - \frac{r}{ct_0} \right) \left( 1 + \left( \frac{{H_f}^2}{{H_0}^2} \right) \left( \frac{r}{ct_0} \right) \right)^{-1} \tag{183}$$

$$H_f(r)^2 = \frac{({H_f}^2 - \frac{rH_0}{c} {H_0}^2) {H_0}^2}{({H_0}^2 + \frac{rH_0}{c} {H_f}^2)} \ , \tag{184}$$

$$H_f(r) = H_0 \sqrt{\frac{{H_f}^2 - \frac{rH_0}{c} {H_0}^2}{{H_0}^2 + \frac{rH_0}{c} {H_f}^2}} \ . \tag{185}$$

Hence, in a frame with peculiar speed $v_f$ and expansion parameter $H_f$, Eq. (185) gives the relative expansion parameter $H_f(r)$ as a function of distance $r$. Notice that, similar to Eq. (180), as $r$ goes to zero, $H_f(r)$ goes to the frame expansion parameter $H_f$. Thus, $H_f(0) = H_f$.

### 1. *Frame Extent $x_0$*

Here, a new parameter $x_0$, termed the "frame extent", is introduced that is defined as the distance where $H_f(r)$ goes to zero. The frame extent $x_0$ is derived via Eq. (185) as follows:

$$\begin{aligned} {H_f}^2 - \frac{x_0 H_0}{c} {H_0}^2 &= 0 \ , \\ x_0 &= \frac{c {H_f}^2}{{H_0}^3} \ . \end{aligned} \tag{186}$$

Notice, for light, which sees an expansion parameter of $H_0$, Eq. (186) reduces to Eq. (112)—where $x_0$ goes to $r_0$:

$$\begin{aligned} x_0 &= \frac{c \cancel{{H_0}^2}}{\cancel{{H_0}^3}} \ , \\ x_0 = r_0 &= \frac{c}{H_0} \ . \end{aligned}$$

Thus, the upper limit of the frame extent $x_0$ is the size of the universe $r_0$. The lower limit of $x_0$ is zero, which is seen with a frame expansion parameter $H_f$ of zero.

Note that there is a difference between the frame extent $x_0$ and the frame size $r_f$: $x_0$ is an observable metric, whereas $r_f$ is conceptual. With Eqs. (159) and (112), restated below, $r_f$ relates to $x_0$ as follows:

$$\begin{aligned} r_f &= r_0 \frac{H_f}{H_0} \ , \\ r_0 &= \frac{c}{H_0} \ , \\ r_f &= \frac{c H_f}{{H_0}^2} \ , \\ r_f \frac{H_f}{H_0} &= \frac{c {H_f}^2}{{H_0}^3} = x_0 \ , \\ r_f H_f &= x_0 H_0 \ . \end{aligned} \tag{187}$$

Looking at Eq. (187), with $H_f$ being less than or equal to $H_0$, the frame extent $x_0$ must be less than or equal to the frame size $r_f$. As $H_f$ goes to $H_0$, $r_f$ goes to $x_0$; and as $H_f$ goes to $H_0$, both $r_f$ and $x_0$ go to $r_0$. As $H_f$ goes to zero—looking at Eqs. (159) and (187)—both $r_f$ and $x_0$ go to zero.

With Eq. (107), Eq. (187) further equates to:

$$r_f H_f = x_0 H_0 = v_f \ . \tag{188}$$

Thus, in relation to $r_f$, $x_0$ is the distance in the Hubble frame where the rate of expansion $v_f$ is equivalent to the rate of expansion of the moving frame at $r_f$. Keep in mind that $v_f$ is also the peculiar speed of the moving frame in the Hubble frame.

### 2. *Relative Frame Constant $k_f(r)$*

If measuring the expansion parameter of the parent frame across a distance can result in a relative value—described by $H_f(r)$, which deviates from $H_f$, where does this leave frame constant $k_f$?

Recall from Section X that the positions and motions of the particles comprising a system have no bearing on the expansion parameter of the frame containing the system. The expansion parameter is a property of the frame alone.

This is still the case in the present situation. Further, it is still true that all particles in the system have the same frame constant $k_f$, which is defined by Eq. (109) as the expansion parameter per unit mass. Thus $k_f$ can be calculated by dividing the frame expansion parameter $H_f$ by the total system mass $m_t$. This relation still holds as well.

The frame expansion parameter $H_f$ remains in effect and is distributed across all particles in the system—as described by Eq. (109). In relation to the peculiar speed of the frame, any point in the frame could be considered as the instantaneous "origin"—where $v_f(r) = v_f(0) = v_f$. Thus, any single point would see the frame having an expansion parameter of $H_f(r) = H_f(0) = H_f$. Because every particle in the system agrees on the frame's expansion parameter, it can be imagined that they all have the same state—which is to say the same frame constant $k_f$.

However, while particles *in isolation* have the same

frame constant $k_f$, akin to $H_f(r)$, a first particle will see a second particle in the system—at a distance $r$—as having a smaller, relative frame constant $k_f(r)$. Reciprocally, the second particle will see the first particle as having this same frame constant—$k_f(r)$. Building on Eq. (109), a relation for $k_f(r)$ is as follows:

$$k_f(r) = \frac{H_i(r)}{m_i} = \frac{H_f(r)}{m_t} \ . \tag{189}$$

If the relative expansion parameter $H_f(r)$ varies with distance—with one particle seeing another as existing in a relative frame that varies with distance—is it possible that $H_f(r)$ also varies with time and speed?

Looking at Eq. (163), $H_f$ is already a function of time and speed—$H_0$ and $v_f$. Recall that $H_0$ is defined as the inverse of the Hubble time $t_0$ and thus, by definition, changes with time—asymptotically approaching zero. $v_f$ is the peculiar speed relative to the Hubble frame and asymptotically approaches zero as well. Recall that inertial frames with non-zero peculiar speeds are always decelerating in the Hubble frame.

Thus, the expansion parameter $H_f$ of a moving frame decreases over time—asymptotically approaching zero. It's not unreasonable, then, to imagine that the expansion parameter would decrease over distance as well—as described by relative expansion parameter $H_f(r)$. **Importantly, like $H_f$, $H_f(r)$ is a property of the frame and not its contents.**

Again, particles in isolation will all still measure the parent frame as having an expansion parameter of $H_f$—regardless of their positions and velocities relative to the frame. It's only when two particles, separated by a distance, measure the frame in unison that they see a relative value $H_f(r)$, which differs from the frame parameter $H_f$. Therefore, the frame's relative expansion parameter weakens with time *and* distance. Hence, measuring the frame at different times and across varying distances will give disparate results.

Note that while $H_f$ *will* diminish over time, the rate of change of $H_0$ and $v_f$ in Eq. (163) is negligible—as evidenced by $\dot{H}_0$ in Eq. (115), which calculates to an extremely small rate. To put this number in perspective: In another 13.8 billion years—the estimated age of the universe—the Hubble parameter will have not quite dropped from 70 to 69 km s$^{-1}$ Mpc$^{-1}$.

### 3. *A 10-Mpc Rotation Curve*

Fig. 13 shows the rotation curve of a simulated galaxy that extends out to 10 Mpc. The curve was generated identically to the other curves herein—via Eq. (70)—but with $H_f$ in this equation having been replaced by $H_f(r)$—as given by Eq. (185).

The cyan line in Fig. 13 plots the curve for a galaxy with only a bulge—no stellar and gas disks. The blue line with small dashes plots the curve for the case where the equivalent galaxy mass is concentrated at a point. The parameters for this galaxy are nearly identical to those of the Milky Way:

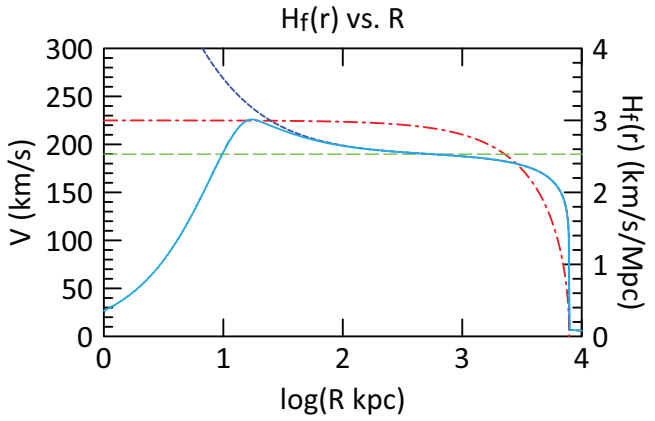


FIG. 13. A simulated galaxy with only a bulge. The net rotation curve is drawn as a solid cyan line. The blue line with small dashes is the rotation curve with the galaxy mass concentrated at a point. The green dashed line plots $v_{flat}$, and the red dash-dot line plots $H_f(r)$ vs. distance.

$$\begin{aligned} m_t &= 1.67 \times 10^{41}\,\text{kg} \ , \\ H_f &= 3.0\,\text{km}\,\text{s}^{-1}\text{Mpc}^{-1} \ , \\ v_{flat} &= 190\,\text{km}\,\text{s}^{-1} \ , \\ x_0 &= 7.87\,\text{Mpc} \ . \end{aligned}$$

The red dash-dot line plots $H_f(r)$ vs. distance. Notice that $H_f(r)$ remains substantially flat out to 1 Mpc—where it has only dropped from 3.0 to 2.8 km s$^{-1}$ Mpc$^{-1}$. From 1 to 6 Mpc, $H_f(r)$ declines nearly linearly to 1.5 km s$^{-1}$ Mpc$^{-1}$. Beyond 6 Mpc, there is a rapid decline to zero at 7.87 Mpc, which is the value of frame extent $x_0$ for the parent frame—as calculated via Eq. (185). At this distance and beyond, $H_f(r)$ is zero, and the gravitational acceleration between particles in the frame is purely Newtonian.

The green dashed line plots $v_{flat}$ for the galaxy, which calculates to 190 km s$^{-1}$. The rotation curve is nearly flat from 100 kpc to 2.8 Mpc. At 100 kpc, the rotational velocity is 5% above $v_{flat}$ (at around 200 km/s). By 2.8 Mpc, the velocity has fallen to 5% below $v_{flat}$ (at roughly 180 km/s), which constitutes a slope of -7.4 km s$^{-1}$ Mpc$^{-1}$.

Referring back to the isolated galaxies with rotation curves that remain substantially flat out to 1 Mpc—presented by Mistele et al. [17], it's predicted that, if the technology existed to look beyond 1 Mpc, these curves would eventually show declines similar to the curve of Fig. 13. Further, it's predicted that there's a distance—the frame extent $x_0$—for each curve where the rotational velocity effectively drops to zero.

Notably, with $x_0$ being a function of the frame's expansion parameter $H_f$, galaxies with small expansion parameters will have smaller frame extents and rotation curves that reflect this limit. This leaves the question: What is

TABLE I. A Sample of Galaxies With Relative Expansion Parameters at $r_{max}$.

| Galaxy | $H_f$ (km s$^{-1}$ Mpc$^{-1}$) | $v_{flat}$ (km s$^{-1}$) | $r_{max}$ (kpc) | $H_f(r)$ (km s$^{-1}$ Mpc$^{-1}$) | $v'_{flat}$ (km s$^{-1}$) | $x_0$ (kpc) |
|---|---|---|---|---|---|---|
| Cam B | .07 | 10.7 | 1.68 | .055 | 10.0 | 4.28 |
| NGC 7793 | .35 | 54.7 | 7.97 | .337 | 54.1 | 107 |
| NGC 2366 | 1.3 | 47.3 | 6.02 | 1.297 | 47.2 | 1480 |
| NGC 0055 | 1.3 | 74.2 | 13.36 | 1.29 | 74.1 | 1480 |
| NGC 6789 | 3.0 | 35.5 | .73 | 3.0 | 35.5 | 7870 |
| UGC 07524 | 3.0 | 82.9 | 10.50 | 3.0 | 82.9 | 7870 |

the consequence of not having corrected for distance (via Eq. (185)) on the rotation curves of Appendix XXIV—especially those with small expansion parameters?

Table I shows a sample of galaxies with the relative parameter $H_f(r)$ calculated at $r_{max}$—with $r_{max}$ marking the extent of the rotation curve. Also included in the table is $v'_{flat}$, which is calculated via Eq. (167) using $H_f(r)$ as opposed to $H_f$. Note that $v'_{flat}$ is purely illustrative. It's only meant to indicate any potential error in the rotation curve as a consequence of using a constant expansion parameter to generate the curve. As shown in Fig. 13, $v_{flat}$—as implied by the name—is flat with respect to distance by definition.

Looking at the galaxy with the smallest frame expansion parameter $H_f$ in Appendix XXIV—with an $H_f$ of .07 km s$^{-1}$ Mpc$^{-1}$—Cam B has an $H_f(r)$ that is 21% lower at .055 km s$^{-1}$ Mpc$^{-1}$. This, however, only translates to a 6% drop in rotational velocity at $r_{max}$—as rotational velocity is a function of $H_f$ raised to the power of 1/4—as given by Eq. (167).

Hence, in Table I, with Cam B having a $v'_{flat}$ of 10.0 vs. 10.7 for $v_{flat}$, it's surmised that the curve—as drawn in Appendix XXIV with a constant expansion parameter—is within the margin of error—especially given that this particular curve is a poor fit in the first place.

NGC 7793 has the next lowest $H_f$ in the sample at .35 km s$^{-1}$ Mpc$^{-1}$. Its $v'_{flat}$ is only 1% lower than $v_{flat}$—indicating that, as is the case with Cam B, the curve in Appendix XXIV is drawn with acceptable accuracy. The situation improves—the margin between $v'_{flat}$ and $v_{flat}$ decreases—for the remaining galaxies in the table with higher values of $H_f$. This could also be deduced by comparing $r_{max}$ for these galaxies with $x_0$. Qualitatively, looking at the table, when $x_0$ is an order of magnitude larger than $r_{max}$, it's reasonable to use a constant expansion parameter across the span of the rotation curve.

In summary, the expansion component of acceleration does not extend indefinitely but has a specific reach, and only within this range does it make a meaningful contribution to the motions of bodies. In galactic subsystems such as our Solar System, its effect is negligible and does not measurably contribute to the motions of bodies. Even out to 10 light-years, the expansion component is so small relative to the Newtonian component—orders of magnitude less—that it can safely be ignored. However, in the range of kpc to Mpc, the expansion component becomes dominant, but as frame extent $x_0$ is approached, this component rapidly drops to zero.

Upon consideration, the expansion component of acceleration *must* have a limited range. If rotation curves remained flat indefinitely, then the accelerating fields underpinning those curves would have to extend indefinitely as well. Were this the case, the pull between bodies across vast distances would be far too large for the universe to have the structure and dynamics we observe, where galaxies, on average, are moving apart at speeds that increase with distance.

## XIX. DYNAMIC MASS

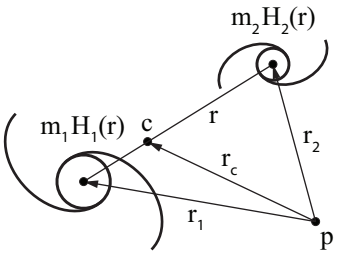


FIG. 14.

While the range of the expansion component is finite, it can still extend far enough to affect nearby galaxies. For example, the simulated galaxy of Section XVIII with a frame expansion parameter $H_f$ of 3 km s$^{-1}$ Mpc$^{-1}$ has a frame extent $x_0$ of 7.87 Mpc, which encompasses most if not all of the galaxies in the Local Group. It's not unreasonable to imagine that 3 km s$^{-1}$ Mpc$^{-1}$ would be near the average expansion parameter for galaxies. Recall that the Milky Way has an estimated $H_f$ of 3.04 km s$^{-1}$ Mpc$^{-1}$; and as shown in Fig. 10, an $H_f$ of 3.09 km s$^{-1}$ Mpc$^{-1}$ corresponds to the MOND constant $a_0$, which has been checked against a large catalog of galaxies.

In Section XVII, it was reasoned that the main galaxies of the Local Group—the Milky Way, M31, and M33, taken in any combination, do not comprise a system as defined in the section. Yet, they are gravitationally bound—with each having a frame extent of roughly 8 Mpc—corresponding to a frame expansion parameter on the order of 3 km s$^{-1}$ Mpc$^{-1}$.

To explore how these galaxies influence each other, refer to Fig. 14, which shows two galaxies of different mass, expansion parameter, and frame constant moving in the Hubble frame. Note that there is no frame expansion parameter $H_f$ for the galaxy pair because the pair does not comprise a system! Recall from Section XVII that all particles in a system, by definition, must have the same frame constant $k_f$. The frame constant of galaxy one in the figure is $H_1/m_1$, whereas the frame constant of galaxy two is $H_2/m_2$.

The acceleration with respect to galaxy one at distance $r$ is given by Eqs. (185) and (70):

$$H_1(r) = H_0\sqrt{\frac{{H_1}^2 - \frac{rH_0}{c}{H_0}^2}{{H_0}^2 + \frac{rH_0}{c}{H_1}^2}} \ , \tag{190}$$

$$a_1 = \frac{m_1 G}{r}\left(\frac{1}{r} + \frac{2\sqrt{cH_1(r)}}{\sqrt{m_1 G}}\right) \ . \tag{191}$$

Here, it's assumed that galaxies one and two are sufficiently far apart that they can be considered as point masses.

The acceleration with respect to galaxy two at distance $r$ is thus:

$$H_2(r) = H_0\sqrt{\frac{{H_2}^2 - \frac{rH_0}{c}{H_0}^2}{{H_0}^2 + \frac{rH_0}{c}{H_2}^2}} \ , \tag{192}$$

$$a_2 = \frac{m_2 G}{r}\left(\frac{1}{r} + \frac{2\sqrt{cH_2(r)}}{\sqrt{m_2 G}}\right) \ . \tag{193}$$

Looking at Eqs. (191) and (193), the following inequality is apparent:

$$m_2 a_1 \neq m_1 a_2 \ .$$

Here, it's presumed that particles external to a system see the same acceleration as particles within the system. The particles of galaxy two experience an acceleration $a_1$ toward galaxy one and likewise, the particles of galaxy one experience an acceleration $a_2$ toward galaxy two.

Thus, referring to Fig. 14, an inertial observer at point $p$ would not see point $c$—the barycenter of galaxies one and two—maintaining constant velocity over time:

$$\frac{d}{dt}(\vec{r}_c) \neq 0 \ .$$

There is, however, a "dynamic mass" ${m_1}'$ and dynamic mass ${m_2}'$ such that the following equation is satisfied:

$${m_2}' a_1 = {m_1}' a_2 \ . \tag{194}$$

With Eq. (194), relations for ${m_1}'$ and ${m_2}'$ are as follows:

$$\frac{{m_1}'}{{m_2}'} = \frac{a_1}{a_2} \ ,$$

$$\frac{{m_1}'}{{m_2}'} = \frac{\frac{m_1 G}{r}\left(\frac{1}{r} + \frac{2\sqrt{cH_1(r)}}{\sqrt{m_1 G}}\right)}{\frac{m_2 G}{r}\left(\frac{1}{r} + \frac{2\sqrt{cH_2(r)}}{\sqrt{m_2 G}}\right)} \ ,$$

$$\frac{{m_1}'}{{m_2}'} = \frac{m_1\left(1 + \frac{2r\sqrt{cH_1(r)}}{\sqrt{m_1 G}}\right)}{m_2\left(1 + \frac{2r\sqrt{cH_2(r)}}{\sqrt{m_2 G}}\right)} \ ,$$

$${m_1}' = m_1\left(1 + \frac{2r\sqrt{cH_1(r)}}{\sqrt{m_1 G}}\right) \ , \tag{195}$$

$${m_2}' = m_2\left(1 + \frac{2r\sqrt{cH_2(r)}}{\sqrt{m_2 G}}\right) \ . \tag{196}$$

With Eq. (185), restated below, and Eqs. (195) and (196), a general relation for dynamic mass $m'$—as a function of baryonic mass $m$, frame expansion parameter $H_f$, and distance $r$—is as follows:

$$H_f(r) = H_0\sqrt{\frac{{H_f}^2 - \frac{rH_0}{c}{H_0}^2}{{H_0}^2 + \frac{rH_0}{c}{H_f}^2}} \ ,$$

$$m' = m\left(1 + \frac{2r\sqrt{cH_f(r)}}{\sqrt{mG}}\right) \ . \tag{197}$$

Looking at Eq. (197), the dynamic mass $m'$ is comprised of two components—the baryonic term $m$ and the dynamic term $m(2r\sqrt{cH_f(r)}/\sqrt{mG})$. Recognize that the dynamic term is only apparent with respect to a second mass at a distance $r$—and thus is only meaningful in the context of Eq. (194). The implication of this equation is that the momentum of two interacting particles—in the general case where those particles may or may not belong to the same system—is only conserved in the case where those masses are considered as dynamic—as described by Eqs. (185) and (197). As will be shown below, the dynamic terms in Eq. (194) cancel out when the two masses are part of the same system.

The logic behind dynamic mass is thus: A galaxy or, generally, a system of bodies, with a frame expansion parameter $H_f$ of zero, has a dynamic mass $m'$ that is equivalent to its baryonic mass $m$. All of the motions in this system are purely Newtonian. A system, however, with a non-zero $H_f$, has internal motions where bodies have elevated speeds that don't comport with the observable mass. Such a system could be construed as having missing mass or "dark mass"—where the larger the expansion parameter $H_f$, the greater the mass discrepancy. Thus, the expansion parameter of a given system can be thought of as amplifying the system's mass and increasing its inertia.

The equations for dynamic mass are applicable *within* systems as well as between systems. For example,

Eq. (194)—as applied to two bodies within and part of a system—resolves as follows:

$$m_2{}'a_1 = m_1{}'a_2 \ ,$$
$$m_2\left(1+\frac{2r\sqrt{cH_2(r)}}{\sqrt{m_2G}}\right)a_1 = m_1\left(1+\frac{2r\sqrt{cH_1(r)}}{\sqrt{m_1G}}\right)a_2 \ ,$$
$$k_f(r) = \frac{H_1(r)}{m_1} = \frac{H_2(r)}{m_2} \ ,$$
$$\cancel{m_2\left(1+\frac{2r\sqrt{ck_f(r)}}{\sqrt{G}}\right)a_1 = m_1\left(1+\frac{2r\sqrt{ck_f(r)}}{\sqrt{G}}\right)a_2} \ ,$$
$$m_2a_1 = m_1a_2 \ .$$

Bodies within a system all see the same frame expansion parameter $H_f$ and have the same frame constant $k_f$. Two bodies separated by distance $r$, in unison, see the frame as having a relative expansion parameter $H_f(r)$, and each body sees the other as having a relative frame constant $k_f(r)$, and both agree on its value. Thus, the dynamic terms of $m_1{}'$ and $m_2{}'$ cancel, and Eq. (194) reduces to the familiar Third Law of Motion—with non-dynamic mass terms.

If, however, $m_1{}'$ and $m_2{}'$ represent bodies or particles in separate systems with different relative frame constants $k_1(r)$ and $k_2(r)$, the dynamic terms of these masses do not cancel:

$$m_2{}'a_1 = m_1{}'a_2 \ ,$$
$$m_2\left(1+\frac{2r\sqrt{cH_2(r)}}{\sqrt{m_2G}}\right)a_1 = m_1\left(1+\frac{2r\sqrt{cH_1(r)}}{\sqrt{m_1G}}\right)a_2 \ ,$$
$$\left(k_1(r)=\frac{H_1(r)}{m_1}\right) \neq \left(k_2(r)=\frac{H_2(r)}{m_2}\right) \ ,$$
$$m_2\left(1+\frac{2r\sqrt{ck_2(r)}}{\sqrt{G}}\right)a_1 = m_1\left(1+\frac{2r\sqrt{ck_1(r)}}{\sqrt{G}}\right)a_2 \ .$$

Including the $a_1$ and $a_2$ terms, gives this:

$$\frac{m_1m_2G}{r^2}\left(1+\frac{2r\sqrt{cH_2(r)}}{\sqrt{m_2G}}\right)\left(1+\frac{2r\sqrt{cH_1(r)}}{\sqrt{m_1G}}\right) = \frac{m_1m_2G}{r^2}\left(1+\frac{2r\sqrt{cH_1(r)}}{\sqrt{m_1G}}\right)\left(1+\frac{2r\sqrt{cH_2(r)}}{\sqrt{m_2G}}\right) \ .$$

Notice that, beyond the frame extents of $m_1$ and $m_2$—where $H_1(r)$ and $H_2(r)$ go to zero, the above equation resolves to the familiar relation for Newtonian gravity:

$$\frac{m_1m_2G}{r^2}\left(1+\frac{2r\sqrt{\cancelto{0}{cH_2(r)}}}{\sqrt{m_2G}}\right)\left(1+\frac{2r\sqrt{\cancelto{0}{cH_1(r)}}}{\sqrt{m_1G}}\right) = \frac{m_1m_2G}{r^2}\left(1+\frac{2r\sqrt{\cancelto{0}{cH_1(r)}}}{\sqrt{m_1G}}\right)\left(1+\frac{2r\sqrt{\cancelto{0}{cH_2(r)}}}{\sqrt{m_2G}}\right) \ ,$$
$$\frac{m_1m_2G}{r^2} = \frac{m_1m_2G}{r^2} \ .$$

The center of two dynamic masses is termed the "dynamic barycenter". Referring back to Fig. 14, if point $c$ were the dynamic barycenter of galaxies one and two—which is to say the center of $m_1{}'$ and $m_2{}'$, an observer at point $p$ *would* see point $c$ maintaining constant velocity over time. However, with $m_1{}'$ and $m_2{}'$ being dynamic, the ratio of distances from $c$ to each galaxy would evolve over time.

If the galaxies of the Local Group are bound within the frame extents of the three main galaxies—at roughly 8 Mpc, it's reasonable to imagine that this is the case for other galaxy groups and clusters. When thinking about larger structures, it's not necessary that every galaxy reside within the frame extent of every other galaxy. In other words, galaxies or groups can be chained together, where only the frame extents of individual links (or series of links) overlap. Extrapolating further, is it possible that the large-scale structures we observe in the universe—such as filaments and walls—are the result of such chaining—a phenomenon that allows these structures to form and remain stable over billions of years?

## XX. MASS DENSITY OF THE UNIVERSE

Continuing the discussion from Section XIV, the mass $m_0$ of the universe is given by Eq. (150):

$$m_0 = \frac{cH_0{r_0}^2}{G} \ ,$$

where $H_0$ and $r_0$ are the expansion parameter and size of the universe, respectively, in the rest frame of an inertial observer.

As reasoned in Section XIV, all inertial observers should agree on the total mass of the universe $m_0$. And, as deduced in Section XIII, any given inertial observer—regardless of his peculiar speed—should perpetually see himself as being located at the center of the universe. A peculiar speed of zero is synonymous with being at rest in the Hubble frame—which is to say, at rest in the frame of the coincident Hubble coordinate.

It's posited that, with this and the above equation in mind, the contained mass $m_c$ at a given radius $r$ in the rest frame of a Hubble coordinate—where $r$ is a distance in the frame—is as follows:

$$m_c = \frac{cH_0r^2}{G} \ . \tag{198}$$

Eq. (198) describes an idealized case, termed the "ground state", where mass is evenly distributed, and the particles that comprise the contained mass are at rest in the Hubble frame. As discussed, particles at rest in the Hubble frame are moving in the Hubble flow. In the ground state, all particles move precisely in the Hubble flow—with peculiar speeds of zero. Thus, in the ground state, particles in the universe are electrically neutral, have zero kinetic energy relative to the Hubble frame,

and zero vibrational energy. This, in turn, applies to Eq. (150), which gives the net rest mass of the universe in the ground state.

In reality, however, particles and systems of particles—under the influence of gravity—are generally found to be in constant motion relative to the Hubble frame. This is termed the "dynamic state". However, as the scale at which the universe is observed increases, the universe appears increasingly homogeneous and isotropic. Bodies look to largely be moving in the Hubble flow—which is to say, at large scales, the structure of the universe approaches that described by the ground state. With this in mind, investigating the ground state and how this state evolves over time can inform an understanding of the dynamic state. In this section, it will be shown that the deconvolution of Eq. (198) can reveal important aspects of the ground state—mass density, how mass moves over time, and how mass is created in exchange for the expansion of space.

The speed $v$ of a coordinate at a distance $r$ in the rest frame of an inertial observer is given by Eq. (110). The derivative of this equation with respect to $r$ is as follows:

$$
\begin{aligned}
&v = rH_0 \ , \\
&\frac{dv}{dr} = H_0 + r\frac{dH_0}{dr} \ , && (199) \\
&\cancelto{0}{\frac{dv}{dt}}\frac{dr}{dr} = \frac{dr}{dt}\left(H_0 + r\frac{dH_0}{dr}\right) \ , && (200) \\
&\frac{dH_0}{dr} = -\frac{H_0}{r} \ . && (201)
\end{aligned}
$$

Notice that the left side of Eq. (200) goes to zero with the employment of Eq. (123)—which holds that the speed $v$ of a receding coordinate remains constant over time. Plugging Eq. (201) into Eq. (199) shows that $v$ remains constant over distance $r$ as well:

$$
\begin{aligned}
&\frac{dv}{dr} = H_0 + \cancel{r}\left(-\frac{H_0}{\cancel{r}}\right) \ , \\
&\frac{dv}{dr} = 0 \ . && (202)
\end{aligned}
$$

Taking the derivative of Eq. (198) with respect to $r$ gives the following:

$$
\begin{aligned}
&\frac{dm_c}{dr} = \frac{c}{G}\left(\frac{dH_0}{dr}r^2 + 2H_0 r\right) \ , \\
&\frac{dm_c}{dr} = \frac{c}{G}\left(-\frac{H_0}{\cancel{r}}\cancel{r^2} + 2H_0 r\right) \ , && (203) \\
&\frac{dm_c}{dr} = \frac{cH_0 r}{G} \ , && (204) \\
&\frac{dm_c}{dr} = \frac{cv_c}{G} \ . && (205)
\end{aligned}
$$

Plugging Eq. (201) into Eq. (203) gives Eq. (204). Plugging Eq. (110) into Eq. (204) resolves to Eq. (205)—the latter showing that $dm_c/dr$ is invariant with respect to distance *and time* for a given Hubble coordinate $v_c$. The reference frame of $m_c$ is a Hubble coordinate, and any given coordinate $v_c$ at a distance $r$ in this rest frame—that is receding according to Eq. (110)—is also a Hubble coordinate.

The area density $\rho_A$ of a layer as a function of $v_c$ derives from Eq. (205):

$$
\begin{aligned}
&dm_c = \frac{cv_c dr}{G} \ , \\
&A_c = 4\pi r^2 \ , \\
&dA_c = 8\pi r dr \ , \\
&\frac{dm_c}{dA_c} = \frac{cv_c \cancel{dr}}{8\pi G r \cancel{dr}} \ , \\
&\rho_A = \frac{cv_c}{8\pi G r} \ , && (206) \\
&\rho_A = \frac{cv_c H_0}{8\pi G r H_0} = \frac{c\cancel{v_c} H_0}{8\pi G \cancel{v_c}} \ , && (207) \\
&\rho_A = \frac{cH_0}{8\pi G} \ . && (208)
\end{aligned}
$$

Eq. (206) shows that $\rho_A$ is a function of $v_c$ and $r$. Multiplying Eq. (206) by $H_0/H_0$ gives Eq. (207), which—via Eq. (110)—reduces to Eq. (208). Interestingly, recalling Eq. (113), Eq. (208) shows that the area density $\rho_A$ in a given frame is purely a function of time in that frame—with area density decreasing over time. This aligns with the Hubble flow, where the mass of the universe at a large scale is observed to be spreading apart—decreasing in area density.

With Eq. (205) and the relation for differential volume $dV$, the volume density (or density) $\rho$ is thus:

$$
\begin{aligned}
&dV_c = 4\pi r^2 dr \ , \\
&\frac{dm_c}{dV_c} = \frac{cv_c dr}{4\pi G r^2 dr} = \frac{cH_0 \cancel{r} \cancel{dr}}{4\pi G \cancel{r^2} \cancel{dr}} \ , \\
&\rho = \frac{cH_0}{4\pi G r} = \frac{{cH_0}^2}{4\pi G r H_0} \ , \\
&\rho = \frac{{cH_0}^2}{4\pi G v_c} \ , && (209) \\
&\rho = \frac{2H_0}{v_c}\rho_A \ . && (210)
\end{aligned}
$$

Eq. (209) gives the volume density $\rho$ at coordinate $v_c$ as a function of $v_c$. Eq. (210) gives density $\rho_c$ as a function of area density $\rho_A$. Depth, in these two equations, is embodied by the Hubble coordinate $v_c$, which is a more convenient measure of distance than $r$—as it remains constant over time. Compared with the equation for $\rho_A$—where area density is decreasing along with $H_0$ (as described by Eq. (115)), $\rho$ decreases by the square of $H_0$, which accounts for mass spreading out both tangentially and radially.

Comparing the average density contained by coordi-

nate $v_c$ to the density at $v_c$ gives this:

$$\rho_{ave} = \frac{m_c}{V_c} = \frac{cH_0 r^2}{G}\frac{3}{4\pi r^3} ,$$
$$\rho_{ave} = \frac{3cH_0{}^2}{4\pi G v_c} = 3\rho . \qquad (211)$$

The average density $\rho_{ave}$ is simply the mass contained by a volume divided by that volume. Eq. (211) shows that the average density in the volume is three times the density at the Hubble coordinate defining the volume; and thus, in the ground state, there is a gradient in density with respect to distance.

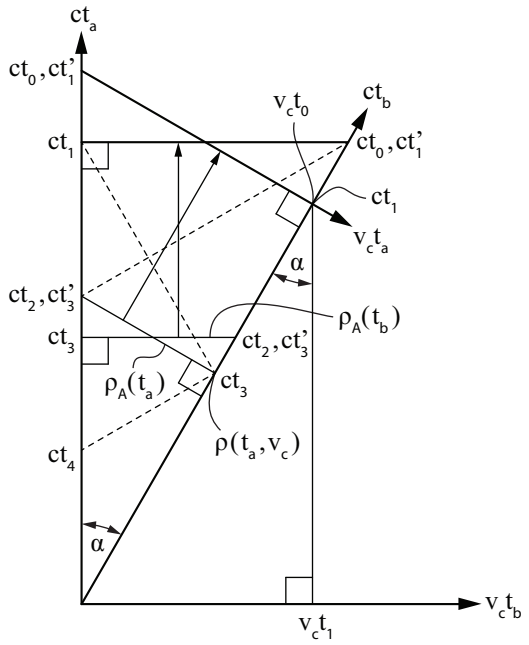


FIG. 15.

Fig. 15 is a spacetime diagram that relates time and distance in the rest frame of a Hubble coordinate to that of a moving frame. In this case, the moving frame $b$ is a Hubble coordinate with speed $v_c$. The time and distance axes of the rest frame $a$ are $ct_a$ and $v_c t_a$, respectively; and the time and distance axes of the moving frame are $ct_b$ and $v_c t_b$. The geometry of the diagram is such that two principles are satisfied: One, the speed between a fixed point in the rest frame and a fixed point in the moving frame is the same in both frames; and two, the speed of light calculates to $c$ in both frames. Similar to the spacetime diagrams of Figs. 9 and 12, the world lines of Hubble coordinates $a$ and $b$ converge at the universe's initial event. As before, $t_0$ is the Hubble time in the rest frame.

From the perspective of an observer in the rest frame, the moving frame will have traveled a distance of $v_c t_0$ *in the rest frame*. Here, $t_0$ corresponds to $t'_1$, which is timespan $t_1$ in the moving frame *as observed in the rest frame*. As taught by special relativity, a clock moving in the rest frame ticks more slowly than an identical clock that is static in the rest frame. This is known as "time dilation". The speed of a clock is measured in tick events per unit time. As the denominator in this fraction grows larger, the clock rate slows. Notice in the diagram that the span of time $t'_1$—referred to as "coordinate time"—is longer than $t_1$, which is "proper time" in the moving frame; and thus, *in the rest frame*, the moving clock is ticking slower.

An observer in the moving frame, counting off ticks on his clock, would calculate that he traveled a distance of $v_c t_1$ in the rest frame. An observer in the rest frame, *looking at his clock*—and with $t_1$ associated with an event that both observers agree upon—would calculate that the moving frame traveled a longer distance: $v_c t_0$. Thus, from the perspective of the moving observer, distances in the frame of travel, in the direction of travel, are "length contracted" relative to what an observer at rest in the frame of travel would measure.

In the diagram, distance and time are orthogonal. Specifically, distance in the rest frame—as measured by an observer in the moving frame—is orthogonal to time in the rest frame. In congruence, distance in the rest frame—as measured by an observer in the rest frame—is orthogonal to time in the moving frame. This geometry allows observers in both frames to agree on their relative speed and to agree on the speed of light.

Distance in the rest frame along the $v_c t_a$ axis increases at speed $v_c$ as follows:

$$\sin(\alpha) = \frac{v_c t_0}{c t_0} = \frac{v_c}{c} .$$

In the moving frame, along the $v_c t_b$ axis, distance also increases at speed $v_c$:

$$\sin(\alpha) = \frac{v_c t_1}{c t_1} = \frac{v_c}{c} .$$

Thus, speed $v_c$ is consistent in the two frames.

Light (represented by dashed lines) emitted by an observer in the rest frame at $t_2$ travels through time a span of $c(t_1 - t_2)$ to reach an observer in the moving frame. The distance in the rest frame that this beam of light will have traveled is represented by the line drawn between $ct_2$ on the $ct_a$ axis and $ct_3$ on the $ct_b$ axis. Notice that the lengths of these lines are equivalent, which is to say that light travels equal lengths through space and time.

In the moving frame, this beam will have traveled through time a span of $c(t_0 - t_3)$ and a distance in space depicted by the line between $ct_1$ on the $ct_a$ axis and $ct_0$ on the $ct_b$ axis. Again, these distances are equivalent; thus, both observers—in the rest frame and the moving frame—measure light as traveling at $c$.

Distance in the rest frame can be measured by bouncing light off a mirror. This is shown in the diagram by the dashed line from $ct_4$ on the $ct_a$ axis to $ct_3$ on the $ct_b$ axis, which reflects back to $ct_1$ on the $ct_a$ axis. Dividing the total travel time by two, an observer would

conclude that the beam of light hit the mirror at time $t_2$ and covered a distance in space (and time) of $c(t_2 - t_4)$.

Imagine, further, two lights in the rest frame offset by a given distance. In the diagram, one light is at the midpoint of the solid line connecting $ct_2$ on the $ct_a$ axis and $ct_3$ on the $ct_b$ axis, and the second light is at the endpoint of this line. Both lights are timed to flash simultaneously at time $t_2$ in the rest frame. One path of light would trace the dashed line from $ct_3$ on the $ct_b$ axis to $ct_1$ on the $ct_a$ axis. The other path (not drawn) from the midpoint would be parallel to this dashed line and would be detected by the observer exactly midway between $t_2$ and $t_1$. The observer—accounting for distance—would conclude that both lights flashed simultaneously. Thus, it can be said that all events in parallel with the $v_c t_a$ axis are simultaneous in the rest frame; and by the same logic, all events parallel with the $v_c t_b$ axis are simultaneous in the moving frame.

Under the principle that the laws of physics should be consistent between frames $a$ and $b$, identical clocks at rest in each frame should tick at the same rate. Thus, it's imagined that observers in both frames would agree on the current age and mass of the universe—$t_0$ and $m_0$. Further, looking at Eq. (208)—which is a function of $H_0$ (and thus, $t_0$), both observers would see the universe—in its ground state—as having the same area density $\rho_A$ in relation to their respective clocks.

At a given point in time on the $ct_a$ axis, $\rho_A$, which is invariant with respect to distance, is constant along the $v_c t_a$ axis—the line on which events in frame $a$ are simultaneous. This line moves forward in time—with $\rho_A$ decreasing simultaneously at points along its length according to Eq. (208). Likewise, in frame $b$, $\rho_A$ is constant along the $v_c t_b$ axis. In the diagram, both lines of constant density move forward at the same rate in their respective frames.

With the understanding that there's nothing special about frames $a$ and $b$ in the diagram—as these two frames could represent any two Hubble coordinates in the universe, it's imagined that an observer in the rest frame of *any* Hubble coordinate in the universe would see a uniform area density extending indefinitely in all directions. This is in line with the cosmological principle, which holds that, at a large enough scale, the universe appears homogeneous and isotropic.

The volume density $\rho$ as given by Eq. (210), however, is a function of two parameters: time $t_0$ and speed $v_c$ of a distant Hubble coordinate—where $\rho$ is the density at coordinate $v_c$ at $t_0$ in the rest frame. Looking at the spacetime diagram, an observer in frame $a$, at local time $t_0$, would calculate the same density at the point where the $v_c t_a$ and $ct_b$ axes intersect—as an observer in frame $b$ would calculate at the intersection of $v_c t_b$ and $ct_a$—at $t_0$ in his frame. Both observers would attribute the same volume density to the other's coordinate.

Thus, in the ground state, density can only be calculated in the rest frame of a Hubble coordinate relative to a second distant Hubble coordinate. Moreover, observers in different rest frames at different speeds relative to a given coordinate would attribute different densities to that coordinate. This is analogous to length contraction, where physical distances are not absolute. It's concluded, therefore, that there is no absolute volume density in the universe. Volume density is relative to the speed of the Hubble coordinate at which density is calculated.

## XXI. GROUND STATE OF THE UNIVERSE

Taking the derivative of Eq. (198) with respect to time gives this:

$$\frac{dm_c}{dt} = \frac{c}{G}\left(\frac{dH_0}{dt}r^2 + 2H_0 r\frac{dr}{dt}\right) , \tag{212}$$

$$\dot{m}_c = \frac{c}{G}\left(-{H_0}^2 r^2 + 2H_0 r\frac{dr}{dt}\right) , \tag{213}$$

$$\dot{m}_c = \frac{c}{G}\left(-{v_c}^2 + 2{v_c}^2\right) , \tag{214}$$

$$\dot{m}_c = \frac{c{v_c}^2}{G} . \tag{215}$$

Eq. (115) is plugged into Eq. (212), which gives Eq. (213); and Eq. (110) is plugged into Eq. (213)—allowing $\dot{m}_c$ to be described in terms of $v_c$. Notice that, similar to Eq. (156) (which gives the power of the universe), the rate of mass change contained by a radius $r$—or said alternatively, encapsulated within a given Hubble coordinate $v_c$—is constant with respect to time. In the case where the Hubble coordinate demarks the extent of the universe—where $v_c$ goes to $c$, Eq. (215) reduces to Eq. (156).

Alternatively, $\dot{m}_c$ can be defined as a function of $m_c$ as follows:

$$\begin{aligned} m_c &= \frac{cH_0 r^2}{G}\frac{H_0}{H_0} , \\ m_c &= \frac{c{v_c}^2}{G}\frac{1}{H_0} , \\ \dot{m}_c &= m_c H_0 . \end{aligned} \tag{216}$$

The implication of Eqs. (215) and (216) is that the mass contained by any Hubble coordinate is increasing over time. It, thus, has to be concluded that the mass of the universe is continuously increasing everywhere.

This can be visualized in Fig. 16, which shows the mass $m_c$ contained by a given Hubble coordinate $v_c$ depicted as the area $A_c$ of a rectangle with side lengths of $(c/G)v_c$ and $r$:

$$m_c = A_c = \frac{c}{G}v_c \cdot r . \tag{217}$$

Line $dm_c/dr$ vs. $v_c$ is simply a plot of Eq. (205). Eq. (217) is derived by plugging Eq. (110) into Eq. (198).

As shown in the figure, line $dm_c/dr$ vs. $v_c$ maintains the same slope over time. The only movement in Fig. 16 is along $r(t)$. At the birth of the universe—when $r_0$ *and*

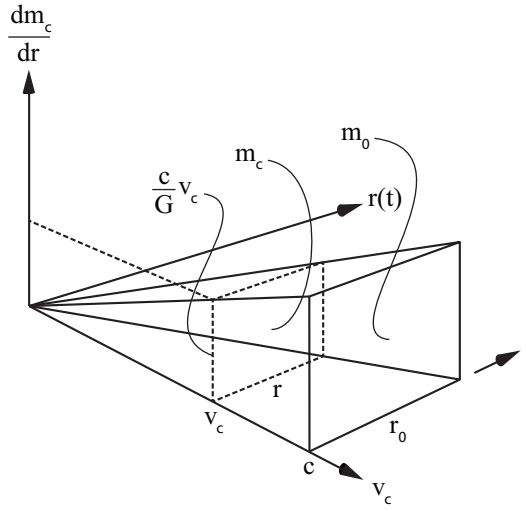


FIG. 16.

$t_0$ are zero—the area of the rectangle at $c$ is zero—along with all other rectangles along the $v_c$ axis. As time progresses and the universe expands, these rectangles increase in area—representing the increase in mass across the span of Hubble coordinates from 0 to $c$.

Taking the partial derivative of Eq. (198) with respect to $r$—holding time constant—gives this:

$$\frac{\partial m_c}{\partial r} = \frac{2cH_0 r}{G} \ . \tag{218}$$

With $H_0$ defined as the inverse of $t_0$, constant time translates to a constant expansion parameter $H_0$.

To visualize how $\partial m_c/\partial r$ relates to $dm_c/dr$, refer to Fig. 17, which shows the $r(t)$–$dm_c/dr$ plane of Fig. 16 for a given Hubble coordinate $v_c$.

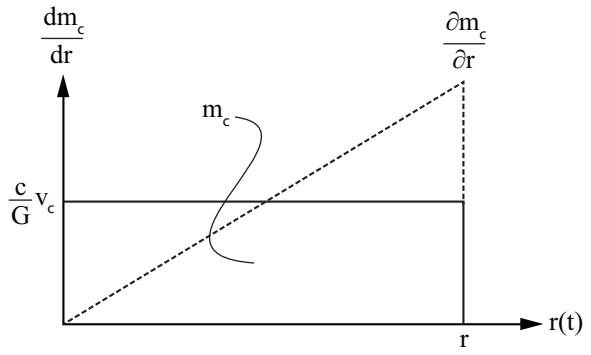


FIG. 17.

While the full derivative of $m_c$ with respect to $r$, $dm_c/dr$—where $r$ represents a moving coordinate—is constant over distance *and time*, the partial derivative $\partial m_c/\partial r$ increases linearly with $r$. Notice that in both cases, the area under the curve gives the contained mass $m_c$.

Alternatively, the partial derivative of Eq. (198) with respect to time—at a constant $r$—is thus:

$$\begin{aligned} m_c &= \frac{cH_0 r^2}{G} \ , \\ \frac{\partial m_c}{\partial t} &= \frac{c}{G}\frac{dH_0}{dt} r^2 \ , \\ \frac{\partial m_c}{\partial t} &= \frac{-cH_0{}^2 r^2}{G} \ , \qquad (219) \\ \frac{\partial m_c}{\partial t} &= \frac{-cv_c{}^2}{G} \ , \qquad (220) \\ \frac{\partial m_c}{\partial t} &= -m_c H_0 \ . \qquad (221) \end{aligned}$$

Note the negative sign in Eqs. (219) and (220)—indicating that a volume fixed at $r$ actually loses mass, which implies that mass is moving across $r$. Interestingly, Eq. (221) shows that the rate of loss in this control volume is equivalent to the rate of mass–gain in an expanding volume with a moving $r$—the latter given by Eq. (216).

A fractional mass $\Delta m_c$ moving across a small distance $\Delta r$ at speed $v_c$ has a mass-flow rate of $\dot{m}_c$:

$$\dot{m}_c = \frac{\Delta m_c v_c}{\Delta r} \ . \tag{222}$$

In differential form, Eq. (222) reduces as follows:

$$\begin{aligned} \dot{m}_c &= \frac{dm_c}{dr} v_c \ , \\ \dot{m}_c &= \frac{cv_c{}^2}{G} \ . \end{aligned}$$

Note the equivalence between the above mass-flow equation and Eq. (220), which indicates that the differential mass at a given Hubble coordinate is moving in concert with the coordinate at speed $v_c$. This movement applies to all Hubble coordinates, and thus, it's reasoned that all of the mass of the universe is moving in sync with these coordinates—which is to say, moving in the Hubble flow.

This mass flow describes the ground state—previously defined as the case where all particles comprising the mass of the universe are precisely in the Hubble flow with no particle having a non-zero peculiar speed—and where the mass at a given coordinate is distributed evenly across a surface defined by that coordinate.

However, Eq. (220) only accounts for the flow of existing mass across a boundary, but it doesn't account for the addition of mass, which is hypothetically increasing everywhere—as described by Eq. (215) and Fig. 16. Where and how is mass created?

### 1. *Creation of Space and Mass*

With Eq. (205), the fractional mass at two Hubble coordinates $v_1$ and $v_2$—where $v_2$ is slightly greater than

$v_1$—is thus:

$$\Delta m_1 = \frac{cv_1}{G}\Delta r \ , \tag{223}$$

$$\Delta m_2 = \frac{cv_2}{G}\Delta r \ . \tag{224}$$

Eqs. (223) and (224) confirm that the fractional mass across a minute distance $\Delta r$ remains constant over time and distance—assuming that $\Delta r$ remains constant, which is asserted here. Over time, as the distance between coordinates $v_1$ and $v_2$ increases, at a certain point, this distance will be greater than $\Delta r$—at which point, it's imagined that there is now space for a new coordinate.

The presumption here is that space does not expand continuously but in quanta—with each created quantum of space constituting a new coordinate. As reasoned in previous sections, mass is created as a consequence of this expansion. As space expands in quanta, mass is created in quanta; or alternatively said: Because the particles that make up matter could only be created in quanta—if they are manifested from expanding space, space must expand by quanta.

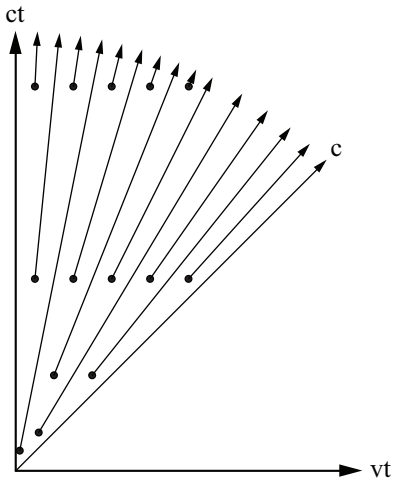


FIG. 18.

This mechanism of mass creation can be visualized in Fig. 18, which shows an array of Hubble coordinates fanning out. Black dots in the figure represent particles that are created in the spaces between these coordinates. The arrows emanating from these dots are the world lines of these particles and new Hubble coordinates created in concert. Notice that the world lines of coordinates created after the initial event all look to emanate from the initial event.

In Fig. 16, the increase in contained mass that is visualized as the growth of area $A_c$ can be imagined as occurring as a result of the coordinate density increasing along the $v_c$ axis. Expansion in $r$ creates room for additional coordinates, which, in turn, increases the mass contained by $r$.

Imagined another way, consider $\Delta m_1$ and $\Delta m_2$ as layers of an expanding onion. As a void grows between these layers—which constitutes expanding space, mass is created in unison with that expansion. Referring back to Eq. (206), the area density $\rho_A$ at a given Hubble coordinate $v_c$ decreases with $r$—which would be expected with a fixed mass being distributed over an increasing area. Importantly, new mass does not fill the voids within this expanding layer. The layer corresponds to an existing Hubble coordinate, and mass is only created upon the manifestation of a new coordinate—when a new layer is added to the onion.

If a particle is created in conjunction with a Hubble coordinate, there's no reason, upon creation, for this particle—at least, initially—to be moving relative to that coordinate. It's imagined that this is why there is a tendency for the matter of the universe to be moving in the Hubble flow. Mass is created in conjunction with Hubble coordinates and is initially at rest relative to these coordinates—which is to say at rest in the Hubble frame. These coordinates, however, are receding from each other, and thus, newly created mass will be moving in concert, which is to say, in the Hubble flow. But this leaves the following questions: Why would this motion persist? Why, under the influence of gravity, wouldn't the mass of the universe eventually reverse course and collapse in on itself?

### *2. Hubble Flow*

To recap, in the ground state, all particles created in the Hubble flow perpetually remain in the Hubble flow as they expand out in the rest frame of a Hubble coordinate at constant velocities. In the rest frame of a Hubble coordinate, at a given moment in time, the area density $\rho_A$ is invariant with respect to distance. This was shown by Eq. (208) and Fig. 15.

Further, if the universe is finite, which is deemed to be the case, an observer in the rest frame of a Hubble coordinate—moreover, *any* Hubble coordinate—will, thus, see himself as being located at the center of the universe. In the ground state, with time running reverse, not only will all particles in the universe converge on the observer's location, they will all converge at the same time—where $t_0 = 0$. Moreover, this will be the case for *any* observer in the rest frame of *any* Hubble coordinate. Thus, in the ground state, every particle sees itself at the center of the universe, and because mass, in the ground state, is homogeneous and isotropic, every particle is at the barycenter of all other particles.

At the barycenter, the gravitational fields of all surrounding particles cancel. Thus, when the universe is in the ground state, in the rest frame of *any* given particle, the net gravitational acceleration acting upon that particle is zero. Because this is the case for every particle in the universe, in the reference frame of a given particle, all other particles will continue to move indefinitely in the Hubble flow. Almost tautologically, because each particle sees all other particles moving in the Hubble flow, all

particles continue to move in the Hubble flow.

Importantly, in the ground state, a given particle does **not** recede from another particle because the space between those particles is expanding. Particles recede because they were created at rest in a dynamic frame—where any two particles separated by a distance will naturally be in motion relative to each other. A second particle will continue to move at constant velocity relative to the first because there are no net gravitational fields acting upon either. As these particles continue to drift apart, coincidentally, space expands in parallel at the rate of recession.

Further, because the recession rate of a given particle is constant over time, as the distance to this particle increases, for space to expand at the same rate, mathematically, the Hubble parameter $H_0$ must decrease in concert. This is described by Eq. (115), which shows $H_0$ decreasing at the necessary rate (as given by Eq. (123)) purely as a function of time—which *happens* to satisfy this requirement.

With that said, at the current age of the universe—13.8 billion years—in another 13.8 billion years, the Hubble parameter will only have decreased by roughly 1%. So, at present, the Hubble parameter can effectively be considered as constant. If the universe were in the ground state—*imagining the case where measurements could be made in this universe*, the expansion of the universe would look uniform and isotropic, and measurements of the Hubble parameter would be consistent across all regions of the cosmos.

### *3. The Dynamic State*

The ground state, however, doesn't describe the universe we observe—which is highly dynamic. Even if the ground state existed for a moment—tantamount to a pencil balanced on its tip—it would quickly devolve to the dynamic state. Any perturbation would cause nearby particles to coalesce, and this slight concentration of mass would result in the net gravitational field in the vicinity of these particles increasing in strength above the baseline of zero. This strengthening field would, in turn, accelerate additional local particles toward the gathering mass—further amplifying the field in a feedback loop. As gathering particles increase in speed—with potential energy converting to kinetic energy—they would eventually collide and radiate heat. Clearly, the dynamic state is a higher-energy state than the ground state. Where did this energy come from?

It's posited that all energy in the universe is ultimately borrowed from the vacuum. This includes the creation of mass *and* the potential energy that induces the local movement of that mass. Energy flow is accounted for by changes in the size and shape of the vacuum. Energy is borrowed to create mass, which is reflected by the expansion (or creation) of space; and the concentration of mass is reflected by local curvature in spacetime.

In the ground state, all particles move in the Hubble flow at constant velocities with respect to each other because there is no net accelerating field acting upon these particles. It's thus concluded that the spacetime of the ground state is flat—*as if* the universe in the ground state has zero mass. As particles coalesce—transitioning from the ground state to the dynamic state, the spacetime around these particles becomes locally curved. Potential energy is converted to kinetic energy.

However, the net potential energy of the universe in the ground state is zero. Particles spread apart at constant velocities—indefinitely. Thus, as particles transition from the ground state to the dynamic state, the net potential energy of the universe decreases *from a baseline of zero*. In effect, energy is borrowed from the vacuum to accelerate these particles—with spacetime curving, increasingly, in concert.

If, at a moment in time immediately after the transition from the ground state to the dynamic state, all particles in motion—via force—were restored to their former positions in the ground state, spacetime would decurve. The work being done on these particles would increase the potential energy of the universe (which was briefly negative) back to zero as spacetime is pulled flat.

The ground state also describes a universe with zero entropy. Every particle is perfectly ordered—at rest in the Hubble frame. There is zero kinetic energy (relative to the Hubble frame) and zero vibrational energy in this state. Thus, as measured by an observer at rest in the Hubble frame, the temperature of the universe in the ground state is absolute zero.

As particles begin to coalesce in different regions, entropy increases in these regions, and energy flows from the vacuum to these particles as they gather and gain kinetic energy—raising the average temperature of the universe. As generally observed, energy flows in the direction that increases the total entropy of the universe.

In this vein, it can be imagined that increasing entropy is what makes the universe dynamic—putting its mass in motion. Both entropy and the curvature of spacetime immediately increase from baselines of zero as particles transition from the ground state to the dynamic state—implying that the two phenomena are related. Further, if the expansion of space is a function of time, is curvature a function of entropy? Interestingly, both time and the total entropy of the universe are only ever seen to be moving in one direction—increasing.

In the dynamic state—as is the case in the ground state, the recessional motion of two distant bodies is **not** a consequence of space expanding in the void—at least not directly. Once created, the motions of particles are *only* a function of their locations in the Hubble flow at the time of creation and the fields acting upon them. Particles aggregate into bodies, systems of bodies, and galaxies. The chaining of galaxies and mass flows gives rise to large-scale structures such as filaments and walls, and immense voids.

Yet—in measurements of the Hubble parameter based

on the recessional speeds of distant bodies in disparate regions of the universe—the Hubble parameter, when defined as the inverse of Hubble time, falls squarely in the range of measured values. Thus, the peculiar speeds of galaxies, at least at this point in time, have not overwhelmed their recessional speeds at large scales. Across large distances, bodies are largely receding according to Hubble's law, which is to say moving in the Hubble flow. Again, with the ground state in mind, it is imagined that bodies are largely found to be moving in the Hubble flow because the proximal particles that formed those bodies were created at rest in the Hubble frame.

## XXII. SUMMARY

The present thesis holds that, upon creation, particles are at rest in the Hubble frame. Because this frame is dynamic, two particles at rest in the Hubble frame, separated by a distance, will initially be receding from each other—with the recessional speed given by Hubble's law. As long as there are no accelerating fields acting upon these particles, they will continue to move at constant velocity with respect to each other—drifting apart at the same speed in perpetuity. Coincidentally, space will always be expanding between these particles at the same rate. This is because the Hubble parameter $H_0$ decreases over time at precisely the rate where the recessional speed given by Hubble's law remains invariant.

Fundamental to the present thesis is the principle that $H_0$ is mathematically the inverse of the Hubble time $t_0$, and thus, $H_0$ must decrease as $t_0$ increases. This relation—as shown by Eqs. (121)–(123)—yields constant recessional speeds.

The correlation between the Hubble time of 13.787 billion years (the estimated age of the universe [4]) and its inverse—70.92 km $s^{-1}$ $Mpc^{-1}$, which falls squarely in the range of measurements for $H_0$ [19], seems too unlikely to be explainable as a coincidence.

Similarly, it's posited that in all frames, the universe is expanding at $c$ in all directions. Because the rate of expansion remains invariant, the universe has always been and will always be expanding at $c$—a concept that is known as "coasting cosmology".

Coupled with the expansion of space is the creation of mass, which occurs continuously as the universe expands—where mass is added to the universe at a rate given by the Planck power. This relation was not presumed but arrived at indirectly in Section XIV. Thus, at the present Hubble time, the mass of the universe $m_0$ calculates to 1.78E53 kg, which is reasonably close to the current estimate of 1.5E53 kg [3].

Note that this estimate only accounts for baryonic matter—disregarding dark matter and dark energy, which, under ΛCDM, comprise 95% of the mass of the universe [29]. The present thesis holds that baryonic matter is the only matter in the universe, and thus there is no dark matter *nor dark energy*. The mass of the universe $m_0$ and the contained mass $m_c$ at a distance $r$ is given by Eqs. (153) and (198):

$$m_0 = \frac{c^3 t_0}{G} \ ,$$
$$m_c = \frac{c H_0 r^2}{G} \ .$$

As all primary metrics of the universe are direct functions of time $t_0$—the expansion parameter $H_0$, the size $r_0$, and the mass $m_0$, the present model is termed "Time-Driven Cosmology".

Expanding space has no direct effect on matter. It does, however, affect fields—with the most salient example being the stretching of a photon's wavelength as it travels through expanding space. It's imagined that expanding space can also affect gravitational fields—magnifying those fields such that in large systems such as galaxies there are notable effects. Counterintuitively, expanding space increases the probability of bodies gathering into larger structures as opposed to drifting apart.

It can be shown that any frame with a non-zero peculiar speed relative to the Hubble frame is decelerating in the Hubble frame. This deceleration is proportional to peculiar speed $v_f$—as given by Eq. (134):

$$a_f = -v_f H_0 \ .$$

It's presumed that this deceleration has physical effects. As $v_f$ goes to zero, deceleration $a_f$ goes to zero—where these physical effects disappear.

For light, deceleration $a_f$ is maximized—as described Eq. (135):

$$a_f = -c H_0 \ .$$

The observed effect on light—as it decelerates—is redshift. Interestingly, redshift can be explained in two contexts: the wavelength of a photon being stretched over time *or* a photon losing energy as it travels in a decelerating field.

Because any point in space can be the origin of expansion, it's imagined that any frame moving in the Hubble frame can have its own origin of expansion—with the moving frame having an expansion parameter of $H_f$. A photon, for example, can be considered to exist in a frame moving at a peculiar speed of $c$—with that frame having an expansion parameter of $H_0$. A general relation for the expansion parameter $H_f$ of a frame with a peculiar speed of $v_f$ is given by Eq. (163):

$$H_f = \sqrt{\frac{v_f}{c}} H_0 \ .$$

Notice that, as $v_f$ goes zero, $H_f$ goes to zero and as $v_f$ goes to $c$, $H_f$ goes to $H_0$. Thus, a frame traveling at $c$ sees the full expansion parameter of the parent frame, which is to say the universe—$H_0$.

It's posited that gravitational fields are also subject to

being redshifted. It's imagined that a redshifted gravitational field has an additional accelerating component termed the "expansion component" on top of the Newtonian component, which is embodied by Eq. (70). The net acceleration $a_n$ relative to a reference mass $m_r$ at distance $r$—in the Newtonian limit—is thus:

$$a_n = \frac{m_r G}{r}\left(\frac{1}{r} + \frac{2\sqrt{cH_f}}{\sqrt{m_t G}}\right) .$$

Here, $m_t$ is the mass of a system with an expansion parameter $H_f$—the latter a function of the system's peculiar speed $v_f$ as described by Eq. (163). When applied to galaxies, this equation produces flat rotation curves in agreement with observations. Unlike MOND, these equations further predict that there will be cases where the rotation curve of a given galaxy has some level of Keplerian decline—and where a galaxy with a peculiar speed of zero would have entirely Newtonian orbits!

The mechanism for the expansion component is thus: While the redshift of light progresses over time, the strength of a gravitational field, as a function of the source mass, remains invariant—assuming a constant mass. Thus, as a gravitational field is redshifted, it is continuously re-informed by the source mass. The tension between redshift and re-information results in an additional acceleration component. This effect, covered in Section IV, is based upon Eq. (21):

$$\vec{a} = -\frac{2\vec{c}}{\Delta t_u} .$$

Eq. (21) relates the acceleration of a particle in a field to the field's propagation speed of $c$ and the time uncertainty in the field at the particle's location. This relation—derived via the uncertainty principle—is hypothesized to be a general relation for accelerations in fields.

The universe can be described by two states—the "ground state" and the "dynamic state". The ground state is an idealized case where all of the particles of the universe move precisely in the Hubble flow—where no particle has a peculiar speed. Every particle in the universe, in the ground state, is perpetually at rest in the frame of a Hubble coordinate, and in this frame, all other particles are in recession—moving exactly according to Hubble's law from zero to $c$. In the ground state, the contained mass $m_c$ is given by Eq. (198). From this equation, Eq. (208) is derived, which is a relation for area density $\rho_A$ in the rest frame of any Hubble coordinate:

$$\rho_A = \frac{cH_0}{8\pi G} .$$

Notice that $\rho_A$ is invariant with respect to distance and only changes with time—with $H_0$ being the inverse of Hubble time $t_0$. Thus, in the ground state, all observers in their own rest frames will measure the same area density at a given proper time in their frames.

Taking the time derivative of Eq. (198) yields interesting insights. For example, the mass at a given Hubble coordinate $v_c$ remains invariant over time as the coordinate recedes. Another realization is that new mass is created between layers of moving mass as those layers separate—as a consequence of space expanding (or being created) between those layers. Importantly, it's imagined that all new particles are created at rest in the Hubble frame.

In the ground state, as a consequence of the universe expanding at $c$ in all frames of reference and mass being created in concert with space—as described by Eq. (198) and the derivatives thereof, each particle in the universe, in its rest frame, is at the barycenter of all other particles. As such, in its rest frame, there is no net accelerating field acting upon any individual particle. Thus, once created, particles move at constant velocities with respect to each other—each coincident with the Hubble coordinate that was created in unison. Particles naturally spread apart in the Hubble flow because there is no net gravitational field that would affect this motion.

The ground state, however, is purely hypothetical. In the real universe, particles are free to gather into dynamic structures. Even if the ground state were to exist for a moment, it would quickly devolve to the dynamic state. Concepts pertinent to the ground state can inform an understanding of the dynamic state. For example, it's imagined that it would be unlikely for a body in the dynamic state to exist precisely at the barycenter of all other bodies. Even a slight offset from the barycenter would elicit some level of acceleration relative to those bodies. As the scale at which the universe is observed increases, however, it looks increasingly like that described by the ground state—homogeneous and isotropic, with bodies largely moving in the Hubble flow.

## XXIII. THE GALACTIC MODEL

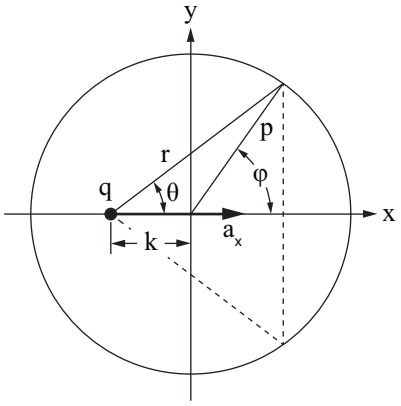


FIG. 19.

The galactic-rotation curves presented in Appendix XXIV were generated according to the following

method: The bulge is modeled as a sphere with a density that varies according to radius $p$, and the disc is modeled as a zero-thickness plate that varies in surface density according to radius $p$. Density, at a given radius, is constant with respect to angle, and thus, local features in the disc such as spiral arms and bars are ignored.

Both models are described by Fig. 19, where, for the bulge, the circle represents a layer of the sphere and the vertical dashed line represents the ring that is formed by the intersection of that layer at radius $p$ and a plane perpendicular to axis $x$. For the disc, the circle marks a radial offset $p$ in a top-down view of the disc. In both models, $\vec{r}$ is a vector between point $q$ at offset $k$ from the $y$ axis and a mass–element at $p$.

For the bulge, the mass $m_r$ of a ring at radius $p$ is thus:

$$V_r = \frac{2\pi}{3}(\cos\phi_1 - \cos\phi_2)({p_2}^3 - {p_1}^3) \ , \tag{225}$$

$$m_r = \rho(p)V_r \ . \tag{226}$$

The volume $V_r$ of the ring bound by radii $p_1$ and $p_2$, and angles $phi_1$ and $phi_2$ is given by Eq. (225). The mass is computed via Eq. (226), where the average density between $p_1$ and $p_2$ is multiplied by the volume. Notice that when $\phi_1 = 0$, $\phi_2 = \pi$, and $p_1 = 0$, $V_r$ is the volume of a sphere of radius $p_2$.

Relative to point $q$ at offset $k$, the distance $r$ to a differential element of ring mass is constant with respect to the revolved angle about the $x$ axis, and thus, the acceleration along $\vec{r}$ from the gravitational field of a ring element is equal in magnitude to that of all elements of equal size across this angle. With a vector pointing to each element, the sum of these vectors yields the net acceleration $a_x$ at point $q$ with respect to a ring of mass $m_r$. The radial components of the vector sum all cancel, leaving $a_x$ pointing along the $x$ axis as follows:

$$p = \frac{p_1 + p_2}{2} \ , \tag{227}$$

$$\phi = \frac{\phi_1 + \phi_2}{2} \ , \tag{228}$$

$$r = \sqrt{p^2 + 2p\cos\phi k + k^2} \ , \tag{229}$$

$$\cos\theta = \frac{p\cos\phi + k}{r} \ , \tag{230}$$

$$a_x = \frac{m_r G}{r}\left(\frac{1}{r} + \frac{2\sqrt{cH_f}}{\sqrt{m_t G}}\right)\cos\theta \ , \tag{231}$$

$$\frac{v^2}{r} = a_x \ , \tag{232}$$

$$v = \sqrt{a_x r} \ . \tag{233}$$

The acceleration at point $q$ along $\vec{r}$ from a mass element of the ring is given by Eq. (70), and the sum of these acceleration vectors is given by Eq. (231). Notice that when point $q$ is centered in the ring—where $\theta = \pi/2$—the net acceleration is zero, as expected. To compute only the Newtonian component of $a_x$, $H_f$, in Eq. (231), is set to zero. Eq. (232) is the familiar relation between tangential speed $v$—where the motion is circular—and centripetal acceleration, which, in this case, is $a_x$. The rotation curves were drawn with the assumption of circular motion—with the rotational velocity $v$ given by Eq. (233).

To calculate the net acceleration $a_x$ at a given offset $k$ from the gravitational field of the full bulge, the bulge is divided into a series of thin layers—with each layer having a certain density $\rho(p)$. Each layer is divided into a series of thin rings orthogonal to the $x$ axis. Eqs. (225) and (226) are used to calculate the mass of a ring defined by radii $p_1$ and $p_2$, and angles $\phi_1$ and $\phi_2$. Eqs. (227)–(231) are then used to calculate the acceleration $a_x$ towards the ring. Running this calculation for small increments of $\phi$ from 0 to $\pi$ at a given $p_1$ and $p_2$—which defines a shell—and summing $a_x$ for each increment, gives the acceleration towards the shell. Running the shell calculation for small increments of $p$ from 0 to the bulge radius, and summing the shell acceleration for each increment, gives the net acceleration $a_b$ towards the bulge. As a test of the code, offset $k$ can be placed inside and outside of the bulge and $a_b$ can be tested to see if Newton's shell theorem is confirmed—with $H_f$ in Eq. (231) set to zero.

The algorithm is nearly identical for the disc calculation. Instead of calculating a ring mass, however, the mass of a pair of arc elements—where one element is the mirror of the other about the $x$ axis—is calculated as follows:

$$A_r = (\phi_2 - \phi_1)({p_2}^2 - {p_1}^2) \ , \tag{234}$$

$$m_r = \rho(p)A_r \ . \tag{235}$$

Looking down at the disc—the view depicted in Fig. 19, a finite area element $A_r$ of the disc is defined by radii $p_1$ and $p_2$, and angles $\phi_1$ and $\phi_2$. The mass of this element $m_r$ is given by Eq. (235), where this area is multiplied by the surface density $\rho(p)$ at radius $p$. Notice that in the relation for $A_r$—Eq. (234), the area element is double the size that would be contained within the arc between $\phi_1$ and $\phi_2$. The area $A_r$ for the arc from 0 to $\pi$ yields, with $p_1$ set to zero, the area of a circle of radius $p_2$ and not a half circle. $A_r$, and by extension, $m_r$, refer to an element–pair mirrored about the $x$ axis.

Looking at Fig. 19, $\vec{r}$ points to a disc element, and the mirror of this vector, drawn as a dashed line, points to the reflected element in the pair. Because of the symmetry about the $x$ axis, the radial components of the acceleration vectors from point $q$ cancel, leaving $a_x$ aligned along the $x$ axis—as was the case for the bulge. Thus, $m_r$ for a disc-element pair—as calculated by Eq. (235)—can be fed directly into Eqs. (227)–(231) to compute the gravitational acceleration $a_x$ towards the pair. This calculation is run for small increments of $\phi$ from 0 to $\pi$ at a given $p_1$ and $p_2$, which gives the acceleration towards a ring of the disc. Integrating across the disk from zero to the disc radius by small increments of $p$ and summing $a_x$ for each ring gives the net acceleration $a_d$ towards the disc.

## XXIV. GALACTIC ROTATION CURVES

TABLE II. A Selection of Nearby SPARC Galaxies (mass models).

| Galaxy | Dark-matter model | $\Upsilon_b$ | $\Upsilon_d$ | Distance (Mpc) | CMB redshift (km s$^{-1}$) | $r_{max}$ (kpc) |
|---|---|---|---|---|---|---|
| Cam B | NFW flat | 0 | .37 | 3.5 | 23 | 1.68 |
| DDO 064 | Burkert | 0 | .49 | 3.800-7.110 | 784 | 3.03 |
| DDO 154 | coreNFW flat | 0 | .29 | 4.04 | 639 | 5.97 |
| DDO 168 | Lucky13 LCDM | 0 | .55 | 4.25 | 380 | 4.07 |
| ESO 444-G084 | NFW LCDM | 0 | .54 | 4.53 | 870 | 4.42 |
| IC 2574 | DC14 flat | 0 | .44 | 3.890-3.940 | 148 | 10.20 |
| NGC 0055 | Einasto flat | 0 | .49 | 1.850-2.340 | 115 | 13.36 |
| NGC 0247 | coreNFW LCDM[a] | 0 | 1.0 | 3.270-3.670 | 143 | 14.50 |
| NGC 0300 | Lucky13 LCDM | 0 | .73 | 1.790-2.170 | 91 | 12.04 |
| NGC 2366 | Burkert | 0 | .38 | 3.200-3.340 | 134 | 6.02 |
| NGC 2403 | Burkert | 0 | .90 | 3.010-3.930 | 182 | 19.60 |
| NGC 2915 | Burkert | 0 | .42 | 3.580-4.290 | 588 | 9.90 |
| NGC 2976 | Burkert | 0 | .48 | 3.520-3.630 | 90 | 2.25 |
| NGC 3109 | NFW LCDM | 0 | .51 | 1.333 | 738 | 7.16 |
| NGC 3741 | Burkert | 0 | .77 | 3.150-3.230 | 456 | 7.13 |
| NGC 4068 | coreNFW LCDM | 0 | .45 | 4.3 | 784 | 2.28 |
| NGC 4214 | NFW LCDM | 0 | .54 | 2.700-2.930 | 550 | 5.63 |
| NGC 6789 | DC14 LCDM[a] | 0 | 1.0 | 3.6 | 275 | 0.73 |
| NGC 6946 | Burkert | .63 | .58 | 4.51 | 133 | 18.90 |
| NGC 7793 | Burkert | 0 | .56 | 3.390-3.840 | 53 | 7.97 |
| UGC 04305 | Burkert | 0 | .50 | 3.24 | 203 | 5.45 |
| UGC 04483 | Burkert | 0 | .50 | 3.2 | 213 | 1.21 |
| UGC 07232 | Burkert | 0 | .50 | 2.95 | 486 | .82 |
| UGC 07524 | DC14 flat | 0 | .43 | 4.410-4.610 | 585 | 10.50 |
| UGC 07559 | coreNFW LCDM | 0 | .43 | 4.97 | 470 | 2.50 |
| UGC 07577 | coreNFW LCDM | 0 | .37 | 2.6 | 417 | 1.50 |
| UGC 07866 | coreNFW LCDM | 0 | .48 | 4.57 | 592 | 2.29 |
| UGC 08490 | DC14 LCDM | 0 | .96 | 4.790-5.550 | 322 | 12.50 |
| UGCA 444 | Burkert | 0 | .49 | 0.93 | 457 | 2.60 |

[a] Error bars are from this dark-matter model, but the mass-to-light ratio is less than that given by the model.
[b] Mass-to-light ratios were sourced from the SPARC database [34].
[c] Distance and redshift data were sourced from the *NASA/IPAC Extragalactic Database* [35].

TABLE III. A Selection of Nearby SPARC Galaxies ($H_f$ and $k_f$).

| Galaxy | Mass (kg) | $H_f$ (km s$^{-1}$ Mpc$^{-1}$) | $k_f$ (kg$^{-1}$ s$^{-1}$) | $v_{flat}$ (km s$^{-1}$) | Poor fit | Outlier |
|---|---|---|---|---|---|---|
| Cam B | 7.12E37 | .07 | 3.19E−59 | 11 | x | |
| DDO 064 | 6.90E38 | 4.0 | 1.88E−58 | 52 | | |
| DDO 154 | 4.75E38 | 3.8 | 2.59E−58 | 47 | | |
| DDO 168 | 7.69E38 | 2.5 | 1.05E−58 | 47 | | |
| ESO 444-G084 | 4.49E38 | 4.0 | 2.89E−58 | 46 | | |
| IC 2574 | 3.24E39 | 1.8 | 1.80E−59 | 62 | | |
| NGC 0055 | 8.97E39 | 1.3 | 4.70E−60 | 74 | | |
| NGC 0247 | 1.62E40 | 1.5 | 3.00E−60 | 89 | | |
| NGC 0300 | 6.21E39 | .90 | 4.70E−60 | 62 | | |
| NGC 2366 | 1.48E39 | 1.3 | 2.85E−59 | 47 | | |
| NGC 2403 | 2.52E40 | 3.1 | 3.99E−60 | 119 | | x |
| NGC 2915 | 1.56E39 | 12 | 2.49E−58 | 83 | x | x |
| NGC 2976 | 2.30E39 | 1.9 | 2.68E−59 | 58 | | |
| NGC 3109 | 1.35E39 | 3.6 | 8.64E−59 | 60 | | |
| NGC 3741 | 4.99E38 | 5.0 | 3.25E−58 | 50 | | |
| NGC 4068 | 4.84E38 | 2.5 | 1.67E−58 | 42 | | |
| NGC 4214 | 1.44E39 | 3.0 | 6.75E−59 | 58 | | |
| NGC 6789 | 2.05E38 | 3.0 | 4.74E−58 | 36 | | |
| NGC 6946 | 7.23E40 | 1.1 | 4.93E−61 | 120 | | |
| NGC 7793 | 9.83E39 | .35 | 1.15E−60 | 55 | | |
| UGC 04305 | 1.70E39 | 2.0 | 3.81E−59 | 54 | x | |
| UGC 04483 | 8.18E37 | 1.8 | 7.13E−58 | 25 | | |
| UGC 07232 | 1.74E38 | 4.0 | 7.45E−58 | 37 | | x |
| UGC 07524 | 6.06E39 | 3.0 | 1.60E−59 | 83 | x | |
| UGC 07559 | 3.10E38 | 1.5 | 1.57E−58 | 33 | | x |
| UGC 07577 | 7.55E37 | .70 | 3.00E−58 | 19 | | x |
| UGC 07866 | 2.23E38 | 3.0 | 4.36E−58 | 36 | | |
| UGC 08490 | 4.95E39 | 2.2 | 1.44E−59 | 73 | | |
| UGCA 444 | 1.88E38 | 3.2 | 5.52E−58 | 35 | | |

In the following graphs, the units for the vertical axes are km $s^{-1}$, and the units for the horizontal axes are kpc. The Newtonian curve for the stellar disk is drawn with a dashed blue line. The Newtonian contribution from the gas disk is drawn with a dashed magenta line with larger dashes, and the bulge contribution is drawn as a dotted green line. The net rotation curve, generated via Eq. (70), is drawn as a solid cyan line.

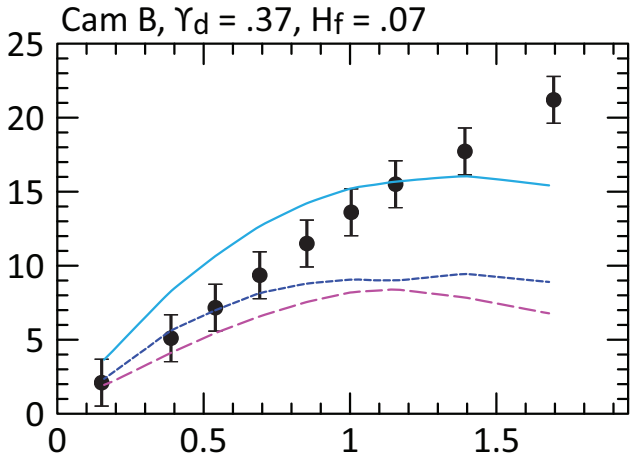


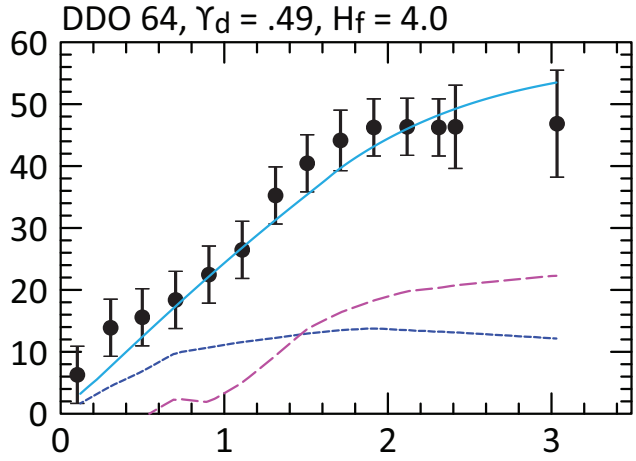


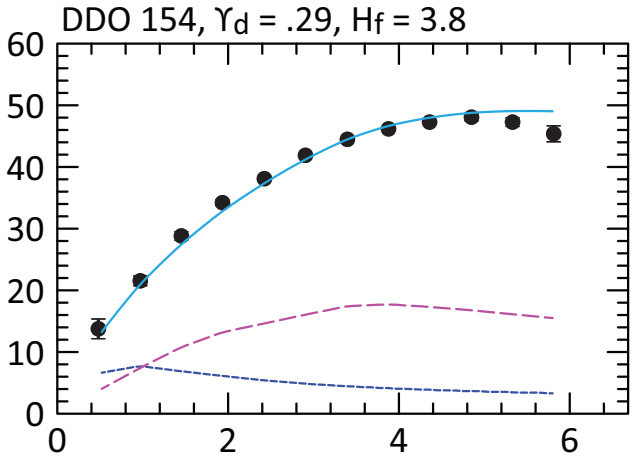


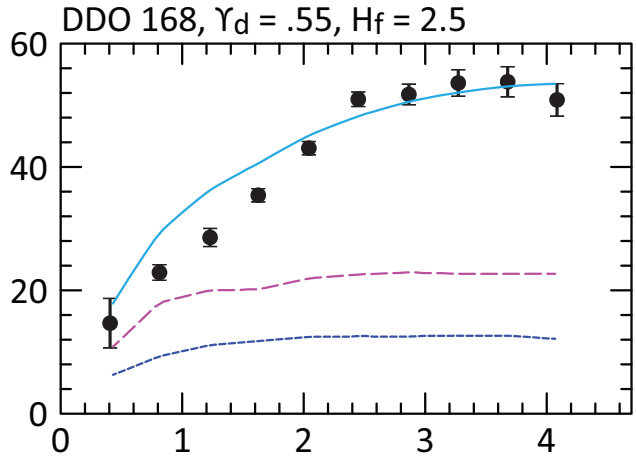


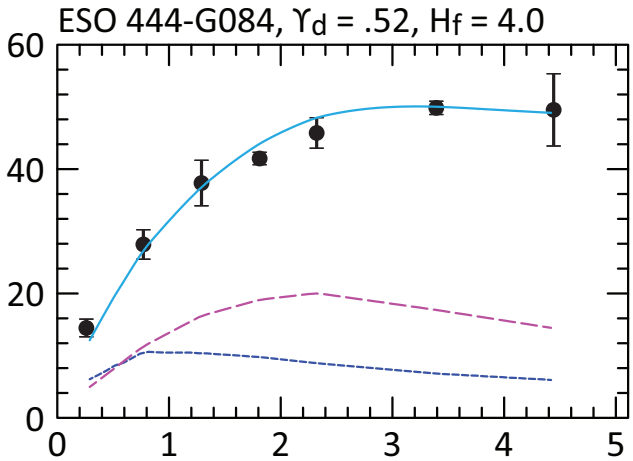


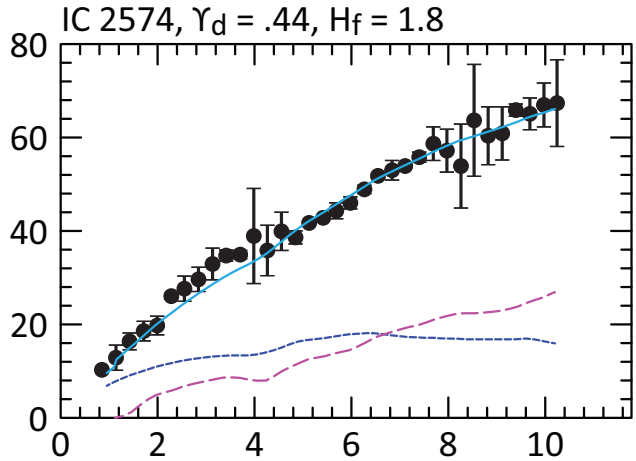

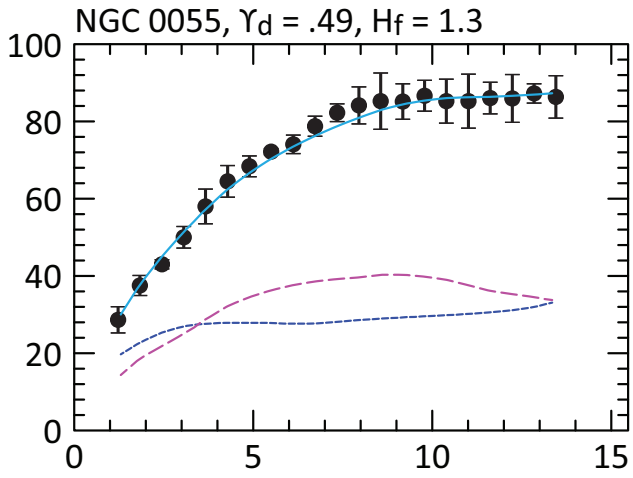
NGC 0055, ϒd = .49, Hf = 1.3
0
20
40
60
80
100
0
5
10
15

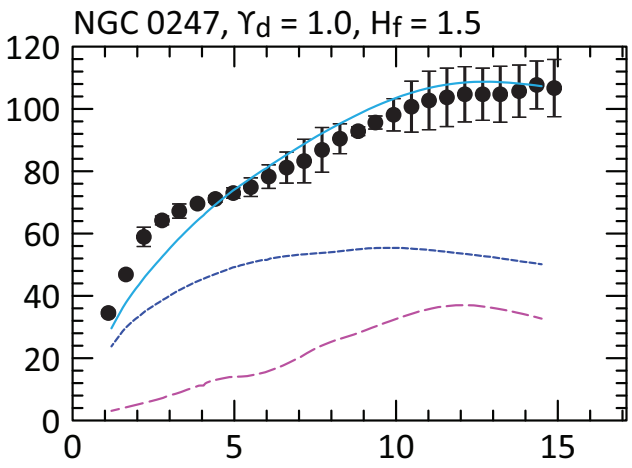
NGC 0247, ϒd = 1.0, Hf = 1.5
0
20
40
60
80
100
120
0
5
10
15

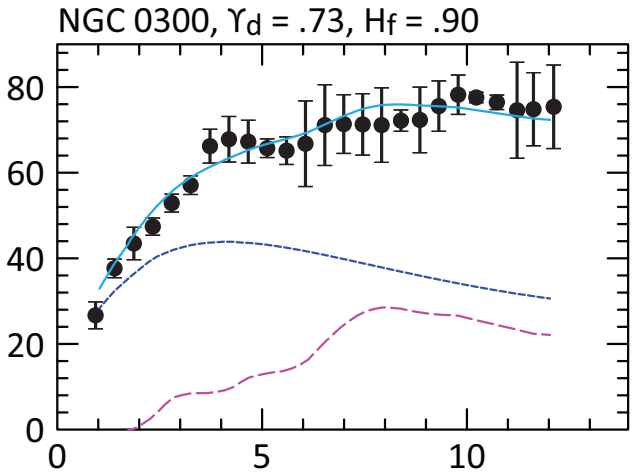
NGC 0300, ϒd = .73, Hf = .90
0
20
40
60
80
0
5
10

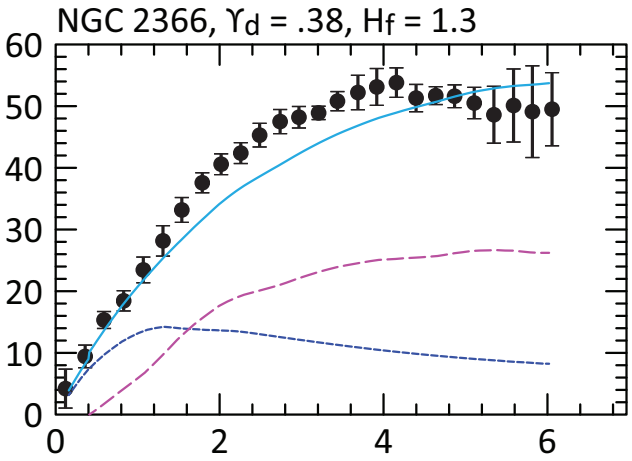
NGC 2366, ϒd = .38, Hf = 1.3
0
10
20
30
40
50
60
0
2
4
6

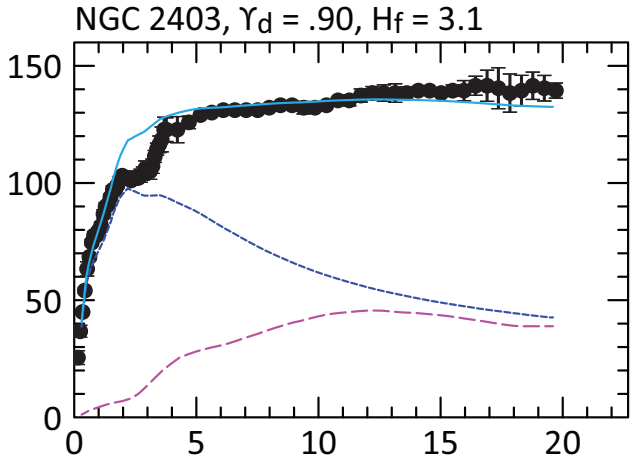
NGC 2403, ϒd = .90, Hf = 3.1
0
50
100
150
0
5
10
15
20

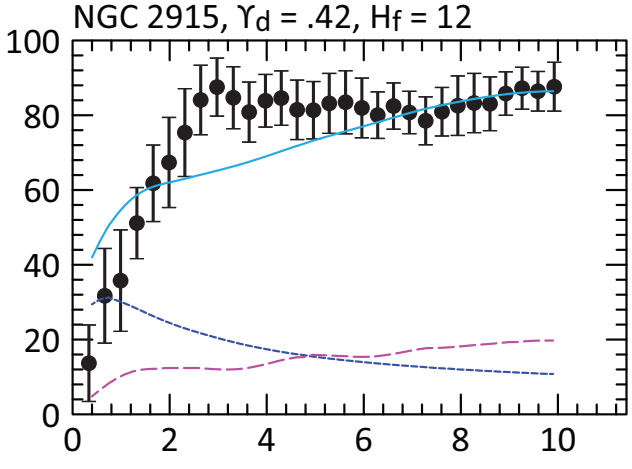
NGC 2915, ϒd = .42, Hf = 12
0
20
40
60
80
100
0
2
4
6
8
10

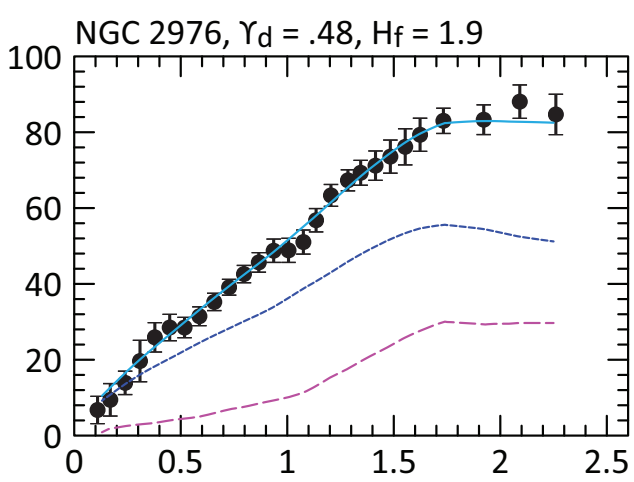
NGC 2976, Υd = .48, Hf = 1.9

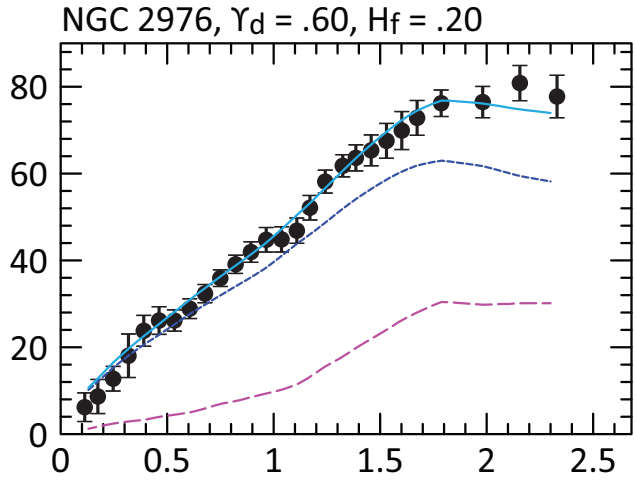
NGC 2976, Υd = .60, Hf = .20

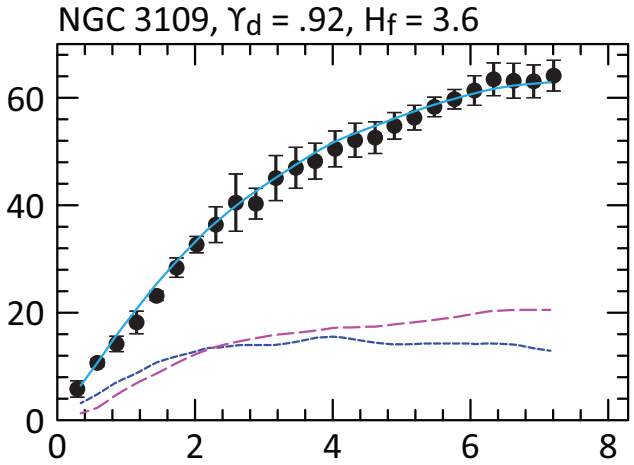
NGC 3109, Υd = .92, Hf = 3.6

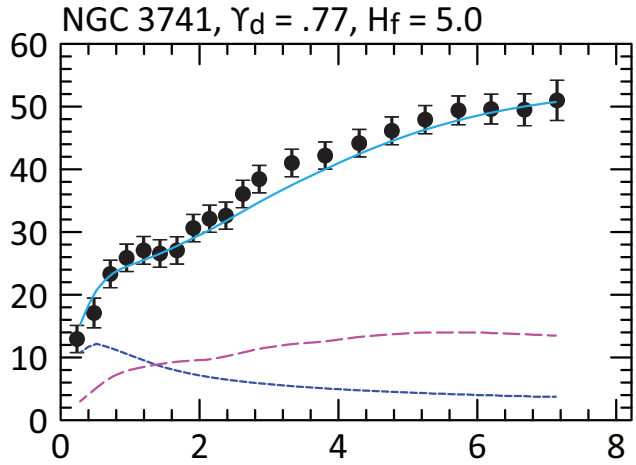
NGC 3741, Υd = .77, Hf = 5.0

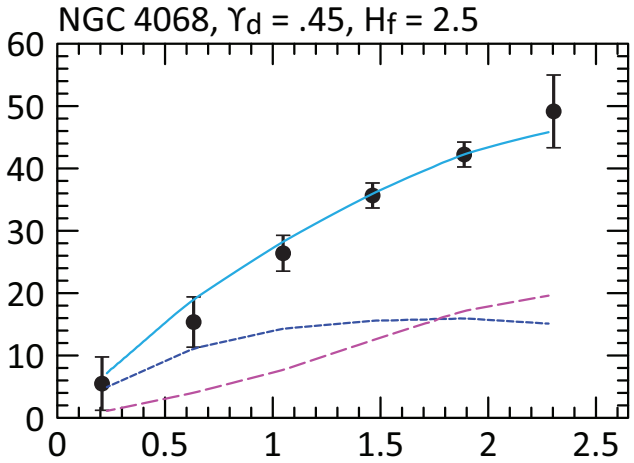
NGC 4068, Υd = .45, Hf = 2.5

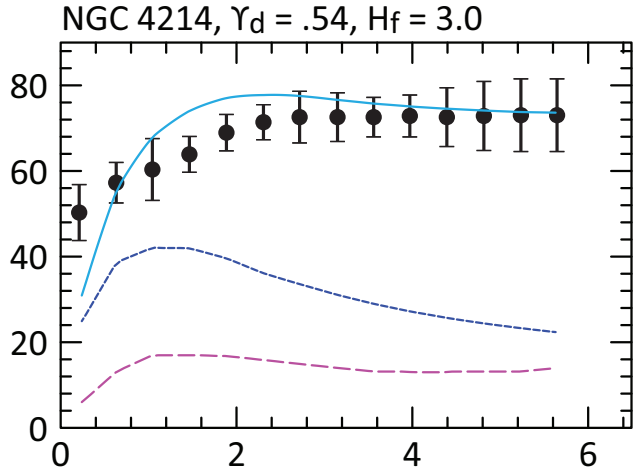
NGC 4214, Υd = .54, Hf = 3.0

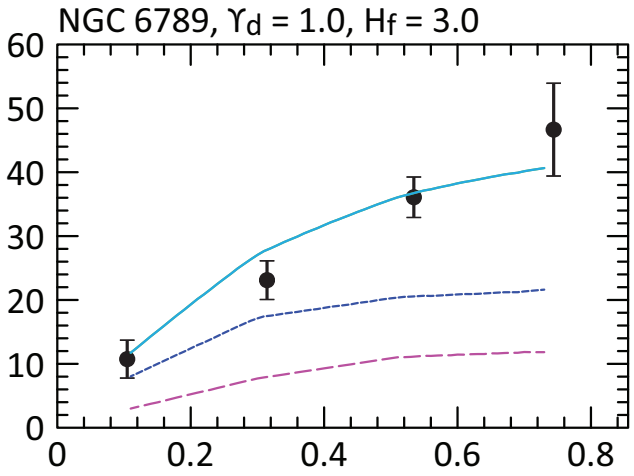
NGC 6789, ϒd = 1.0, Hf = 3.0
60
50
40
30
20
10
0
0
0.2
0.4
0.6
0.8

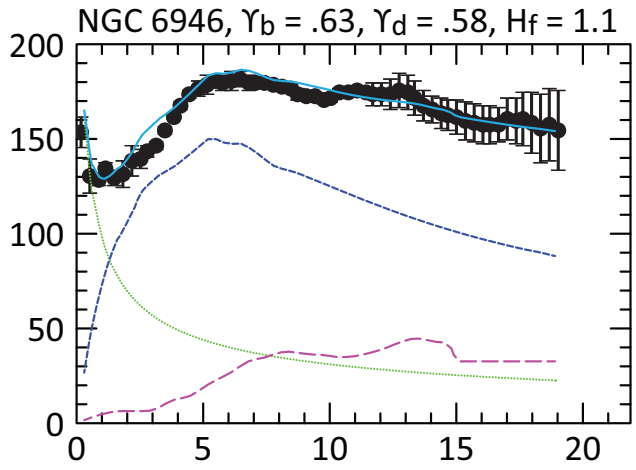
NGC 6946, ϒb = .63, ϒd = .58, Hf = 1.1
200
150
100
50
0
0
5
10
15
20

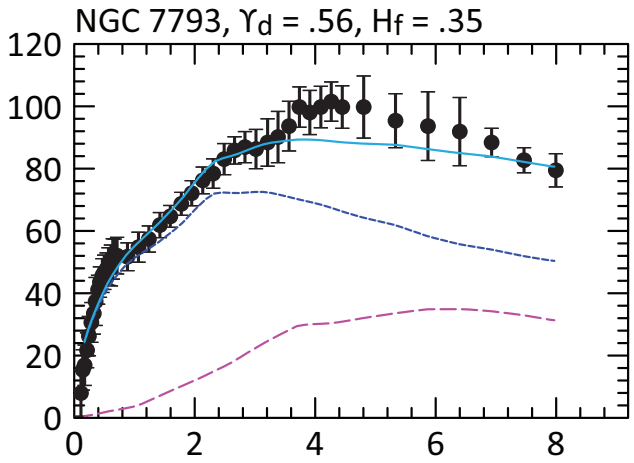
NGC 7793, ϒd = .56, Hf = .35
120
100
80
60
40
20
0
0
2
4
6
8

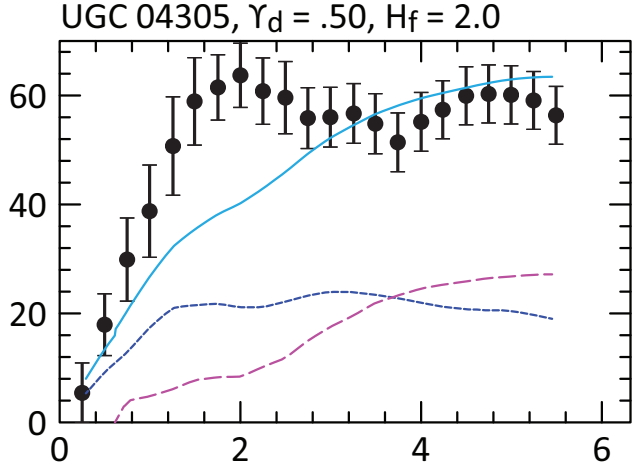
UGC 04305, ϒd = .50, Hf = 2.0
60
40
20
0
0
2
4
6

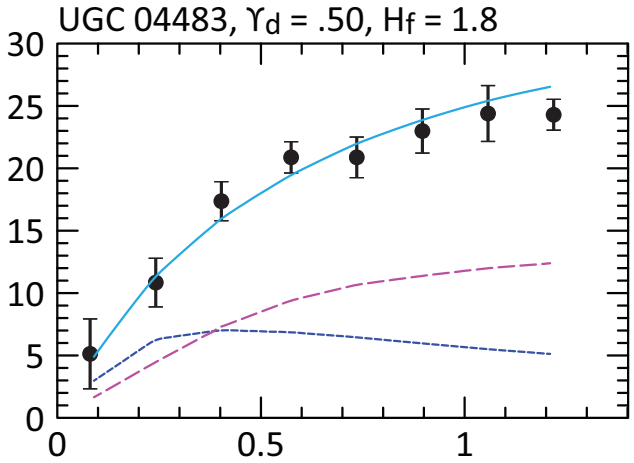
UGC 04483, ϒd = .50, Hf = 1.8
30
25
20
15
10
5
0
0
0.5
1

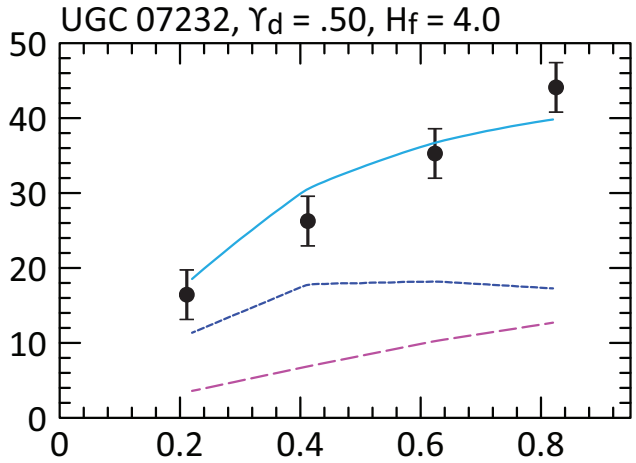
UGC 07232, ϒd = .50, Hf = 4.0
50
40
30
20
10
0
0
0.2
0.4
0.6
0.8

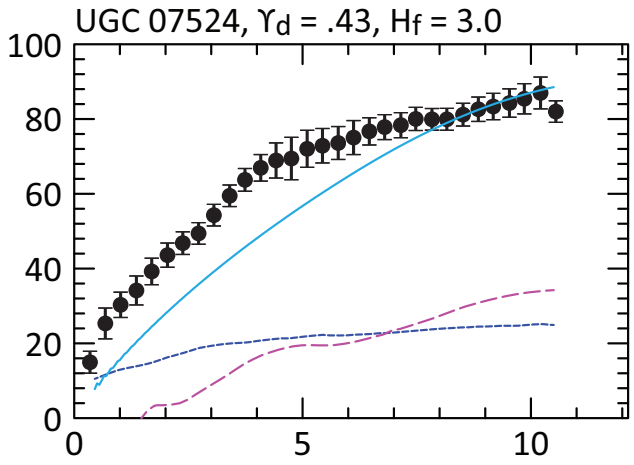
UGC 07524, ϒd = .43, Hf = 3.0
100
80
60
40
20
0
0
5
10

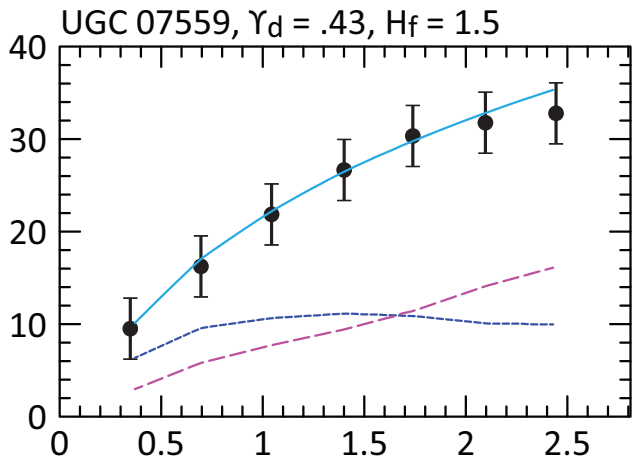
UGC 07559, ϒd = .43, Hf = 1.5
40
30
20
10
0
0
0.5
1
1.5
2
2.5

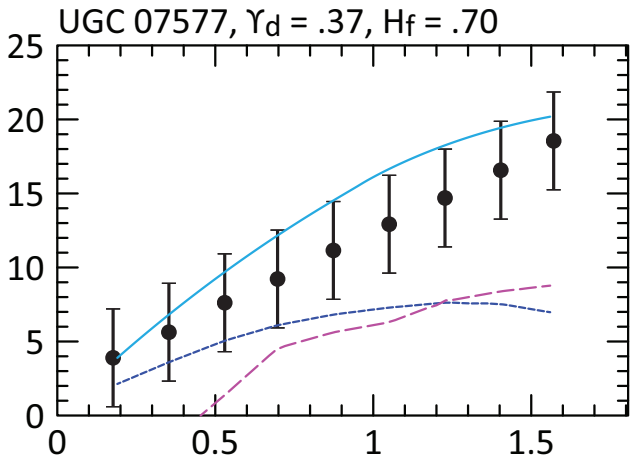
UGC 07577, ϒd = .37, Hf = .70
25
20
15
10
5
0
0
0.5
1
1.5

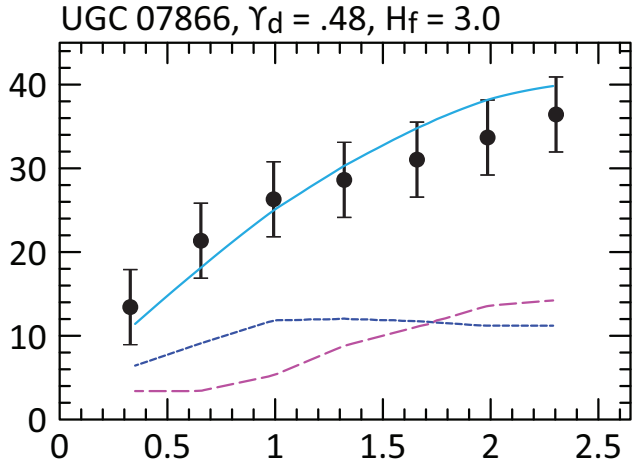
UGC 07866, ϒd = .48, Hf = 3.0
40
30
20
10
0
0
0.5
1
1.5
2
2.5

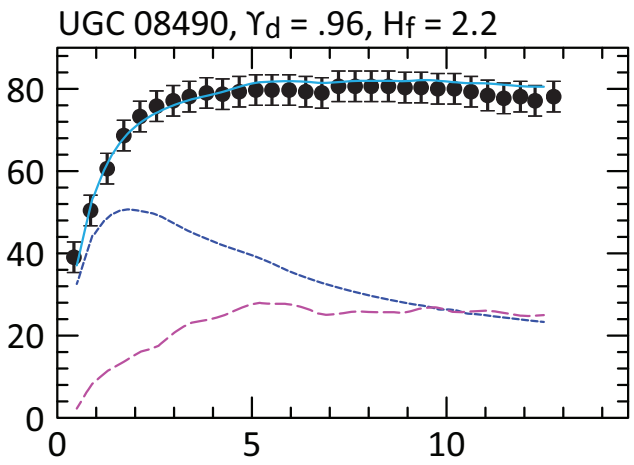
UGC 08490, ϒd = .96, Hf = 2.2
80
60
40
20
0
0
5
10

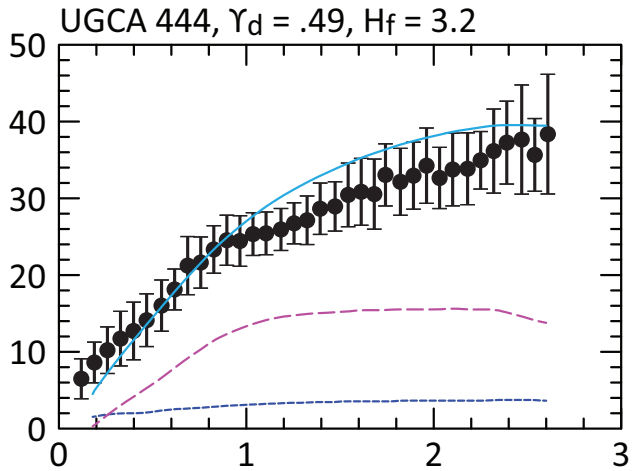
UGCA 444, ϒd = .49, Hf = 3.2
50
40
30
20
10
0
0
1
2
3

[1] R. S. Park, W. M. Folkner, A. S. Konopliv, J. G. Williams, D. E. Smith, and M. T. Zuber, Precession of mercury's perihelion from ranging to the messenger spacecraft, The Astronomical Journal **153**, 121 (2017).

[2] F. Shu, *The Physical Universe: An Introduction to Astronomy*, G - Reference,Information and Interdisciplinary Subjects Series (University Science Books, 1982).

[3] Wikipedia contributors, Observable universe — Wikipedia, the free encyclopedia (2026), [Online; accessed 31-May-2026].

[4] N. Aghanim, Y. Akrami, M. Ashdown, J. Aumont, C. Baccigalupi, M. Ballardini, A. J. Banday, R. B. Barreiro, N. Bartolo, S. Basak, R. Battye, K. Benabed, J.-P. Bernard, M. Bersanelli, P. Bielewicz, J. J. Bock, J. R. Bond, J. Borrill, F. R. Bouchet, F. Boulanger, M. Bucher, C. Burigana, R. C. Butler, E. Calabrese, J.-F. Cardoso, J. Carron, A. Challinor, H. C. Chiang, J. Chluba, L. P. L. Colombo, C. Combet, D. Contreras, B. P. Crill, F. Cuttaia, P. de Bernardis, G. de Zotti, J. Delabrouille, J.-M. Delouis, E. Di Valentino, J. M. Diego, O. Doré, M. Douspis, A. Ducout, X. Dupac, S. Dusini, G. Efstathiou, F. Elsner, T. A. Enßlin, H. K. Eriksen, Y. Fantaye, M. Farhang, J. Fergusson, R. Fernandez-Cobos, F. Finelli, F. Forastieri, M. Frailis, A. A. Fraisse, E. Franceschi, A. Frolov, S. Galeotta, S. Galli, K. Ganga, R. T. Génova-Santos, M. Gerbino, T. Ghosh, J. González-Nuevo, K. M. Górski, S. Gratton, A. Gruppuso, J. E. Gudmundsson, J. Hamann, W. Handley, F. K. Hansen, D. Herranz, S. R. Hildebrandt, E. Hivon, Z. Huang, A. H. Jaffe, W. C. Jones, A. Karakci, E. Keihänen, R. Keskitalo, K. Kiiveri, J. Kim, T. S. Kisner, L. Knox, N. Krachmalnicoff, M. Kunz, H. Kurki-Suonio, G. Lagache, J.-M. Lamarre, A. Lasenby, M. Lattanzi, C. R. Lawrence, M. Le Jeune, P. Lemos, J. Lesgourgues, F. Levrier, A. Lewis, M. Liguori, P. B. Lilje, M. Lilley, V. Lindholm, M. López-Caniego, P. M. Lubin, Y.-Z. Ma, J. F. Macías-Pérez, G. Maggio, D. Maino, N. Mandolesi, A. Mangilli, A. Marcos-Caballero, M. Maris, P. G. Martin, M. Martinelli, E. Martínez-González, S. Matarrese, N. Mauri, J. D. McEwen, P. R. Meinhold, A. Melchiorri, A. Mennella, M. Migliaccio, M. Millea, S. Mitra, M.-A. Miville-Deschênes, D. Molinari, L. Montier, G. Morgante, A. Moss, P. Natoli, H. U. Nørgaard-Nielsen, L. Pagano, D. Paoletti, B. Partridge, G. Patanchon, H. V. Peiris, F. Perrotta, V. Pettorino, F. Piacentini, L. Polastri, G. Polenta, J.-L. Puget, J. P. Rachen, M. Reinecke, M. Remazeilles, A. Renzi, G. Rocha, C. Rosset, G. Roudier, J. A. Rubiño-Martín, B. Ruiz-Granados, L. Salvati, M. Sandri, M. Savelainen, D. Scott, E. P. S. Shellard, C. Sirignano, G. Sirri, L. D. Spencer, R. Sunyaev, A.-S. Suur-Uski, J. A. Tauber, D. Tavagnacco, M. Tenti, L. Toffolatti, M. Tomasi, T. Trombetti, L. Valenziano, J. Valiviita, B. Van Tent, L. Vibert, P. Vielva, F. Villa, N. Vittorio, B. D. Wandelt, I. K. Wehus, M. White, S. D. M. White, A. Zacchei, and A. Zonca, Planck2018 results: Vi. cosmological parameters, Astronomy amp; Astrophysics **641**, A6 (2020).

[5] M. Milgrom, A modification of the newtonian dynamics as a possible alternative to the hidden mass hypothesis, Astrophysical Journal, Letters **270**, 365 (1983).

[6] M. Milgrom, A modification of the newtonian dynamics - implications for galaxies, Astrophysical Journal, Letters **270**, 371–389 (1983).

[7] M. Milgrom, A modification of the newtonian dynamics - implications for galaxy systems, Astrophysical Journal, Letters **270**, 384 (1983).

[8] K. G. Begeman, A. H. Broeils, and R. H. Sanders, Extended rotation curves of spiral galaxies : dark haloes and modified dynamics., **249**, 523 (1991).

[9] R. B. Tully and J. R. Fisher, A new method of determining distances to galaxies, Astronomy and Astrophysics **54**, 661–673 (1977).

[10] S. S. McGaugh, J. M. Schombert, G. D. Bothun, and W. J. G. de Blok, The baryonic tully-fisher relation, The Astrophysical Journal **533**, L99 (2000).

[11] S. S. McGaugh, The baryonic tully-fisher relation of galaxies with extended rotation curves and the stellar mass of rotating galaxies, The Astrophysical Journal **632**, 859 (2005).

[12] S. S. McGaugh and W. J. G. de Blok, Testing the hypothesis of modified dynamics with low surface brightness galaxies and other evidence, Astrophysical Journal, Letters **499**, 66 (1998).

[13] R. H. Sanders, Modified newtonian dynamics: A falsification of cold darkmatter, Advances in Astronomy (2009), 752439.

[14] S. S. McGaugh, Novel test of modified newtonian dynamics with gas rich galaxies, Physical Review Letters **106** (2011), 121303.

[15] S. S. McGaugh, The baryonic tully-fisher relation of gas-rich galaxies as a test of cdm and mond, Astronomical Journal **143** (2012), 40.

[16] F. Lelli, S. S. McGaugh, and J. M. Schombert, The small scatter of the baryonic tully–fisher relation, The Astrophysical Journal Letters **816**, L14 (2016).

[17] T. Mistele, S. McGaugh, F. Lelli, J. Schombert, and P. Li, Indefinitely flat circular velocities and the baryonic tully–fisher relation from weak lensing, The Astrophysical Journal Letters **969**, L3 (2024).

[18] S. S. McGaugh, Testing galaxy formation and dark matter with low surface brightness galaxies, Studies in History and Philosophy of Science **88**, 220 (2021).

[19] A. Sneppen, D. Watson, D. Poznanski, O. Just, A. Bauswein, and R. Wojtak, Measuring the Hubble constant with kilonovae using the expanding photosphere method, **678**, A14 (2023), arXiv:2306.12468 [astro-ph.CO].

[20] D. Brout, D. Scolnic, B. Popovic, A. G. Riess, A. Carr, J. Zuntz, R. Kessler, T. M. Davis, S. Hinton, D. Jones, W. D. Kenworthy, E. R. Peterson, K. Said, G. Taylor, N. Ali, P. Armstrong, P. Charvu, A. Dwomoh, C. Meldorf, A. Palmese, H. Qu, B. M. Rose, B. Sanchez, C. W. Stubbs, M. Vincenzi, C. M. Wood, P. J. Brown, R. Chen, K. Chambers, D. A. Coulter, M. Dai, G. Dimitriadis, A. V. Filippenko, R. J. Foley, S. W. Jha, L. Kelsey, R. P. Kirshner, A. Möller, J. Muir, S. Nadathur, Y.-C. Pan, A. Rest, C. Rojas-Bravo, M. Sako, M. R. Siebert, M. Smith, B. E. Stahl, and P. Wiseman, The Pantheon+ Analysis: Cosmological Constraints, Astrophys. J. **938**, 110 (2022), arXiv:2202.04077 [astro-ph.CO].

[21] W. L. Freedman, B. F. Madore, B. K. Gibson, L. Fer-

rarese, D. D. Kelson, S. Sakai, J. R. Mould, R. C. Kennicutt, Jr., H. C. Ford, J. A. Graham, J. P. Huchra, S. M. G. Hughes, G. D. Illingworth, L. M. Macri, and P. B. Stetson, Final Results from the Hubble Space Telescope Key Project to Measure the Hubble Constant, Astrophys. J. **553**, 47 (2001), arXiv:astro-ph/0012376 [astro-ph].

[22] E. W. Kolb, A Coasting Cosmology, Astrophys. J. **344**, 543 (1989).

[23] R. Monjo, What if the universe expands linearly? a local general relativity to solve the "zero active mass" problem, The Astrophysical Journal **967**, 66 (2024).

[24] S. Aiola, E. Calabrese, L. Maurin, S. Naess, B. L. Schmitt, M. H. Abitbol, G. E. Addison, P. A. R. Ade, D. Alonso, M. Amiri, S. Amodeo, E. Angile, J. E. Austermann, T. Baildon, N. Battaglia, J. A. Beall, R. Bean, D. T. Becker, J. R. Bond, S. M. Bruno, V. Calafut, L. E. Campusano, F. Carrero, G. E. Chesmore, H.-m. Cho, S. K. Choi, S. E. Clark, N. F. Cothard, D. Crichton, K. T. Crowley, O. Darwish, R. Datta, E. V. Denison, M. J. Devlin, C. J. Duell, S. M. Duff, A. J. Duivenvoorden, J. Dunkley, R. Dünner, T. Essinger-Hileman, M. Fankhanel, S. Ferraro, A. E. Fox, B. Fuzia, P. A. Gallardo, V. Gluscevic, J. E. Golec, E. Grace, M. Gralla, Y. Guan, K. Hall, M. Halpern, D. Han, P. Hargrave, M. Hasselfield, J. M. Helton, S. Henderson, B. Hensley, J. C. Hill, G. C. Hilton, M. Hilton, A. D. Hincks, R. Hložek, S.-P. P. Ho, J. Hubmayr, K. M. Huffenberger, J. P. Hughes, L. Infante, K. Irwin, R. Jackson, J. Klein, K. Knowles, B. Koopman, A. Kosowsky, V. Lakey, D. Li, Y. Li, Z. Li, M. Lokken, T. Louis, M. Lungu, A. MacInnis, M. Madhavacheril, F. Maldonado, M. Mallaby-Kay, D. Marsden, J. McMahon, F. Menanteau, K. Moodley, T. Morton, T. Namikawa, F. Nati, L. Newburgh, J. P. Nibarger, A. Nicola, M. D. Niemack, M. R. Nolta, J. Orlowski-Sherer, L. A. Page, C. G. Pappas, B. Partridge, P. Phakathi, G. Pisano, H. Prince, R. Puddu, F. J. Qu, J. Rivera, N. Robertson, F. Rojas, M. Salatino, E. Schaan, A. Schillaci, N. Sehgal, B. D. Sherwin, C. Sierra, J. Sievers, C. Sifon, P. Sikhosana, S. Simon, D. N. Spergel, S. T. Staggs, J. Stevens, E. Storer, D. D. Sunder, E. R. Switzer, B. Thorne, R. Thornton, H. Trac, J. Treu, C. Tucker, L. R. Vale, A. V. Engelen, J. V. Lanen, E. M. Vavagiakis, K. Wagoner, Y. Wang, J. T. Ward, E. J. Wollack, Z. Xu, F. Zago, and N. Zhu, The atacama cosmology telescope: Dr4 maps and cosmological parameters, Journal of Cosmology and Astroparticle Physics **2020** (12), 047–047.

[25] G. Efstathiou and S. Gratton, The evidence for a spatially flat universe, Monthly Notices of the Royal Astronomical Society: Letters **496**, L91–L95 (2020).

[26] A. P. Lightman, *Ancient light : our changing view of the universe* (Harvard University Press, 1991).

[27] A. Guth, *The Inflationary Universe* (Addison-Wesley, 1997).

[28] M. D. Lemonick and M. Nash, Cosmic Conundrum, (2004).

[29] T. Abbott, M. Aguena, A. Alarcon, S. Allam, O. Alves, A. Amon, F. Andrade-Oliveira, J. Annis, S. Avila, D. Bacon, E. Baxter, K. Bechtol, M. Becker, G. Bernstein, S. Bhargava, S. Birrer, J. Blazek, A. Brandao-Souza, S. Bridle, D. Brooks, E. Buckley-Geer, D. Burke, H. Camacho, A. Campos, A. Carnero Rosell, M. Carrasco Kind, J. Carretero, F. Castander, R. Cawthon, C. Chang, A. Chen, R. Chen, A. Choi, C. Conselice, J. Cordero, M. Costanzi, M. Crocce, L. da Costa, M. da Silva Pereira, C. Davis, T. Davis, J. De Vicente, J. DeRose, S. Desai, E. Di Valentino, H. Diehl, J. Dietrich, S. Dodelson, P. Doel, C. Doux, A. Drlica-Wagner, K. Eckert, T. Eifler, F. Elsner, J. Elvin-Poole, S. Everett, A. Evrard, X. Fang, A. Farahi, E. Fernandez, I. Ferrero, A. Ferté, P. Fosalba, O. Friedrich, J. Frieman, J. García-Bellido, M. Gatti, E. Gaztanaga, D. Gerdes, T. Giannantonio, G. Giannini, D. Gruen, R. Gruendl, J. Gschwend, G. Gutierrez, I. Harrison, W. Hartley, K. Herner, S. Hinton, D. Hollowood, K. Honscheid, B. Hoyle, E. Huff, D. Huterer, B. Jain, D. James, M. Jarvis, N. Jeffrey, T. Jeltema, A. Kovacs, E. Krause, R. Kron, K. Kuehn, N. Kuropatkin, O. Lahav, P.-F. Leget, P. Lemos, A. Liddle, C. Lidman, M. Lima, H. Lin, N. MacCrann, M. Maia, J. Marshall, P. Martini, J. McCullough, P. Melchior, J. Mena-Fernández, F. Menanteau, R. Miquel, J. Mohr, R. Morgan, J. Muir, J. Myles, S. Nadathur, A. Navarro-Alsina, R. Nichol, R. Ogando, Y. Omori, A. Palmese, S. Pandey, Y. Park, F. Paz-Chinchón, D. Petravick, A. Pieres, A. Plazas Malagón, A. Porredon, J. Prat, M. Raveri, M. Rodriguez-Monroy, R. Rollins, A. Romer, A. Roodman, R. Rosenfeld, A. Ross, E. Rykoff, S. Samuroff, C. Sánchez, E. Sanchez, J. Sanchez, D. Sanchez Cid, V. Scarpine, M. Schubnell, D. Scolnic, L. Secco, S. Serrano, I. Sevilla-Noarbe, E. Sheldon, T. Shin, M. Smith, M. Soares-Santos, E. Suchyta, M. Swanson, M. Tabbutt, G. Tarle, D. Thomas, C. To, A. Troja, M. Troxel, D. Tucker, I. Tutusaus, T. Varga, A. Walker, N. Weaverdyck, R. Wechsler, J. Weller, B. Yanny, B. Yin, Y. Zhang, and J. Zuntz, Dark energy survey year 3 results: Cosmological constraints from galaxy clustering and weak lensing, Physical Review D **105**, 10.1103/physrevd.105.023520 (2022).

[30] E. P. Tryon, Is the Universe a Vacuum Fluctuation?, Nature (London) **246**, 396 (1973).

[31] J. C. Carvalho, Derivation of the mass of the observable universe, International Journal of Theoretical Physics **34**, 2507 (1995).

[32] C. Mercier, Calculation of the mass of the universe, the radius of the universe, the age of the universe and the quantum of speed., Journal of Modern Physics **10**, 980 (2019).

[33] S. Weinberg, *Gravitation and Cosmology* (John Wiley & Sons, 1972).

[34] P. Li, F. Lelli, S. McGaugh, and J. Schombert, A comprehensive catalog of dark matter halo models for sparc galaxies, The Astrophysical Journal Supplement Series **247**, 31 (2020).

[35] NASA/IPAC Extragalactic Database, The NASA/IPAC Extragalactic Database (NED) is operated by the Jet Propulsion Laboratory, California Institute of Technology, under contract with the National Aeronautics and Space Administration.

[36] Hagala, R., Llinares, C., and Mota, D. F., The slingshot effect as a probe of transverse motions of galaxies, AA **628**, A30 (2019).

[37] J. Klačka, M. Šturc, and E. Puha, Milky Way: New Galactic mass model for orbit computations, arXiv e-prints , arXiv:2407.12551 (2024), arXiv:2407.12551 [astro-ph.GA].

[38] A.-C. Eilers, D. W. Hogg, H.-W. Rix, and M. K. Ness, The circular velocity curve of the milky way from 5 to 25

kpc, The Astrophysical Journal **871**, 120 (2019).
[39] H.-F. Wang, Chrobáková, M. López-Corredoira, and F. Sylos Labini, Mapping the milky way disk with gaia dr3: 3d extended kinematic maps and rotation curve to 30 kpc, The Astrophysical Journal **942**, 12 (2022).
[40] Y. Sofue, Dark halos of m31 and the milky way, Publications of the Astronomical Society of Japan **67**, 75 (2015), https://academic.oup.com/pasj/article-pdf/67/4/75/54682398/pasj_67_4_75.pdf.
[41] P. R. Kafle, S. Sharma, G. F. Lewis, A. S. G. Robotham, and S. P. Driver, The need for speed: escape velocity and dynamical mass measurements of the andromeda galaxy, Monthly Notices of the Royal Astronomical Society **475**, 4043 (2018), https://academic.oup.com/mnras/article-pdf/475/3/4043/23934699/sty082.pdf.
[42] E. Corbelli, Dark matter and visible baryons in m33, Monthly Notices of the Royal Astronomical Society **342**, 199 (2003), https://academic.oup.com/mnras/article-pdf/342/1/199/3574568/342-1-199.pdf.
[43] Corbelli, Edvige, Thilker, David, Zibetti, Stefano, Giovanardi, Carlo, and Salucci, Paolo, Dynamical signatures of a cdm-halo and the distribution of the baryons in m33, AA **572**, A23 (2014).
[44] A. Sarajedini, A differential rr lyrae line-of-sight distance between m31 and m33, Monthly Notices of the Royal Astronomical Society **508**, 3035 (2021), https://academic.oup.com/mnras/article-pdf/508/2/3035/40673695/stab2765.pdf.